Proceedings

Seventeenth ACC Cyfronet AGH HPC Users' Conference

KU KDM 2025

Editors: Marek Magryś
Marian Bubak
Robert Pająk
Andrzej Zemła

Zakopane, 2-4 April 2025

Proceedings

Seventeenth ACC Cyfronet AGH HPC Users' Conference

Zakopane
2-4 April 2025

Editors: Marek Magryś
Marian Bubak
Robert Pająk
Andrzej Zemła

Published in April 2025

by Academic Computer Centre Cyfronet AGH
Nawojki 11, 30-950 Kraków, P.O.Box 6, Poland

ISBN 978-83-61433-48-4

Cover design and book typesetting by Joanna Kasina.

Ladies and Gentlemen!

The seventeenth HPC Users' Conference continues the tradition of annual meetings initiated by Cyfronet, bringing together scientists who utilize the PLGrid infrastructure for their research. At the same time, this edition introduces a new format, incorporating a series of training sessions led by experts from ACC Cyfronet AGH and the Polish National Competence Center, along with individual consultations with the PLGrid support team.

The training topics have been carefully selected based on the needs reported by users and the common challenges they encounter in their daily in silico research. I hope this new approach meets the expectations of both long-time conference participants and those who are just beginning to explore computational resources. The agenda covers not only traditional HPC topics but also AI applications, which are becoming a major consumer of computing power at Cyfronet.

Undeniably, our infrastructure users form a large and scientifically active community. This is evidenced by millions of computational jobs executed on Cyfronet supercomputers every year and hundreds of scientific publications acknowledging the use of our systems. Our resources contribute to research projects that drive significant scientific discoveries, optimize technological processes, answer longstanding questions, and solve previously intractable problems. Given this impact, we feel a deep responsibility to ensure that supercomputers, software, and data storage resources are as accessible as possible. This commitment extends to providing diverse hardware architectures and continuously enhancing the PLGrid User Portal − a gateway not only to Cyfronet's supercomputers and other Polish machines integrated into the PLGrid infrastructure, but also to the LUMI supercomputer and quantum computers.

In addition to serving the academic community, Cyfronet has recently expanded its focus to include small and medium-sized enterprises (SMEs) and industrial users. Under the umbrella of European projects such as EuroCC and FFplus, Cyfronet provides businesses with access to advanced computational resources, expertise, and training opportunities. These initiatives aim to enhance the competitiveness of Polish companies by facilitating the adoption of high-performance computing and artificial intelligence technologies in industry. By bridging the gap between research and business, we support innovation-driven growth and the broader digital transformation of the economy.

Cyfronet plays a crucial role in meeting the computational needs of the Polish research community by providing access to Poland's most powerful supercomputers: Helios, Athena, Ares and Prometheus. These state-of-the-art machines support groundbreaking research in various scientific disciplines, including physics, chemistry, life sciences, and artificial intelligence. Helios, the most powerful system in Poland, enables large-scale simulations and AI model training tasks, while Athena, Ares and Prometheus provide researchers with high-performance computing environments tailored to their diverse needs. Through these supercomputers, Cyfronet ensures that Polish scientists have the computational power required to remain competitive on the global stage, fostering innovation and accelerating scientific discovery.

Recently Poland has joined the LUMI-AI consortium, one of several European consortia developing Artificial Intelligence Factories. LUMI-AI will replace LUMI, one of Europe's fastest supercomputers, with a new AI-dedicated system planned for installation in 2027. The projected computing power of this supercomputer will place it among the world's fastest, further strengthening the European supercomputing ecosystem for training advanced AI models and developing dedicated AI solutions. Moreover, the launch of the LUMI-Q consortium quantum computer is approaching. This system, based on superconducting qubits arranged in a star topology, will minimize the number of exchange operations, enabling the execution of highly

complex quantum algorithms. It will consist of 24 physical qubits connected to a central resonator. Access to both LUMI-AI and LUMI-Q resources will be managed through the PLGrid Portal, just as it currently is for the LUMI supercomputer. As the leader of the PLGrid consortium, Cyfronet coordinates Poland's involvement in both initiatives.

Observing today's rapid scientific advancements, I see remarkable dynamism in the interplay of various disciplines and the increasing reliance on the latest technologies, including supercomputers and AI algorithms. To keep pace with this evolution, Cyfronet continuously expands its infrastructure, enhances employee competencies, and ensures the security of stored and processed data. The effectiveness of these efforts has been confirmed by the recent PN-EN ISO/IEC 27001 certification awarded to ACC Cyfronet AGH for its information security management system.

I am delighted that we can offer cutting-edge technologies and specialized knowledge to representatives of scientific institutions and enterprises daily. The HPC Users' Conference is particularly valuable as it allows us, the Cyfronet team, to gain firsthand insights into your work. Through this exchange of experiences − by clearly identifying both needs and possibilities − we can collaboratively advance Polish science and foster the development and implementation of innovations.

While it is tempting to say, "the sky is the limit," astrophysicists remind us that even this boundary can be surpassed. With that in mind, I wish you success in overcoming research challenges and perseverance in achieving your most ambitious goals. I also extend my gratitude to all users for their collaboration in refining our services and guiding us toward new directions for development.

With best regards,

Marek Magryś
Acting Director
ACC Cyfronet AGH

Organization

KU KDM 2025 was organized by the Academic Computer Centre Cyfronet AGH, Nawojki 11, 30-950 Kraków, Poland.

Organizing Committee

Marek Magryś, Joanna Kasina, Magdalena Maryańska, Kamil Mucha, Robert Pająk

KU KDM'25 Program Committee

Andrzej Zemła, PhD (chairman)	Academic Computer Centre Cyfronet AGH
Krzysztof Boryczko, Prof.	AGH University of Krakow
Marian Bubak, PhD	Sano Centre for Computational Medicine / Academic Computer Centre Cyfronet AGH
Joanna Dulińska, Prof.	Cracow University of Technology
Łukasz Dutka, PhD	Academic Computer Centre Cyfronet AGH
Armen Edigarian, Prof.	Jagiellonian University
Andrzej Eilmes, Prof.	Jagiellonian University
Marek Gorgoń, Prof.	AGH University of Krakow
Ernest Jamro, Prof.	AGH University of Krakow / Academic Computer Centre Cyfronet AGH
Zbigniew Kąkol, Prof.	AGH University of Krakow
Marek Kisiel-Dorohinicki, Prof.	AGH University of Krakow
Jacek Kitowski, Prof.	AGH University of Krakow / Academic Computer Centre Cyfronet AGH
Elżbieta Kuligowska, PhD	Academic Computer Centre Cyfronet AGH
Antoni Ligęza, Prof.	AGH University of Krakow
Marek Magryś	Academic Computer Centre Cyfronet AGH
Grzegorz Mazur, PhD	Jagiellonian University / Academic Computer Centre Cyfronet AGH
Janusz Mrozek, PhD	Jagiellonian University
Klemens Noga, PhD	Academic Computer Centre Cyfronet AGH
Janusz Orkisz, Prof.	Cracow University of Technology
Łukasz Rauch, Prof.	AGH University of Krakow
Irena Roterman-Konieczna, Prof.	Jagiellonian University Medical College
Paweł Russek, Prof.	AGH University of Krakow / Academic Computer Centre Cyfronet AGH
Marek Skomorowski, Prof.	Jagiellonian University
Renata Słota, Prof.	AGH University of Krakow
Marek Stanuszek, Prof.	Cracow University of Technology
Mariusz Sterzel, PhD	Academic Computer Centre Cyfronet AGH
Tomasz Szmuc, Prof.	AGH University of Krakow
Piotr Tworzewski, Prof.	Jagiellonian University
Kazimierz Wiatr, Prof.	Academic Computer Centre Cyfronet AGH

Table of Contents

Introduction to Quantum Computing − Optimizing Logistics Case Study

Paweł Gora

Quantum AI Foundation

pawel.gora@qaif.org

In this talk, I will give an introduction to the quantum computing domain, explaining the basic concepts and algorithms, how it is different from the traditional way of computing, and what are the biggest challenges in this field.

I will also explain the difference between circuit-based models and the quantum annealing approach.

Finally, I will present a use case demonstrating how quantum computing could be applied to solve routing problems in logistics.

Relativistic MHD Simulations of Merging and Collapsing Stars

Agnieszka Janiuk

Center for Theoretical Physics, Al. Lotnikow 32/46 , 02-668 Warsaw, Poland

agnes@cft.edu.pl

Keywords: computational astrophysics, numerical relativity, magnetohydrodynamics

1. Introduction

Compact binary mergers and the collapse of massive stars can produce intense transients observable across high-energy wavelengths. Events such as gamma-ray bursts and kilonova emissions are often accompanied by gravitational wave detections, making them crucial sources for multi-messenger astrophysics. To explore these phenomena theoretically, state-of-the-art approaches like numerical relativity and GR magnetohydrodynamic simulations are used. In this talk, I will review the current progress in simulations of mergers and collapsars, and present recent findings from my team, achieved using Polish PL-Grid and European High-Performance Computing facilities.

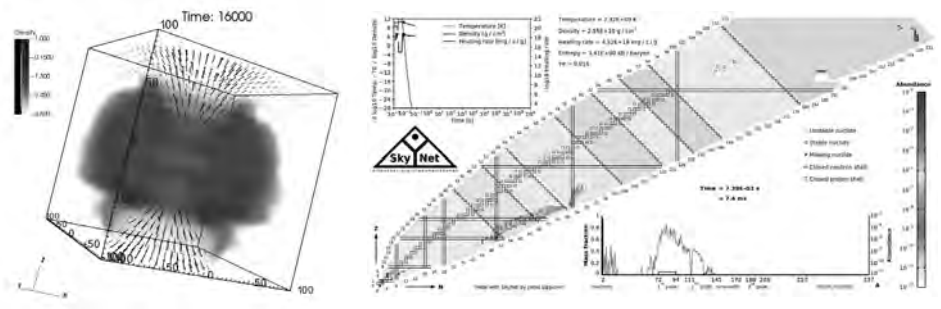

Fig. 1. Left: the 3D visualisation of our HARM-EOS model simulations, with volume rendering odd density field and overplotted velocity vector fields for the evolved state of accreting matter around black hole. The central engine in a form of dense torus launches powerful winds at high latitudes. These winds can be sites of heavy element nucleosynthesis. Right plot visualizes the path of r-process calculations, performed with the Skynet code, utilizing tracers of outflows produced by HARM.

2. Description of the problem

We use our version of the GR MHD code HARM described in [1] and [2], which utilizes numerical algorithms developed initially by [3]. HARM is based on a conservative shock-capturing scheme, with fluxes calculated using classical Harten-Lax-van Leer method. The constrained transport maintains divergence free magnetic field. The background spacetime is fixed by the Kerr metric of the black hole with constant mass and angular momentum. The equation of state of dense matter is implemented in the code with the form of 3-parameter EOS, based on tabulated values computed by minimizing the Helmholtz free energy of particles for a range of densities, temperatures, and compositions [4]. The tracer particle method is implemented in the code to follow the trajectories of outflows on the stored values of density and electron fraction. The nuclear reaction networks calculations are further done with postprocessing using the code Skynet [5]. This publicly available tool is capable to trace the nucleosynthesis in the rapid neu-

tron capture process, including self-heating. Involves large database of over a thousand isotopes. The newest development of HARM-EOS code is planned to include effects of evolving Kerr metric and self-gravity of collapsing star, together with proper microphysics. These calculations are now only in the preliminary stage.

3. Related work

In recent years, only a handful of GR MHD codes which use a composition-dependent EOS exist [6,7]. Our public release of the code, HARM-COOL [1,2] was one of such codes as well. Within the current project, we aim to utilise a new (private) branch of the code under development, named here the HARM-EOS. It has been used already in recent publication [8], where 2-dimensional simulations in GR MHD have been made to address the problem of black hole hyperaccretion.

4. Solution of the problem

We performed set of five 2-D and eight 3-D simulations with varying parameters black hole and disk mass ratio, black hole spins, and initial entropy per-baryon in the EOS. The 3D models were also considering non-axisymmetric perturbations in the torus, that might enhance wind outflow rates. The standard resolution was 288*256(*1/64/128) grid points in radial and polar (and azimulhal) directions, respectively. These models in fixed Kerr metric were meant to mimic the outcome of compact binary mergers in vacuum. In addition, simulations addressed to collapsing stars in evolving Kerr metric were performed (see talk by P. Plonka).

5. Conclusions

We calculated evolution of magnetized torus with 3-parameter EOS driven details microphysics of the short GRB central engine. Our results were used to produce heavy element nucleosynthesis patterns as well as synthetic kilonova lightcurves for a range of BH-disk mass ratios and range of black hole spin parameters. We find strong correlation between the black hole's spin and ejected wind mass, hence predictions for observed kilonova signal may differ. Also, because only a fraction (~20%) of BHNS binaries gain a high BH spin, or results are important for constraining compact binary evolution scenarios. Our models do not provide direct method to distinguish between BH-NS and NS-NS progenitors, but can be useful to explain resulting kilonova LC slopes.

Acknowledgements. This research has been supported by grant No. 2019/35/B/ST9/04000 from the Polish NCN and computing allocation on the ARES system at ACC Cyfronet AGH under the grants no. PLG/2023/016178, PLG/2024/016972. We also utilized two grants on LUMI supercomputing facility, first EHPC-DEV-2024D03-076 for code development and performance tests, and recently within the proper computational grant PLL/2024/07/017501.

References

1. A. Janiuk, 2017, ApJ, 837, 39.
2. A. Janiuk, 2019, ApJ, 882, 163.
3. C. Gammie, McKinney, J. C., & Tóth, G. 2003, ApJ, 589, 444.
4. F. X. Timmes & F.D. Swesty 2000, ApJSS, 126, 501.
5. J. Lippuner & L. Roberts, 2017, ApJS, 233, 18.
6. C. Palenzuela, 2015, Phys Rev D., 92, 044045.
7. D. Siegel, et al., 2018, ApJ, 859, 71.
8. A. A. Zdziarski, et al., 2024, ApJL, 967, 9.

Bielik: the Road to the Polish Large Language Model

Remigiusz Kinas

Speakleash/Bielik.ai

remigiusz.kinas@gmail.com

The presentation will detail the history of the Bielik models, starting from the beginning of the collaboration between SpeakLeash and ACC Cyfronet AGH to the publication of various versions of the model, such as Bielik v0.1 and Bielik v2.0. Another important part of the presentation will be a discussion of the stages of LLM model preparation, such as model and approach selection, tokenization, baseline training, instructional finetuning, and optimization. Methods for improving data quality will also be presented, including deduplication, cleaning, and anonymization, which are key to obtaining high-quality results. Finally, Bielik use cases will be presented. Among them will be answers to questions about how the model can be tailored to meet specific needs, and how its flexibility and low cost of use make it an attractive choice for a variety of applications.

Automated Management of 3D Digital Cultural Heritage Objects in Eureka3D with Onedata

Michał Orzechowski[1,2,3], Łukasz Opioła[2], Ignacio Lamata Martínez[5], Marinos Ioannides[4], Panayiotis N. Panayiotou[4], Łukasz Dutka[2], Renata G. Słota[1], Jacek Kitowski[1,2]

[1]AGH University of Krakow, Adama Mickiewicza 30, Krakow, Poland
[2]Academic Computer Centre Cyfronet AGH, Nawojki 11, Krakow, Poland
[3] Sano Centre for Computational Medicine, Kraków, Poland
[4] UNESCO Chair on Digital Cultural Heritage at Cyprus University of Technology, Research Centre MNEMOSYNE, Limassol, Cyprus
[5] EGI Foundation, Research Centre MNEMOSYNE, Amsterdam, The Netherlands

{morzech, rena, kito}@agh.edu.pl, lukasz.dutka@cyfronet.pl

Keywords: data management, metadata management, workflow processing, cultural heritage, digitisation

1. Introduction

In recent years, the European Union has invested significantly in the digitalisation of Cultural Heritage (CH) assets, supporting museums, libraries, and archives in preserving and providing access to their collections. Alongside EU funding, private and public initiatives, such as those by Google and the Smithsonian Institute, have advanced the digitalisation of CH, particularly through 2D and 3D technologies. However, challenges persist in efficiently sharing large 3D models across platforms like Europeana [1], which requires high-quality online visualization, metadata management, and proper storage systems. The novelty of this paper lies in its proposed solution for overcoming these challenges. One of the main contributions is the integration of metadata and paradata management into a unified data management platform, enabling better organization and access to 3D models. Additionally, the paper introduces automated workflows for processing data, metadata, and paradata, which streamlines the management process. The implementation of the Europeana Data Model as part of the platform further enhances the ability to manage and publish Cultural Heritage Objects (CHO) in line with Europeana's standards. This solution is designed to simplify 3D model handling and improve sharing within Europeana, fostering better collaboration across the European Cultural Heritage sector.

2. Cultural heritage object processing

The 3D digitization of CHOs is complex, requiring tailored workflows for each object type. A generic workflow includes digitization, authenticated upload via EGI Check-in to the Onedata [2] platform, automated processing, and publication as a CHO record accessible via 3D Viewer and Europeana.

EGI Check-in provides federated authentication and authorization, crucial for protecting digital assets. It integrates with CH institution identity management solutions, supporting standards like OIDC and OAuth. Onedata facilitates data and metadata processing. Content providers upload 3D models and metadata, triggering validation workflows. Metadata is ingested, and 3D models are annotated. Lower-resolution models are generated for publication. Finally, CHOs are published as public shares with metadata and paradata, accessible via 3D Viewer.

CHO publication requires data ingestion, metadata/paradata management, automated workflows, PID minting, and OAI-PMH advertisement, aligning with Europeana's EDM. Europeana uses EDM, an RDF-based framework, for metadata aggregation. Integration requires online

3D models (oEmbed compatible) and OAI-PMH accessible EDM-mapped metadata. Onedata supports this via a dynamic EDM form, pre-filled with ingested metadata. Onedata's metadata engine was extended to support EDM, and the OAI-PMH service was enhanced for Europeana harvesting. PID minting is integrated with EUDAT B2HANDLE. A REST API automates the ingestion-to-publication process.

These enhancements were validated within the EGI DataHub [3], a distributed data management platform. The extended Onedata platform provides a comprehensive solution for CHO management and publication, including EDM metadata annotation, PID assignment, OAI-PMH advertisement, and Europeana harvesting.

Onedata's integrated automation workflows address data management challenges. Workflows are composed and executed within Onedata, orchestrating actions on data collection. Lambdas, data processing functions, operate on user data via Onedata's built-in automation engine. Lambdas run in a containerized fashion on Kubernetes, with sidecar injection for Oneclient access to the Onedata filesystem. Workflows consist of lambdas, workflow schemas (blueprints), and inventories (registries). Lambdas are tasks with custom logic, workflow schemas define processing pipelines with lanes and parallel boxes, and inventories manage shared definitions.

The EUreka3D [4] project, which focused on 3D digital transformation of cultural heritage, used this system. It involves capture, cloud infrastructure (Onedata), and delivery (Europeana publication). Onedata's capabilities were crucial for managing and sharing 3D collections, enabling content providers to achieve project goals. Onedata infrastructure, automation workflow engine, the Eureka3D Viewer, and DataHub service are all hosted on the Cyfronet Openstack cloud utilizing 80 VCPU and 170GB of RAM.

3. Results and conclusions

The integration of diverse historical sources, digitized data, and metadata is a focus of many projects, with challenges arising from the rapid advancement of 3D digitization technologies for CHO. Existing systems need better metadata management for improved data interconnectivity. The Eureka3D project proposes a flexible automated workflow system that integrates data management with various processing backends, using FaaS for scalability. Declarative workflows, archiving, and versioning support reproducibility and tracking the evolution of 3D CHOs. The approach also aims to publish CHOs on platforms like Europeana and EOSC.

Acknowledgements. This work is co-financed in part by the "International Co-financed Projects" program (projects no. 5398/DIGITAL/2023/2 and 5399/DIGITAL/2023/2). JK and RGS are grateful for support from the Polish Ministry of Science and Higher Education subvention assigned to AGH University of Krakow.

References

1. Europeana: discover Europe's digital cultural heritage. https://www.europeana.eu
2. Orzechowski, M., Wrzeszcz, M., Kryza, B., Dutka, Ł., Słota, R.G., & Kitowski, J. (2023). Indexing legacy data-sets for global access and processing in multi-cloud environments. Future Generation Computer Systems, 147, 150-159. https://doi.org/10.1016/j.future.2023.05.024
3. *EGI DataHub*. https://datahub.egi.eu/
4. EUreka3D. (2025). *European Union's REKonstructed Content in 3D (EUreka3D)*. Retrieved January 8, 2025, from https://eureka3d.eu/

QHyper: an Integration Library for Hybrid Quantum-Classical Optimization

Tomasz Lamża[1,2,*], Justyna Zawalska[1,2,*], Kacper Jurek[1,2],
Mariusz Sterzel[2], Katarzyna Rycerz[1,2]

[1] AGH University of Krakow, Institute of Computer Science, al. Mickiewicza 30, 30-059 Krakow, Poland
[2] Academic Computer Center Cyfronet AGH, Nawojki 11 Street, 30-950 Krakow, Poland
[*]Authors contributed equally

{jzawalska,kzajac}@agh.edu.pl

Keywords: QHyper, Quantum Optimization, Hyperparameter Optimization, Variational Algorithms, Quantum Annealing, Penalties

1. Introduction

QHyper is a Python library for hybrid quantum-classical combinatorial optimization. It offers a flexible interface for problem formulation, supports various solvers, and enables (hyper)parameter optimization. Designed for diverse applications, QHyper facilitates efficient experimentation. Its simplest use is as a standalone tool for solving optimization problems.

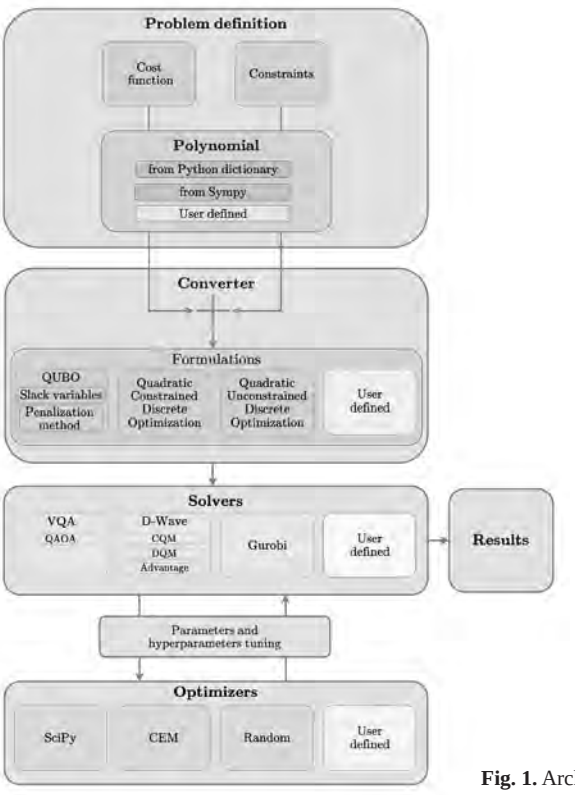

Fig. 1. Architecture of QHyper.

2. Description of the problem

There is a lack of a common API that could be used to connect different solvers needed for the convenience of the researcher in one place. To this end, we have created a modular software that allows users to run gate-based variational quantum algorithms, quantum annealing, and classical optimizers and compare their results. In addition, all essential properties of an optimization experiment can be easily defined using a simple configuration file, streamlining the research process.

3. Related work

There are only a few software tools unifying solvers for both techniques, namely QPLEX [1], QC Ware Forge [2], and Qibo [3]. However, no existing tools currently offer an interface for defining (hyper)optimizers or specifying experiment properties using a simple configuration file.

4. Solution of the problem

QHyper provides unifying architecture covering diverse requirements of computational experiments ranging from formulating combinatorial problems, through selecting and running solvers and objective function hyperparameters optimization. The rich set of solvers and the designed interface allows users to add custom optimization problems, own solvers, and necessary optimizers making QHyper extensible on every level of usability.

5. Conclusions

With its simple configuration options and seamless integration with Jupyter Notebooks, QHyper offers a user-friendly and efficient tool for combinatorial optimization. Its versatility makes it valuable for practitioners, engineers, and researchers, supporting a wide range of applications.

Link to documentation: `https://qhyper.readthedocs.io`

Acknowledgements. The research presented in this paper received support from the funds assigned by Polish Ministry of Science and Technology to AGH University. We gratefully acknowledge Polish high-performance computing infrastructure PLGrid (HPC Center: ACK Cyfronet AGH) for providing computer facilities and support within computational grant no. PLG/2024/017208.

References

1. J. Giraldo, J. Ossorio, N. M. Villegas, G. Tamura, U. Stege, QPLEX: Realizing the Integration of Quantum Computing into Combinatorial Optimization Software, arXiv:2307.14308 Jul. 2023). `URL https://doi.org/10.48550/arXiv.2307.14308`
2. QC Ware Forge. `https://qcware.readthedocs.io/en/latest/reference/optimization.html#`
3. S. Carrazza, S. Efthymiou, M. Lazzarin, A. Pasquale, An open-source modular framework for quantum computing, Journal of Physics: Conference Series 2438 (1) (2023) 012148, arXiv:2202.07017 `https://doi.org/10.1088/1742-6596/2438/1/012148`

Modeling of the Molecular Structure and the Modulated Nematic Phase

Bartosz Nikiel, Antoni Kocot

University of Silesia in Katowice, ul. Bankowa 12, 40-007 Katowice, Poland

bnikiel02@gmail.com, antoni.kocot@us.edu.pl

Keywords: liquid crystals, nematic order, molecular interaction

1. Introduction

The synthesis of a compound with an enantiotropic ferroelectric nematic phase, whose molecular structure is based on DIO, was carried out. Further modifications of the chemical structure led to the discovery of a new chiral liquid crystal phase, in which polar order coexists with the spontaneous formation of a helical structure composed of achiral molecules. We conducted studies on orientational order and changes in the dipole transition moment using infrared spectroscopy. The primary objective of the research is to gain a better understanding of the distinct molecular structural effects on the development of the polar order, phase biaxiality, spatial modulation of the nematic phases of bent and wedge shape molecules to develop design rules for materials forming a predominately weakly tilted polar phase.

2. Description of the problem

Using DFT simulations of the electronic structure of the molecules, rotational barriers were determined and the most probable conformers that could appear in real samples were optimized. At least two energetically stable conformations for the molecules were found for each of the bridges connecting the rings [1]. However, due to the small torsional barrier of the bridges, nearest neighbour interactions can significantly affect the conformations and vibrations of a given molecule [2,3]. The simulated theoretical spectra were used to identify the most important bands in the experimental spectra, as well as to determine the directions of the dipole transition moments of the molecules. Molecular parameters (dipole moment and its components) and theoretical IR and Raman spectra were determined for the isolated molecule and in the presence of neighbours. The components (|| and⊥) of the transition dipole moment and the derivative polarizability tensor were calculated, which allowed for the determination of theoretical polarization spectra, which were then used to determine the order parameters.

3. Related work

The ferroelectric nematic has become an extremely “hot” research topic. Current experiments suggest that the stabilization of the nematic phase can be related to the observed strong softening of one of Frank’s three elastic constants in the adjacent uniaxial nematic phase [4].

4. Solution of the problem

The software that has been used is Gaussian 16 which enabled computing the necessary data about the nematic order.

Geometry optimizations and vibrational calculations were performed using the DFT method (B3LYP) in Gaussian16 software with the 6-311G+(d,p) basis set. The main difference between the calculated and experimental spectra is the intensity of the vibrational peaks, which clearly depends on the molecular interaction.

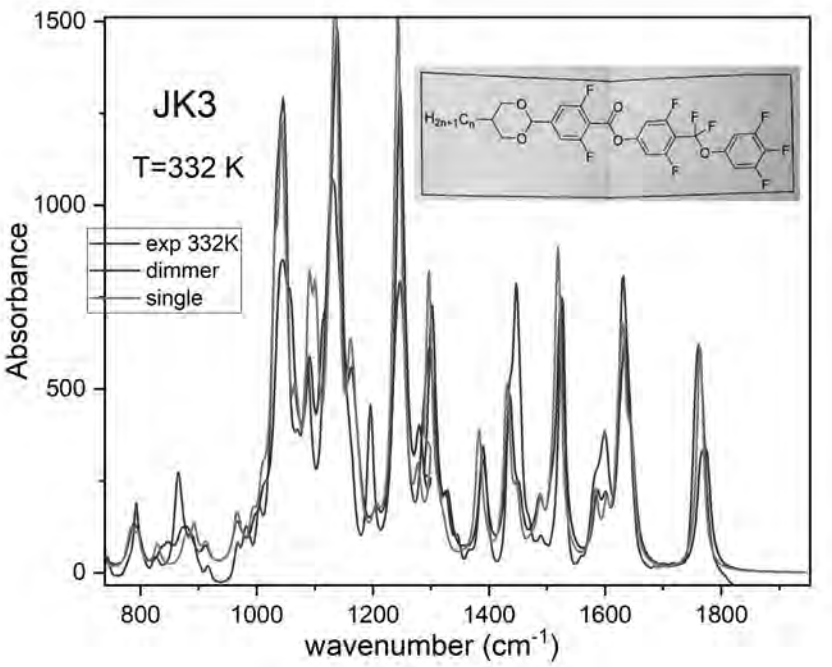

Fig. 1. Comparison of calculated and experimental spectra of the liquid crystal (JK3 sample, n=3).

5. Conclusions

Previous studies on materials forming the twist-band phase have indicated a significant role of intermolecular interactions, therefore, we expect similar results in the case of ferroelectric nematics.

Acknowledgements. This work/research has been supported by OPUS-23 and ACC Cyfronet AGH. The numerical experiment was possible through computing allocation on the Prometheus system at ACC Cyfronet AGH under the grant plgferlcr**.**

References

1. A. Kocot , B. Loska, Y. Arakawa and K. Merkel, Structure of the twist-bend nematic phase with respect to the orientational molecular order of the thioether-linked dimers. Phys. Rev., E . 105, 044701 (2022).
2. K. Merkel, B. Loska, C. Welch, G. H. Mehl, A. Kocot**,** The role of intermolecular interactions in stabilizing the structure of the nematic twist-bend phase, RSC Advances., 5, 2917-2925 (2021).
3. K. Merkel, B. Loska, C. Welch, G. H. Mehl, A. Kocot., Molecular biaxiality determines the helical structure, Phys. Chem. Chem. Phys., 7, 4151-4160 (2021).
4. Karcz et al., Science 384, 1096-1099 (2024).

HPC-Driven Analysis of LGAD Waveforms for Proton Beam Monitoring

Leszek Grzanka[1,2], Nicola Minafra[4], Ronan McNulty[3], Maciej Nessel[1], Tomasz Nowak[2], Jan Swakoń[2], Piotr Rzeźnik[1]

[1] AGH University of Krakow, Krakow, Poland
[2] Institute of Nuclear Physics, Polish Academy of Sciences, Krakow, Poland
[3] School of Physics, University College Dublin, Belfield, Dublin 4, Ireland
[4] Department of Physics & Astronomy, University of Kansas, Lawrence, KS 66045, USA

grzanka@agh.edu.pl

Keywords: proton beam, silicon detectors, radiotherapy

1. Introduction

Accurate beam monitoring is essential in proton therapy to verify beam intensity, stability, and patient safety. Low Gain Avalanche Detectors (LGADs), featuring sub-nanosecond timing and radiation hardness, can offer real-time, single-particle detection. This abstract explores our HPC-assisted workflows for analyzing large-scale waveform data from LGADs and evaluating their potential in proton beam monitoring.

2. Description of the problem

Conventional ionization chambers measure aggregated beam current on millisecond timescales, hiding detailed structure at shorter intervals. Fast silicon sensors like LGADs remain under active development. While they have minimal dead time, pileup at high intensities can undermine counting efficiency and must be addressed. Additionally, capturing beam features at multiple timescales and performing time-of-flight studies with multiple detectors generates terabytes of 10 GHz waveforms, requiring HPC solutions for large-scale data analysis.

3. Related work

Studies showed LGADs track single particles in electron [1] or proton beams with sub-ns resolution [2]. However, large-scale waveform acquisition and direct validation against ionization chambers are less explored. Our approach unites HPC-driven analysis with advanced LGAD sensors for full-beam monitoring.

4. Solution of the problem

In experiments at the AIC-144 cyclotron at IFJ PAN in Krakow (58 MeV protons), LGADs captured waveforms at 10 GHz, yielding over 3 TB of data across multiple 0.5 s beam segments. We employed data cleaning, peak finding, and statistical modeling in Python-based workflows, refactored for parallel computing with Dask on the Ares HPC cluster. This setup efficiently handled memory-intensive tasks and resolved sub-ms beam dynamics. Our codes enabled precise beam fluence measurements and LGAD efficiency determinations over a wide current range, including pileup conditions. We explored LGAD efficiency and developed a novel method to mitigate pileup.

5. Conclusions

LGADs accurately measured beam intensity and microstructure in accordance with conventional monitors, while additionally resolving beam time features on micro- and nanosecond

scales. The HPC approach handled hundreds of GB of waveforms, enabling interactive data analysis that surpasses traditional batch processing in adaptability and detail. This study demonstrates the suitability of LGADs for precise proton beam monitoring and underscores the importance of HPC in advanced accelerator research.

Acknowledgements. This work/research has been supported by the Eurolabs Transnational Access Program Grant number EURO-LABS-ALTO-001. The numerical experiment was possible through computing allocation on the Ares system at ACC Cyfronet AGH under the grants plglgad2023 and plglgad2023raw2.

References

1. Isidori, Tommaso, et al. “Performance of a low gain avalanche detector in a medical linac and characterisation of the beam profile.” Physics in Medicine & Biology 66.13 (2021): 135002.
2. Ulrich-Pur, Felix, et al. „First experimental time-of-flight-based proton radiography using low gain avalanche diodes.” arXiv preprint arXiv:2312.15027 (2023).

Three-Step Deep Learning System for Cancer Cell Detection

Jan Krupiński[3], Ernest Jamro[1,2], Maciej Wielgosz[1,2], Paweł Russek[1,2], Agnieszka Dąbrowska-Boruch[1,2], Kazimierz Wiatr[1]

[1] ACC Cyfronet AGH, Nawojki 11, 30-950 Kraków, Poland
[2] AGH University of Krakow, al. Mickiewicza 30, 30-059 Kraków, Poland
[3] Cracow University of Technology, Warszawska 24, 31-155 Kraków, Poland

jan.krupinski@pk.edu.pl, {jamro, wielgosz, russek, adabrow, wiatr}@agh.edu.pl

Keywords: cytology, deep learning, cell detection, image classification

1. Introduction

Deep learning models can be applied in medicine to detect and classify cells in microscope images. In this paper we propose a novel three-step system, consisting of three separate AI models working collectively on different image details: 1) a whole image, 2) a single cell and 3) results from the previous steps. We also evaluate their performance on three different datasets.

2. Description of the problem

Cytopathology poses unique challenges which necessitate the development of specialized systems. Biological cells possess visual features inherently different from everyday objects, and the characteristics of neoplastic cells can be quite subtle. The resolution and density of cells in images can vary with the magnification and equipment used. This variability of conditions makes large and diverse datasets a requirement in training and testing deep learning models.

3. Related Work

Research in cell detection has mainly focused on single-step and two-step detectors [1]. In the two-step methods, the first step proposes regions of interest, followed by classification. Some studies [2,3] have proposed refining whole-image detections by classifying individual cells.

4. Solution of the problem

The developed three-step (3-S) system consists of three (or more) models, trained separately. The reduced size of the models was chosen to prevent overfitting and to facilitate real-time cell detection even on limited-resource devices. In the first step, YOLOv8 [4] detects and classifies the relevant cells in the image. In the second step, each cell is classified again using a different neural network, such as RegNet [5]. In the third step, both outputs of these models as well as basic image features are used as an input for the XGBoost [6] gradient boosting algorithm to make a final classification. The developed 3-S system is presented in Figure 1.

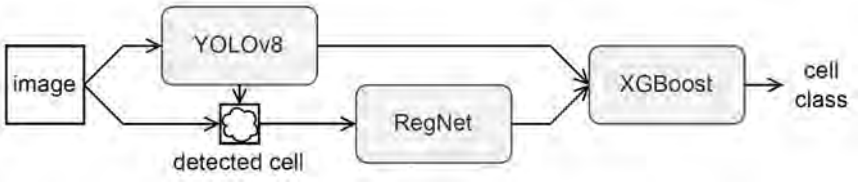

Fig. 1. Three-step (3-S) system consisting of YOLOv8 [1], RegNet [2] and XGBoost [3].

The 3-S system was evaluated for three different tasks, beginning with cell nucleus detection on the DSB2018 [7] dataset which contains around 6,000 nuclei. The 3-S system reached an accuracy of 0.858 for the nuclei class, which is higher when compared to state-of-the-art models [8]. However, the dataset size is rather small, and the images are of limited quality.

The system was also evaluated on the APACC [9] cervical cancer dataset, containing over 21,000 high quality images with four classes of objects. The accuracy for cell classification improved to 0.832 when using RegNet compared to the methods used in the literature [9]. However, the dataset may be less suitable for the detection task because it labels clusters of cells rather than individual cells, which introduces unnecessary ambiguity and lowers the metrics. Furthermore, the dataset is very imbalanced, containing very few unhealthy cells.

Finally, the system was tested on the CyfroVet [10] small animal skin cancer dataset containing over 3,500 images and 12 classes. Here, the overall accuracy increased slightly when compared to just using a YOLOv8 model. However, this required using two additional neural networks at the second step: a simple convolutional neural network, and ViT-B [11]. The results are presented in Table 1.

Tab. 1. Ensemble system results compared to state-of-the-art detection models.

Dataset	DSB2018	DSB2018	APACC	APACC	CyfroVet	CyfroVet
Model	ASFYOLO	3-S System	YOLOv8	3-S System	YOLOv8	3-S System
Accuracy	0.801	0.858	0.22	0.232	0.668	0.670
F-1 macro	0.871	0.871	0.189	0.208	0.642	0.654

5. Conclusions

The paper presents a three-step system for cell detection and classification, which may give better results when compared to state-of-the-art methods on the presented datasets. However, imbalanced and limited data still has a negative impact on the system's performance.

Acknowledgements. The numerical experiment was possible through computing allocation on the Athena system at ACC Cyfronet AGH under the grants plglaoisi24, plgdyplomanci6.

References

1. H. Jianga, et al., „Deep Learning for Computational Cytology: A Survey", Med. Image Analysis, 2022.
2. Y. Nambu, et al., „A screening assistance system for cervical cytology of squamous cell atypia based on a two-step combined CNN algorithm with label smoothing." Cancer Med. 2022 11(2): pp. 520-529.
3. J. Krupiński, et al., „Comparison of One and Two-Step Deep Learning Models for Cytology Image Classification", KUKDM 2024: Sixteenth ACC Cyfronet AGH HPC Users' Conference, 2024.
4. G. Jocher, J. Qiu and A. Chaurasia, „Ultralytics YOLO (Version 8.0.0)": `http://github.com/ultralytics/ultralytics`
5. J. Xu, Y. Pan, et.al., „RegNet: Self-Regulated Network for Image Classification", IEEE Transactions on Neural Networks and Learning Systems, vol. 34, no. 11, 2023.
6. T. Chen and C. Guestrin, „XGBoost: A Scalable Tree Boosting System", Proceedings of the 22nd ACM SIGKDD International Conference on Knowledge Discovery and Data Mining, 2016.
7. A. Goodman, et al., "2018 Data Science Bowl", Kaggle, 2018.
8. M. Kang, C.-M. Ting, F. F. Ting, R. C.-W. Phan „ASF-YOLO: A novel YOLO model with attentional scale sequence fusion for cell instance segmentation", Image Vis. Comput. 147, 2024.
9. D. Kupas, A. Hajdu I. Kovacs et al., „Annotated Pap cell images and smear slices for cell classification", Sci Data 11, 743, 2024.
10. R. Frączek et al., „The System for Automatic Skin Cancer Detection – Achievements and Challenges", KUKDM 2024: Sixteenth ACC Cyfronet AGH HPC Users' Conference, 13-15 March 2024.
11. A. Dosovitskiy, L. Beyer, et. al., „An image is worth 16x16 words: Transformers for image recognition at scale" ICLR, 2021.

SPEECHM: Extendable AI Models Benchmarking Service

Marek Kasztelnik, Szymon Mazurek

Academic Computer Centre Cyfronet AGH, Kraków, Poland

{marek.kasztelnik,szymon.mazurek}@cyfronet.pl

Keywords: AI, evaluation, ranking

1. Introduction

Multimodal AI models are increasingly vital for applications integrating text, audio, and video data, such as real-time speech-to-speech translation, virtual meeting assistants, and language-transparent communication. These models promise transformative potential, but their holistic evaluation remains a significant challenge. Existing benchmarks often focus on isolated tasks rather than comprehensive, multimodal capabilities, leaving a critical gap in assessing real-world applicability.

2. Description of the problem

The evaluation of multimodal AI models, as a part of research in the framework of the Meetween project [1], is fragmented, with most existing benchmarks targeting single-modality tasks such as automatic speech recognition (ASR), text summarization, or machine translation. Existing benchmarks fail to address the complexity of multimodal applications, where synchronized processing of text, speech audio, and video streams is crucial.

3. Related work

Popular benchmarks such as GLUE [2] and SuperGLUE [3] provide a foundation for text-based natural language processing tasks, and ASR-GLUE [4] extends these efforts to speech recognition. However, these benchmarks remain modality-specific, limiting their applicability to multimodal systems. The lack of a holistic benchmarking solution restricts the development of AI systems capable of handling complex, multimodal inputs.

4. Current status of development and plans

SPEECHM (Speech Performance Evaluation Criteria and Holistic Metrics) addresses this gap by introducing a unified, extendable benchmarking service for evaluating multimodal AI models. Inspired by SuperGLUE and ASR-GLUE, SPEECHM offers a standardized and extendable framework for assessing models across multimodal speech perception and generation tasks. The platform (Fig. 1) comprises two key components: (1) Web Application - Organizes and presents tasks, test sets, models, and rankings; (2) HPC Backend: Leverages high-performance computing resources to execute and scale benchmarking, even for GPU-intensive evaluations.

The current version of SPEECHM supports 10 tasks evaluated using 7 metrics–F-score, SacreBLEU, BLEURT, WER, ROUGE, Accuracy, and Exact Match, 8 diverse test sets, including MTEDX, MUSTC, DIPCO, ACL6060, FLORES, ICSI, SpokenSquad, and AUTOMIN. The service will be used during the upcoming International Conference on Spoken Language Translation (IWSLT) challenge [5], demonstrating its precision and versatility.

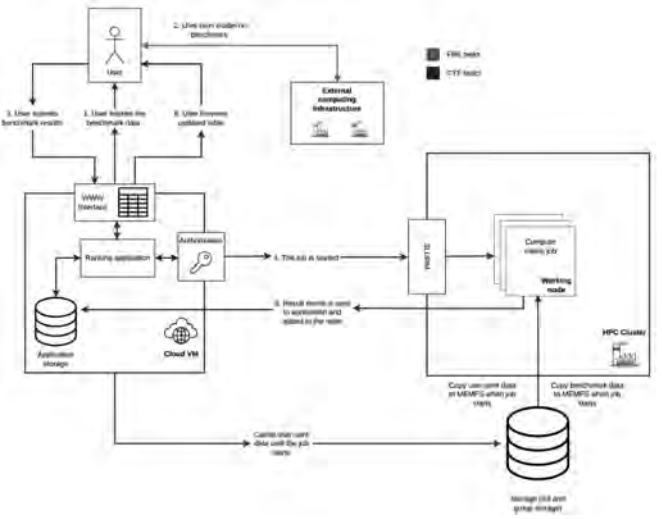

Fig. 1. Architecture of SPEECHM service.

Future development will focus on expanding the range of supported tasks, test sets, and evaluators and introducing mechanisms for organizing AI-focused challenges.

5. Conclusions

SPEECHM offers a novel solution for the holistic evaluation of multimodal AI models, addressing limitations in existing benchmarks. Its unified framework, robust architecture, and diverse test sets enable scalable and fair assessments, supporting the development of advanced AI models for real-world applications. Continued enhancements to the platform will further strengthen its role as a standard for multimodal AI benchmarking.

Acknowledgements. This work has been supported by the European Union's Horizon research and innovation programme under grant agreement No 101135798, project Meetween (My Personal AI Mediator for Virtual MEETtings BetWEEN People). The numerical experiment was possible through computing allocation on the Ares, Athena and Helios systems at ACC Cyfronet AGH under the grants PLG/2024/016971 and PLG/2025/018002.

References

1. The Meetween project, `https://www.meetween.eu/`
2. The General Language Understanding Evaluation (GLUE) benchmark, `https://gluebenchmark.com/`
3. Alex Wang et al. "Superglue: A stickier benchmark for general-purpose language understanding systems." NeurIPS (2019).
4. Feng, L. et al. "ASR-GLUE: A New Multi-task Benchmark for ASR-Robust Natural Language Understanding." ArXiv:2108.13048. (2021).
5. International Conference on Spoken Language Translation (IWSLT) conference, `https://iwslt.org`

Toolkit for Managing Research Data in Medical Simulations on HPC Infrastructure

Taras Zhyhulin[1], Karol Zając[1], Piotr Nowakowski[1,2], Maciej Malawski[1,2], Jan Meizner[1,2], Marek Kasztelnik[2], Piotr Połeć[2]

[1] Sano Centre for Computational Medicine, Czarnowiejska 36, 30-054 Kraków, Poland
[2] ACC Cyfronet AGH, ul. Nawojki 11, 30-950 Kraków, Poland

{t.zhyhulin,k.zajac,p.nowakowski,m.malawski}@sanoscience.org, {jan.meizner,m.kasztelnik,p.polec}@cyfronet.pl

Keywords: integration, data sharing, data repositories, FAIR principles, Open Science, high performance computing, medical simulations

1. Introduction

Modern medical simulations on digital twin models require substantial computational resources, large input datasets, and produce extensive output files that must be securely stored and shared among research team members to prevent data breaches. At the same time, there is a growing trend toward Open Science and FAIR principles, which require researchers to share their data with the community and collaborate within it. Sano Centre for Computational Medicine, in collaboration with ACC Cyfronet AGH, is working to motivate researchers to adhere to Open Science principles by developing infrastructure that facilitates it. The cornerstone of this effort − the previously developed integration of the Model Execution Environment platform with Dataverse and Zenodo repositories − is described in the paper "Integrating Data Repositories with HPC Resources for Streamlined Medical Simulation Model Execution" [1]. Now, we focus on further developing the infrastructure for convenient data sharing by expanding integrated repositories, enhancing the Sano Dataverse instance, and introducing beneficial data-sharing practices. Overall, our goal is to provide a toolkit that simplifies and incentivizes research data sharing and collaboration.

2. Description of the problem

Sharing large volumes of research data requires significant storage, which can be optimized by adopting a standardized approach to data sharing. To encourage researchers to follow this approach, appropriate infrastructure must be provided. Additionally, the scientific community aims to adhere to Open Science and FAIR principles, promoting dataset publication. However, making valuable research data openly available under free licenses allows unrestricted use by the community without direct returns to the original researchers. Therefore, mechanisms should be in place to incentivize community contributions to research before granting access to the data.

3. Related work

An example of an infrastructure that enables HPC simulation and facilitates data sharing is the Galaxy platform. It provides a user-friendly interface for constructing and executing data analysis workflows and integrates with repositories like Zenodo for data retrieval. The platform offers a regularly updated set of domain-specific and general-purpose tools for processing, analysis, and visualization on academic clusters. Additionally, workflows, results, and execution histories can be published for reuse.

4. Solution of the problem

The Model Execution Environment platform has been expanded with integration into the InvenioRDM repository. The Sano Dataverse instance has joined RODBUK, the Kraków Open Research Data Repository, to enhance credibility and increase the dissemination of published research data. Additionally, a rule-based data-sharing practice has been developed and implemented in publishing the DPValid dataset, provided by In Silico World partners.

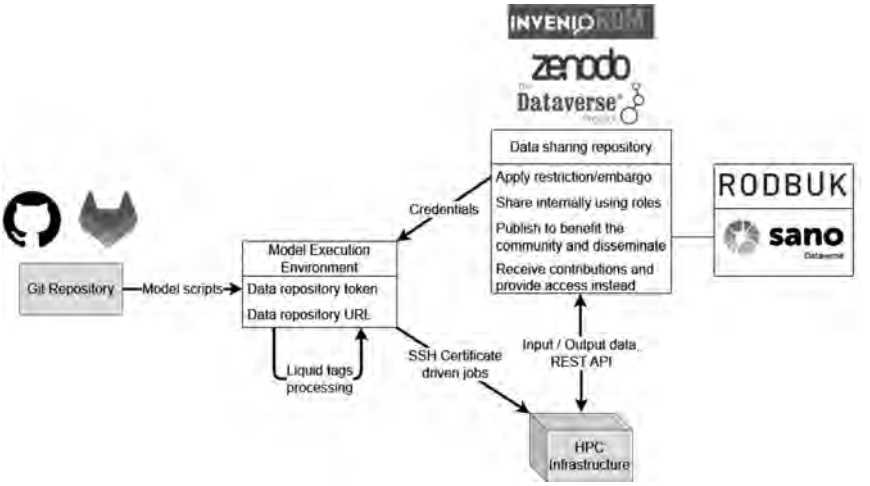

Fig. 1. Infrastructure facilitating data sharing.

5. Conclusions

The developed infrastructure–including the integration of MEE with data repositories, the inclusion of Sano Dataverse as part of RODBUK, and the implementation of a rule-based data--sharing technique–provides a comprehensive toolkit for processing, sharing, and publishing research data. This approach ensures the potential for research contributions even beyond the scope of the related project. Thanks to this toolkit, researchers have access to convenient tools that facilitate data management while adhering to Open Science and FAIR principles. Additionally, the infrastructure ensures security and reliability through RODBUK policies.

Acknowledgement. This publication is partly supported by the EU H2020 grants Sano (857533), ISW (101016503) and by the Minister of Science and Higher Education "Support for the activity of Centers of Excellence established in Poland under Horizon 2020" number MEiN/2023/DIR/3796. We gratefully acknowledge Polish high-performance computing infrastructure PLGrid (HPC Center: ACK Cyfronet AGH) for providing computer facilities and support within computational grant no. PLG/2024/017022.

References

1. Taras Zhyhulin, Karol Zając, Piotr Nowakowski, Maciej Malawski, Marek Kasztelnik, Piotr Połeć, Marian Bubak, „Integrating Data Repositories with HPC Resources for Execution of Simulation Models," w Konferencja Użytkowników Komputerów Dużej Mocy, Zakopane, 2024.
2. The Galaxy Community. The Galaxy platform for accessible, reproducible, and collaborative data analyses: 2024 update, Nucleic Acids Research, 2024;, gkae410, https://doi.org/10.1093/nar/gkae410

Serverless Transcriptomics on the HPC Cluster

Kamil Burkiewicz[1,2], Maciej Malawski[1,2]

[1] Sano Centre for Computational Medicine, Czarnowiejska 36, 30-054 Kraków, Poland
[2] Faculty of Computer Science, AGH University of Krakow, al. Mickiewicza 30, 30-059 Kraków, Poland

{k.burkiewicz, m.malawski}@sanoscience.org

Keywords: transcriptomics, FaaS, AWS, object storage, Apptainer

1. Introduction

When studying the expression of genes at the RNA level, the key problem becomes mapping RNA sequences to a specific reference genome or transcriptome. Many tools have been developed for solving this issue, offering various usage characteristics. One such tool is Salmon [4], which provides estimates of the transcripts quantification by performing lightweight quasi-mapping. Our objective is to use MapReduce paradigm with serverless functions to speed up the Salmon computation on a HPC cluster.

2. Description of the problem

We view the problem as a purely computational one, or CPU-bound. As the RNA reads are independent, the RNA quantification is in principle inherently parallelizable and with input data stored in a read-per-line file format, the data can be easily chunked and run in parallel, resulting in increased speedup in comparison with single threaded implementation.

3. Related work

This work is part of the Transcriptomics Atlas Pipeline [2] project, which was extensively developed over the years and consists now of highly optimized pipelines running Salmon and STAR aligners.

4. Solution of the problem

Inspired by the cloud environment, our computational paradigm of choice is MapReduce with serverless functions, as it ensures massive parallelism and omits the need for synchronization between jobs. We have already successfully implemented such a solution in the AWS cloud using Lambda service as backend. To do so, we used Lithops, a multi-cloud framework for running MapReduce tasks on FaaS architectures. Therefore, to bypass the need for reimplementation of the whole solution within the HPC environment, we exploit the LithopsHPC [1], a version of Lithops that can run under SLURM. It runs containerized Lithops components as SLURM jobs, preparing a platform for the user to create a FaaS abstraction on underlying HPC resources. We successfully ported LithopsHPC from MareNostrum 5 at Barcelona Supercomputing Center to Ares supercomputer at ACC Cyfronet.

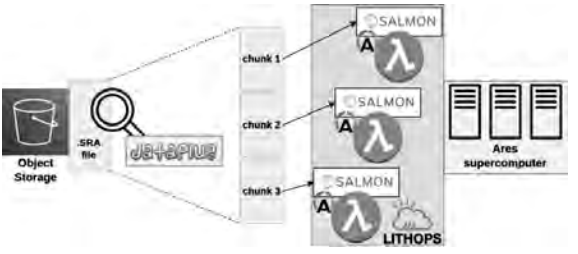

Fig. 1. Scheme of proposed solution.

We also use DataPlug software [3], which is designed to allow for logical partitioning of data into chunks while leaving the input files physically intact. It helps to reduce data movement and provides the possibility to run parallel tasks on small portions of original data. We created an extension for DataPlug that operates on Sequence Read Archives files (SRA), a basic format in the field of transcriptomics. It utilizes S3 compatible object storage.

5. Conclusions

The main contributions of our work can be summarized as follows:

- Implementation of serverless pipeline for transcriptome quantification using Salmon.
- Porting LithopsHPC solution to Ares supercomputer at ACC Cyfronet.
- Benchmarking of solution in HPC environment.

Acknowledgements. This work is supported by the European Union's Horizon 2020 research and innovation programme under grant agreement No 857533 and the International Research Agendas Programme of the Foundation for Polish Science No MAB PLUS/2019/13. This publication was created within the project of the Minister of Science and Higher Education "Support for the activity of Centers of Excellence established in Poland under Horizon 2020" on the basis of the contract number MEiN/2023/DIR/3796. This publication is supported by the European Union's Horizon Europe research and innovation programme under grant agreement NEARDATA No 101092644. The numerical experiment was possible through computing allocation on the Ares system at ACC Cyfronet AGH under the grant plgsano5 (PLG/2024/017108).

References

1. A. B. Arevalo, D. C. Tejeda, A. Call, P. G. López and R. N. Castell, „Enhancing HPC with Serverless Computing: Lithops on MareNostrum5," 2024 IEEE 32nd International Conference on Network Protocols, doi: 10.1109/ICNP61940.2024.10858564
2. P. Kica, S. Lichołai, M. Orzechowski and M. Malawski, "Optimizing Star Aligner for High Throughput Computing in the Cloud," 2024 IEEE International Conference on Cluster Computing Workshops (CLUSTER Workshops), doi: 10.1109/CLUSTERWorkshops61563.2024.00039
3. A. Arjona, P. García-López and D. Barcelona-Pons, "Dataplug: Unlocking extreme data analytics with on-the-fly dynamic partitioning of unstructured data," 2024 IEEE 24th International Symposium on Cluster, Cloud and Internet Computing (CCGrid), doi: 10.1109/CCGrid59990.2024.00069
4. Patro, R., Duggal, G., Love, M. et al., "Salmon provides fast and bias-aware quantification of transcript expression," Nat Methods 14, 417–419 (2017), doi: 10.1038/nmeth.4197

Analysis of Index Access Pattern in STAR RNA-seq Aligner

Jan Meizner[1,2], Piotr Kica[1], Sabina Lichołai[1,2], Maciej Malawski [1,2]

[1] Sano - Centre for Computational Medicine, Czarnowiejska 36, building C5, 30-054 Kraków
[2] ACC Cyfronet AGH, Nawojki 11, 30-950 Kraków

https://sano.science
{j.meizner, p.kica, s.licholai, m.malawski}@sanoscience.org

Keywords: HPC, cloud, cache, performance, RDMA, Ethernet

1. Introduction

This paper describes analysis of memory access pattern in the RNA-seq aligner called Spliced Transcripts Alignment to a Reference (STAR) [1]. The task is computationally and memory challenging as reads contain various types of mutations such as insertions or deletions. The alignment process is key for detection of a gene expression.

2. Description of the problem

As the STAR requires huge amount of computational resources esp. CPU and memory it is an ideal candidate for HPC. However, even HPC resources are not unlimited and finding optimal way to utilize them is crucial. In the case of STAR, we are running multiple processes on multiple nodes. Each of these processes requires access to the same array called the index. While single-node calculations use the shared memory, running them on multiple nodes requires loading the index once per node, which is extremely wasteful memory-wise, esp. as index for the Human genome takes around 30 GB of data [2]. To prevent it we are currently considering utilization of inter-node memory sharing mechanism. However, we hypothesized that the latency of the DRAM is much smaller than one of the interconnect. The goal of our work is to verify this and check the access pattern of STAR would allow caching to provide sufficient performance.

3. Related work

In the course of our research, we have analyzed multiple possible interconnects and compared them to access to directly attached RAM modules. As examples of the interconnects, we have selected InfiniBand [3] and HPE Slingshot [4] as dominant low-latency solutions used for HPC systems, and Ethernet commonly used in the IaaS Clouds [5]. In the Tab. 1 we have collected typical latency for said interconnects as well as for the DDR4 memory.

Tab. 1. Comparison of interconnect and local memory latency.

	Interconnect			Memory
	Slingshot	Infiniband	Ethernet	DDR4
Latency [ns]	300 - 400	50 - 100	10 000	10

As shown in Tab 1 even the best interconnect available at the moment has an order of magnitude higher latency than DDR4 memory which prompted the need to find optimal caching solution.

4. Solution of the problem

As the STAR tool is open source, we were able to provide instrumentation code to collect metrics showing access pattern to the array representing the genomics index that should be shared between nodes. The recompiled code was executed on the Helios supercomputer (CPU partition) which is an ideal environment for the task by enabling high level of parallelization per node while still enabling distribution of workload onto multiple nodes to even further decrease the computation time. Also, the Slingshot interconnect provides very low latency.

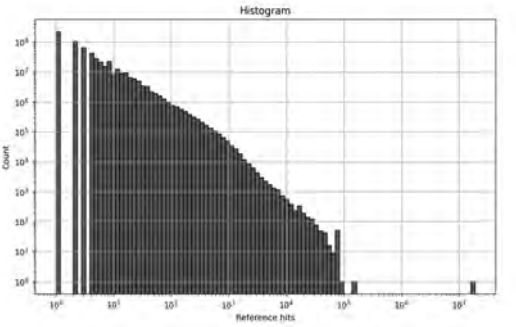

Fig. 1. Histogram showing relation between elements count and number of hits.

We have stored the output in a concise binary HDF5 files with appropriate compression. Using compressed HDF5 files instead of CSV reduces the size of input data by the factor of 10 to enable convenient analysis of multiple cases.

We have also developed a Python script based on NumPy and Pandas libraries to analyze the said file and find access pattern to the index. The result is presented in the Fig. 1 in the form of a histogram.

5. Conclusions

From the histogram in Section 4 we may conclude that caching just around 20% of the index would significantly improve performance of memory access, as such portion of the array is accessed much more frequently than the rest of the data. In the future we are planning to test access pattern for additional cases as well as find the most suitable solution for the implementation of the caching mechanism itself.

Acknowledgements. This publication is partly supported by the EU H2020 grants Sano (857533), NEARDATA (101092644) and by the Minister of Science and Higher Education "Support for the activity of Centers of Excellence established in Poland under Horizon 2020" number MEiN/2023/DIR/3796. We gratefully acknowledge Polish high-performance computing infrastructure PLGrid (HPC Center: ACK Cyfronet AGH) for providing computer facilities and support within computational grant no. PLG/2024/017108.

References

1. A. Dobin, CA Davis, F. Schlesinger, J. Drenkow, C. Zaleski, S. Jha, P. Batut, M. Chaisson, TR Gingeras: STAR: ultrafast universal RNA-seq aligner. Bioinformatics. 2013 Jan 1;29(1):15-21.
2. P. Kica, S. Lichołai, M. Orzechowski, M. Malawski (2024, September). Optimizing Star Aligner for High Throughput Computing in the Cloud. In 2024 IEEE International Conference on Cluster Computing Workshops (CLUSTER Workshops) (pp. 162-163). IEEE.
3. S. Shen, L. Huang, M. Chrapek, T. Schneider, J. Dayal, M. Gajbe, R. Wisniewski, and T. Hoefler: „LLAMP: Assessing Network Latency Tolerance of HPC Applications with Linear Programming." In Proceedings of the International Conference for High Performance Computing, Networking, Storage and Analysis (SC'24), November 2024, 1004–1021. Atlanta, GA, USA: IEEE Press.
4. D. De Sensi, S. Di Girolamo, K. H. McMahon, D. Roweth, and T. Hoefler. „An In-Depth Analysis of the Slingshot Interconnect." In Proceedings of the International Conference for High Performance Computing, Networking, Storage and Analysis (SC20*)*, November 2020.
5. D. De Sensi, T. De Matteis, K. Taranov, S. Di Girolamo, T. Rahn, and T. Hoefler, "Noise in the clouds: Influence of network performance variability on application scalability," Proc. ACM Meas. Anal. Comput. Syst., vol. 6, Dec 2022.

Using High Performance Computing for the Quantification and Personalization of Cardiovascular Models

Karolina Tlałka[1,2], Harry Saxton[3], Ian Halliday[2], Andrew Narracott[2], Maciej Malawski[1,4]

[1] Sano Centre for Computational Medicine, Nawojki 11, 30-072 Kraków, Poland
[2] Division of Clinical Medicine, School of Medicine and Population Health, University of Sheffield, Sheffield, United Kingdom
[3] School of Computer Science, University of Sheffield, Sheffield, United Kingdom
[4] Faculty of Computer Science, AGH University of Krakow, Kraków, Poland

{k.tlalka|m.malawski}@sanoscience.org,
{h.saxton|i.halliday|a.j.narracott}@sheffield.ac.uk

Keywords: cardiovascular models, dynamic systems, sensitivity analysis, global optimization

1. Introduction

The digital twin is the concept of creating virtual representation of a patient and use it to predict the risk of disease, increase the knowledge or find metrics useful in diagnostics [1]. Cardiovascular lumped-parameter models can be coupled with models representing homeostatic processes, such as baroreflex - a neurological mechanism of controlling blood pressure [2]. The most expensive stages of lumped-parameter model development are sensitivity analysis (SA) and personalization (optimization), which are supported by HPC.

2. Computing challenges

Adding the mechanism, which perturbs parameters at every beat leads to an increase in computation time, which becomes even greater by the need to run simulation for a long time to represent the real experiments. Another challenge is a nonlinear nature of the model which requires using global methods for SA and optimization, based on multiple model executions and require convergence. We perform a convergence study of Differential Evolution (DE) optimization [3] for a 4-chamber model coupled with baroreflex model [2], with the loss function based on time series data digitized from [4].

3. Related work

Most of the existing work focus on quantification of closed-loop or open-loop models of baroreflex in local scale [5, 6]. In [7] we showed that there are differences in local and global sensitivity patterns in closed-loop models, hence those models should be analysed globally.

4. Solution of the problem

We used an extended version of published model [7] with the baroreflex model [2]. We calibrated upon the subset of 6 parameters representing the most influential time constants and sympathetic gain of heart period path. Base values are taken from [2]. Julia BBO_adaptive_de_rand_1_bin_radiuslimited() DE algorithm [8] was tested, for the 50 agents and maximum of 1000 iterations. Loss function was the sum of squared difference between simulation outputs and the data (mean arterial pressure, heart rate and stroke volume series from Lower Body Negative Pressure experiment [4]). To test convergence of the study we performed 30 simulations on Ares and assessed the dispersion of calibration subset. Using HPC allowed to reduce computational time ~31 times, from estimated 1500h on local machine to 49h using HPC. The results of the study are presented in Fig. 1. The dispersion for gain and venous time constant is small, but for the other quantities there is a huge variation in optimization outputs.

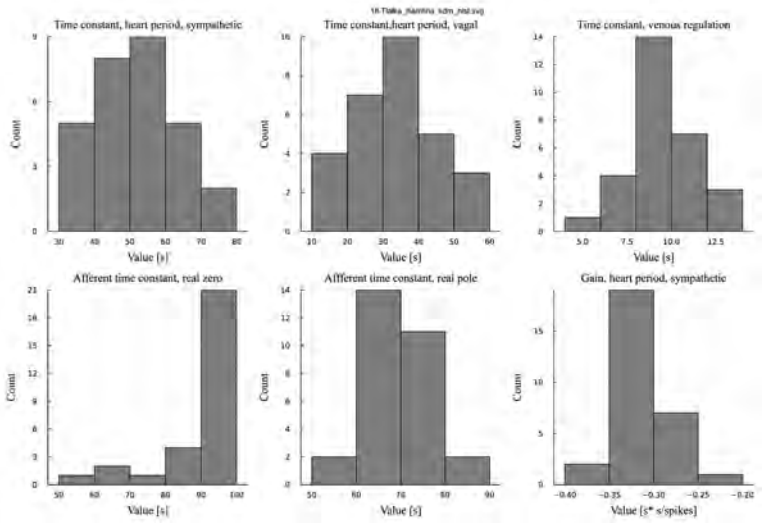

Fig. 1. The results of convergence study.

5. Conclusions

The results suggest that the convergence is not achieved. Possible solutions of the problem include changes within optimizer parameters, decreasing the range of variation for calibrated parameters, or further investigation of loss function structure.

Acknowledgements. The publication was supported by the Ministry of Science and Higher Education "Support for the activity of Centers of Excellence established in Poland under Horizon 2020" on the basis of the contract number MEiN/2023/DIR/3796, by the European Union's Horizon 2020 programme under grant agreement No 857533, by Sano project carried out within the International Research Agendas programme of the Foundation for Polish Science, co-financed by the European Union under the European Regional Development Fund. We gratefully acknowledge Polish high-performance computing infrastructure PLGrid (HPC Centre: ACK Cyfronet AGH) within computational grant no. PLG/2024/017108.

References

1. Zhang K. et al. (2024). Concepts and applications of digital twins in healthcare and medicine. Patterns (New York, N.Y.), 5(8), 101028.
2. Ursino M. (1998). Interaction between carotid baroregulation and the pulsating heart: a mathematical model. The American Journal of Physiology, 275(5), H1733–H1747.
3. Storn R., Price K. (1995). Differential Evolution: A Simple and Efficient Adaptive Scheme for Global Optimization Over Continuous Spaces. Journal of Global Optimization. 23.
4. Høiseth L. Ø. et al. (2015). Tissue oxygen saturation and finger perfusion index in central hypovolemia: influence of pain. Critical care medicine, 43(4), 747–756.
5. Olufsen, M. S. et al. (2006). Modeling baroreflex regulation of heart rate during orthostatic stress. American journal of physiology. Regulatory, integrative and comparative physiology, 291(5), R1355–R1368.
6. Kosinski S. A. et al. (2018). Computational model-based assessment of baroreflex function from response to Valsava maneuver. Journal of Applied Physiology, 125(6): 1944-1967. PMID: 30236047.
7. Tlałka K. et al. (2024) Sensitivity analysis of closed-loop one-chamber and four-chamber models with baroreflex. PLoS Comput Biol 20(12): e1012377.
8. Feldt R. (2013-2021). BlackBoxOptim.jl. Accessed 20.02.2025. Available at: `https://github.com/robertfeldt/BlackBoxOptim.jl`

Bipolar Disorder Characterization from Diffusion MRI: a Deep Learning Approach

Dominika Ciupek[1], Maciej Malawski[1,2], Tomasz Pięciak[3,1]

[1] Sano Centre for Computational Medicine, Kraków, 30-054 Poland
[2] AGH University of Kraków, Kraków, 30-059 Poland
[3] ETSI Telecomunicación, Universidad de Valladolid, Valladolid, 47011 Spain

{d.ciupek, m.malawski}@sanoscience.org, tpieciak@tel.uva.es

Keywords: magnetic resonance imaging, diffusion tensor imaging, bipolar disorder, deep learning

1. Introduction

Diffusion-weighted magnetic resonance imaging (DW MRI) provides unique insights into cellular structure, making the modality an effective tool for the non-invasive assessment of brain microstructure with a particular sensitivity to various neurological disorders [1]. However, proper modeling of the DW signal is essential for extracting quantitative indicators, especially under a limited acquisition procedure. This study explores the potential of employing deep learning (DL) models to estimate diffusion tensor imaging (DTI) [2] microstructural parameters in individuals with bipolar disorder (BP).

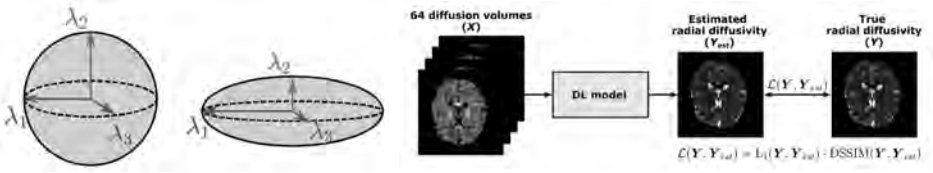

(a) (b)

Fig. 1. (a) Visual representation of DTI model, (b) scheme of microstructural parameters estimation using DL model with a loss function defined as the product of the least absolute error (L_1) and the structural dissimilarity index measure (DSSIM).

2. Diffusion tensor imaging

The diffusion tensor (DT) describes the movement of water molecules using a second-order tensor, algebraically represented as a symmetric, positive definite 3 × 3 matrix with three perpendicular eigenvectors and three positive eigenvalues. It can be visualized geometrically as an ellipsoid, where the major axis aligns with the principal eigenvector, and the axes lengths correspond to the eigenvalues. DT allows for the determination of multiple microstructural parameters, such as the radial diffusivity (RD), the average of the two minor eigenvalues, λ_2 and λ_3 [1]. Typically, the weighted least squares procedure is used to estimate DT parameters, but the process requires specific acquisition protocols and a sufficient number of DW volumes.

3. Related work

DL models have been recently widely used to estimate microstructural parameters such as those presented in the previous section. However, existing research mainly focuses on applying neural networks to acquisition protocols that involve a limited number of DW volumes [3,4,5]. Despite this progress, there is a limited number of detailed analyses of the ability of models to preserve the differences in microstructural parameters between healthy individuals and patients with various neurological disorders [5].

4. Results and Conclusions

The study used the UCLA dataset [6], including healthy individuals and patients with BP. A U-net model was employed to estimate RD, and it was trained in three data configurations: 1) healthy patients, 2) BP, and 3) a combination of both. Training the model on a private computer takes ~4363s/epoch, while using the Athena GPU reduces it to ~46s/epoch. To achieve acceptable accuracy, it is crucial to carefully select hyperparameters, which requires running the network training 12 times for 100 to 200 epochs. Consequently, the total training time on Athena is ~2.5 hours, as it can execute multiple scripts simultaneously. In contrast, training on a private laptop takes ~2,181 hours (90 days), making it impractical without HPC.We conducted analyses using standard metrics, including mean squared error (MSE) and structural similarity index measure (SSIM). We also applied Tract-Based Spatial Statistics (TBSS) to assess the number and location of voxels showing differences in RD between healthy subjects and patients. The results are summarized in Table 1. While all networks performed well according to evaluation metrics, deeper analyses revealed significant differences in the clinical accuracy. To capture more effectively the differences in microstructural parameters between healthy individuals and patients, it is crucial to train the network using data from both groups.

Tab. 1. Evaluation results on BP data of models trained in three configurations.

Bipolar		**Trained models**		
		Healthy	**Bipolar + Healthy**	
Evaluation metrics	**MSE [10^{-5}]**	1.55	1.65	0.68
	SSIM	0.9996	0.9997	0.9998
TBSS analysis	**TP [%]**	8.6	56.4	67.1
	FP [%]	0.0	0.0	0.3

Acknowledgements. The numerical experiment was possible through computing allocation on the Ares and Athena systems at ACC Cyfronet AGH under the grants PLG/2024/016945 and PLG/2025/018009. This work is supported by the European Union's Horizon 2020 research and innovation programme under grant agreement No 857533 and the International Research Agendas Programme of the Foundation for Polish Science No MAB PLUS/2019/13. This publication was created within the project of the Minister of Science and Higher Education "Support for the activity of Centers of Excellence established in Poland under Horizon 2020" on the basis of the contract number MEiN/2023/DIR/3796. Tomasz Pieciak acknowledges the NAWA for grant PPN/BEK/2019/1/00421 and the Ministry of Science and Higher Education under the scholarship for outstanding young scientists (692/STY/13/2018).

References

1. L. J. O'Donnell, et al.: An introduction to diffusion tensor image analysis. Neurosurgery Clinics, 22(2), 2011, pp.185-196.
2. P. J. Basser, et al.: MR diffusion tensor spectroscopy and imaging. Biophysical journal, 66(1), 1994, pp.259-267.
3. E. K. Gibbons, et al.: Simultaneous NODDI and GFA parameter map generation from subsampled q-space imaging using deep learning. Magnetic resonance in medicine, 81(4), 2019, pp.2399-2411.
4. M. Gaviraghi, et al.: A generalized deep learning network for fractional anisotropy reconstruction: Application to epilepsy and multiple sclerosis. Frontiers in Neuroinformatics, 16, 2022.
5. S. Aja-Fernández, et al.: Validation of deep learning techniques for quality augmentation in diffusion MRI for clinical studies. NeuroImage: Clinical, 39, 2023.
6. K. J. Gorgolewski, et al.: Preprocessed consortium for neuropsychiatric phenomics dataset. F1000Research, 6, 2017.

Verification, Validation and Uncertainty Quantification Workflows on High Performance Computers

Karol Zając

Sano – Centre for Computational Personalised Medicine, 36 Czarnowiejska, Kraków, 30-054 Poland

k.zajac@sanoscience.org

Keywords: HPC, VVUQ, Large-Scale, Parallel Computing, EasyVVUQ, Dask Distributed

1. Introduction

Scientific computing often relies on large-scale simulations, requiring substantial computational resources. High-Performance Computing (HPC) enables researchers to perform Verification, Validation, and Uncertainty Quantification (VVUQ) experiments, which often demand thousands of simulations. Running these workflows efficiently requires proper resource management and scalable tools to handle parallel execution and data processing.

2. Description of the problem

Access to HPC is required since running extensive VVUQ experiments on local machines becomes unfeasible due to computational constraints. Moreover, VVUQ workflows can be complex, involving multiple models, large datasets, and dependencies on external software and licenses. Efficiently scheduling and executing such workflows, while ensuring correct resource allocation and parallel execution, remains a challenge.

3. Related work

There exist several automated VVUQ frameworks, such as Dakota and OpenTURNS, but they often lack seamless integration with HPC job schedulers. EasyVVUQ provides a flexible Python-based framework for uncertainty quantification workflows, but scaling it effectively on HPC infrastructure involves additional tooling for workload distribution and appropriate resource management – which, in turn, depends on environment setup and model requirements.

4. Solution to the problem

To address these challenges, we leverage EasyVVUQ combined with both DaskJobQueue and DaskMPI to enable efficient execution of Sensitivity Analysis (SA) and VVUQ workflows on HPC. Following exploration of these solutions, we propose a general workflow for running VVUQ experiments, as presented in Figure 1. This workflow includes:

- Constructing an EasyVVUQ campaign which executes predefined actions.
- Selecting sampling and analysis methods for model parameters and their variability.
- Handling generation of model input files and decoding outputs to obtain quantities of interests.
- Utilizing DaskJobqueue and DaskMPI to distribute campaign tasks across HPC resources, ensuring load balancing and efficient parallel execution.

This setup allows EasyVVUQ to handle both Python-based simulations and external applications, including MPI-based executables. Proper allocation of computational resources, environment configuration, and workflow structuring ensure scalability and reproducibility.

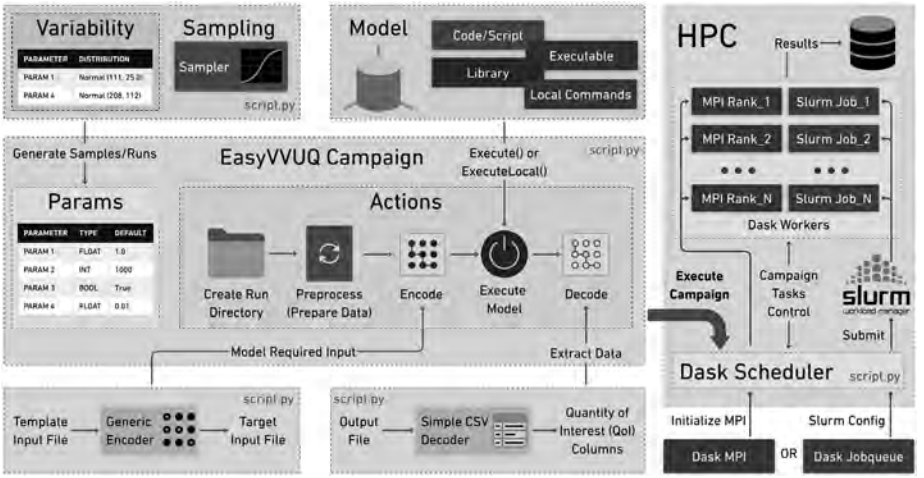

Fig. 1. EasyVVUQ workflow setup along with Dask execution on HPC.

5. Conclusions

Integration of EasyVVUQ with Dask and SLURM facilitates scalable execution of UQ and SA experiments on HPC. This approach improves computational efficiency while allowing flexible resource management. Because it is a generic solution, it can be utilized with any model, including Python-based implementations, more complex software such as Ansys, and even precompiled solutions. The framework has been tested on the Ares cluster at ACC Cyfronet AGH.

Acknowledgements. This publication is part of a project that has received funding from the European Union's Horizon Europe research and innovation programme under grant agreement No. 101136438. We gratefully acknowledge Polish high-performance computing infrastructure PLGrid (HPC Center: ACK Cyfronet AGH) for providing computer facilities and support within computational grants no. PLG/2024/016973 and PLG/2025/018003.

References

1. Kica, P., Otta, M., Czechowic, K., Zajac, K., Nowakowski, P., Narracott, A., Halliday, I., & Malawski, M. (2023). Serverless approach to sensitivity analysis of computational models. 2023 IEEE/ACM 23rd International Symposium on Cluster, Cloud and Internet Computing (CCGrid), 627–639. https://doi.org/10.1109/CCGrid57682.2023.00064
2. Suleimenova, D., Arabnejad, H., Edeling, W., Coster, D., Luk, O., Lakhlili, J., … Groen, D. (2021). Tutorial applications for Verification, Validation and Uncertainty Quantification using VECMA toolkit. Journal of Computational Science, 53. doi:10.1016/j.jocs.2021.101402
3. EasyVVUQ: Uncertainty intervals for everyone, EasyVVUQ documentation web site: https://easyvvuq.readthedocs.io/en/dev/
4. Dask, Dask Distributed documentation web site: https://distributed.dask.org/en/stable/

EDITH Project Roadmap – towards Virtual Human Twins

Marian Bubak[1,2], Marek Kasztelnik[1], Maciej Malawski[1,2], Jan Meizner[1,2], Piotr Nowakowski[1,2], Piotr Połeć[1]

[1]ACC Cyfronet AGH, ul. Nawojki 11, 30-950 Kraków, Poland
[2]Sano Centre for Computational Medicine, Czarnowiejska 36, 30-054 Kraków, Poland

{m.bubak,m.malawski,p.nowakowski}@sanoscience.org,
{m.kasztelnik,p.polec}@cyfronet.pl

Keywords: computational medicine, EDITH, virtual human twin, roadmap

1. Introduction

Computational medicine is an interdisciplinary field integrating knowledge about mechanisms of human physiology and using computational modeling on advanced computing infrastructures to understand and predict diseases. It enables a personalized approach to health treatment: predicting the risk of disease, performing virtual drug tests, advising changes in diet and lifestyle, and identifying therapies and medical procedures [1].

2. Description of the problem

To realize the idea of personalized computational medicine we need high quality mathematical models of human physiology implemented in forms of computer simulation modules and access to medical data, appropriate simulation procedures, supporting software environment, modern computing and storage systems, as well as standardization and certification procedures for medical treatments based on computational medicine [2].

3. Related work

Research in this direction started by Peter Hunter within the Physiome Project [3] was continued in the framework of the Virtual Physiological Human (VHP) [4] by many researchers and institutions like Sano Centre for Computational Medicine [5]. The outcomes of these investigations are presented at the VPH Conferences.

4. Solution of the problem

Recently, a holistic and systematic approach was pursued in the framework of the EU Project EDITH coordinated by Liesbet Geris [6], aiming at practical implementation of the idea of digital twins of humans: from cells and tissues to organs and entire bodies in the form of virtual human twin (VHT). VHT is an integrated, multi-scale, multi-temporal and multi-disciplinary representation of quantitative human physiology and pathology. To put VPH in practice, we require an inclusive ecosystem, implementation a federated repository gathering resources such as models, data sets, algorithms, practices, as well as a simulation platform on top of compute and storage resources. According to the EDITH Roadmap [6], the complexity and scale of VHT demand significant computational resources such as high-performance computing (HPC) to run computationally intensive simulations, training AI-based twins, and perform data-intensive analyses.

Research of the Cyfronet AGH team has resulted in elaboration of a demonstrator which enables running modules of VHT on HPC resources for scale-out studies with processing large amounts of data and “parameter study” types of computations. It enables reproducibility of

computer simulations, execution of computational models controlled by a set of scripts with a versioning system enabling collaborative usage. The functionality of the demonstrator was successfully validated with a set of typical VHT modules on the HPC resources. Currently, it is further developed, and we aim at elaboration of a whole VHT ecosystem for stroke patients [7].

5. Conclusions

The EDITH Roadmap presents a set of recommendations which should enable more efficient research and implementation in practice the idea of the virtual human twin. These recommendations are related to an assessment of creators and consumers in this area, basic building blocks of VHT technologies, VHT infrastructures, ELSI, standards and regulatory aspects, and sustainability conditions. The Cyfronet team main contribution – the demonstrator - may be already exploited in on-going research in computational medicine.

Acknowledgements. We acknowledge the support of EU grants EDITH No 101083771 (Digital Europe), GEMINI No 101136438 (HORIZON), Teaming Sano No 857533, and ACC Cyfronet AGH grant PLG/2023/016723.

References

1. Georgia Tourassi: Computational medicine: Grand challenges and opportunities for revolutionizing personalized healthcare, Frontiers in Medical Engineering, vol. 1, 2023, 10.3389/fmede.2023.1112763
2. Peter Coveney, Roger Highfield: Virtual You. How Building Your Digital Twin will Revolutionize Medicine and Change Your Life, Princeton University Press, 2023.
3. Physiom Project - https://www.auckland.ac.nz/en/abi/our-research/research-groups-themes/physiome-project.html
4. VPH Institute - https://www.vph-institute.org/
5. Sano Centre for Computational Medicine - https://sano.science/
6. EDITH – European Virtual Digital Twin, EU Project, Digital Europe, https://www.edith-csa.eu/
7. GEMINI - A Generation of Multi-scale Digital Twins of Ischaemic and Haemorrhagic Stroke Patients, EU Project, HORIZON, https://dth-gemini.eu/

Enabling Scientists through Marketplace: Simplifying Access to HPC and Research Resources

Michał Kołomański, Wojciech Ziajka, Paweł Gorczyca

Academic Computer Centre Cyfronet AGH, Kraków, Poland

{m.kolomanski, w.ziajka, p.gorczyca}@cyfronet.pl

Keywords HPC, e-infrastructure, scientific workflows, data access

1. Introduction

Access to high-performance computing (HPC), storage, datasets, and publications is essential for modern scientific research. The Marketplace [1] is designed to simplify the discovery, ordering, and usage of these resources, ensuring scientists can efficiently set up their research environments and focus on innovation.

2. Description of the problem

Accessing HPC and large-scale infrastructures remains challenging due to fragmentation, complex procurement, and technical barriers. Researchers need a unified platform to filter available resources, compare offers, and quickly set up their environment. The goal is to streamline workflows, from selecting infrastructure to running computations and retrieving results efficiently.

3. Related work

Previous initiatives (e.g. EOSC Future project [2]) improved resource discoverability, but accessing them remains a challenge. Ordering can be a lengthy process, and setting up the necessary environment, including data transfers, is still a major hurdle. The Marketplace aims to bridge this gap by offering an end-to-end platform that integrates resource discovery, ordering, and workflow management, simplifying research execution.

4. Current status of development and plans

Discoverability is well established − users can filter offers based on access policies, geographical availability, and other criteria. Ordering is facilitated through integration with dedicated JIRA instance, or providers' existing ticketing systems. Nonetheless, to enhance order management, and improve the user and provider experience even more, we are developing a custom Backoffice Ordering System (BOS), which will significantly streamline the process and improve user-provider interactions.

A key ongoing development is the integration of the Marketplace with UPV's Infrastructure Manager (a TOSCA Cloud Orchestrator) [3] to enable the automatic deployment of services in a given environment. Additionally, we are working with CERN's File Transfer Service (FTS) [4] service to ensure seamless data movement between infrastructures. These enhancements will allow researchers to efficiently set up their environments, deploy custom software, and manage data workflows with minimal overhead.

We have also entered a new era − the era of the federation − where multiple nodes (such as scientific communities) form a network and share core functionalities like a catalogue. From now on, the Marketplace also serves as a plug-and-play solution for communities! They no longer need to develop their own catalogue from scratch to share e.g. their data repository. Instead, they can simply adopt our Marketplace, customize it to their needs, deploy it locally, and manage it effortlessly.

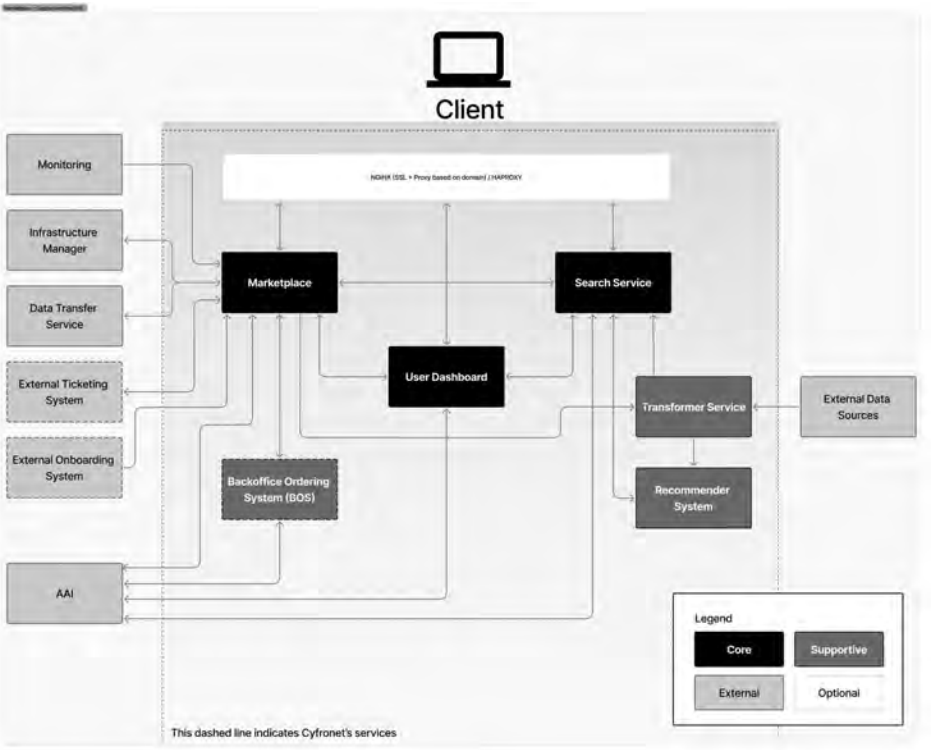

Fig. 1. Architecture of Marketplace service.

5. Conclusions

Providing a unified, intuitive platform for accessing HPC and research resources is key to accelerating modern innovation. The Marketplace plays a crucial role in enabling researchers to focus on discoveries rather than navigating administrative and technical complexities.

Acknowledgements. ACC Cyfronet makes this work possible. The Marketplace is currently being developed within the EOSC Beyond [5].

References

1. Marketplace, `https://search.marketplace.sandbox.eosc-beyond.eu`
2. EOSC Future project, `https://eoscfuture.eu/about/`
3. UPV's Infrastructure Manager, `https://www.grycap.upv.es/im/overview.php`
4. CERN's File Transfer Service, `https://cern.service-now.com/service-portal?id=service_element&name=file-transfer`
5. EOSC Beyond project, `https://www.eosc-beyond.eu/about`

UX Research for HPC Platforms – How to Increase the Adoption of e-Infra Services?

Katarzyna Lechowska-Winiarz, Agnieszka Pułapa, Alicja Świerad

Academic Computer Centre Cyfronet AGH
ul. Nawojki 11, Kraków

k.lechowska-winiarz@cyfronet.pl, a.pulapa@cyfronet.pl,
a.swierad@cyfronet.pl

Keywords: user experience, ux research, hpc, e-infrastructure

1. Introduction

This abstract presents user experience (UX) research findings conducted on the EOSC Marketplace platform. The analysis revealed that complex commands, unintuitive interfaces, and insufficient support hinder access to research infrastructures (RIs). The presented conclusions provide the foundation for recommendations aimed at enhancing platform usability and increasing the accessibility of HPC services for a broader user base.

2. Description of the problem

Research infrastructures are essential for scientific research, yet their growing complexity presents challenges, even for experienced researchers, who may lack advanced IT skills [1]. Platforms providing scientific services are often designed with technically proficient users in mind, unintentionally excluding specialists from other fields. Lowering the entry threshold and equipping users with skills requires a deep understanding of their needs. Tailoring IT tools accordingly will allow a broader audience to fully utilise available resources, maximising their potential for scientific discovery.

3. Related work

Between 2022 and 2024, Cyfronet's Data Processing Laboratory team conducted several UX research studies within the EOSC Marketplace ecosystem, applying UX research methodology presented below (Fig.1). Although the platform does not handle HPC job submissions directly, it plays a crucial role in the RIs ecosystem by enabling scientists and other target users to search for and order services, highly influencing the overall user experience.

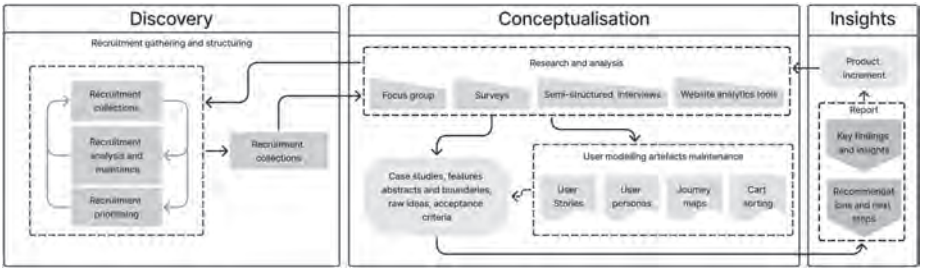

Fig. 1. UX research methodology.

4. Solution of the problem

This presentation will outline the benefits of UX research, and the most common challenges encountered. We will demonstrate how it can increase the accessibility and adoption of scientific services. Our work enabled a thorough analysis of how users from diverse backgrounds search for and utilise resources and how improving platform usability can help researchers from non-technical fields adopt HPC and other advanced digital services more easily.

The DPL team used several widely recognised UX research methods [2], including usability testing, post-questionnaires, and online surveys. In-depth interviews were also carried out with focus groups representing end-users and e-infrastructure service providers, alongside tracking user journeys and conducting behavioral studies using tools such as Google Analytics and Hotjar to assess user interactions.

5. Conclusions

Although user experience studies for e-infrastructure services and tools have not yet gained widespread popularity, the right choice of methods and target groups can be a real game-changer in leveraging the potential of HPC platforms. By addressing usability challenges and improving user experience, we can significantly increase the adoption of HPC services among a broader audience, including scientific, business communities, or governmental bodies.

Acknowledgements. This work has been supported by the European Union's Horizon 2020 and 2021-2027 research and innovation programme.

References

1. Jeremy Cohen, Chris Cantwell, David Moxey, Jeremy Nowell, Peter Austing, Xu Guo, John Darlington, Spencer Sherwin, „ Ensuring an Effective User Experience When Managing and Running Scientific HPC Software", 2015 IEEE 11th International Conference on e-Science, pp.78-87, 2015.
2. Iga Mościchowska, Barbara Rogoś-Turek: Badania jako podstawa projektowania user experience., Wydawnictwo PWN, 2020.

Qommunity: a Library for Community Detection Using Quantum and Classical Methods

Kacper Jurek[1,2], Barbara Wojtarowicz[2], Katarzyna Rycerz[1,2,3], Joan Falcó-Roget[3]

[1] AGH University of Krakow, al. Mickiewicza 30, 30-059 Kraków, Poland
[2] ACC Cyfronet AGH, Nawojki 11, 30-950 Kraków, Poland
[3] Sano Centre for Computational Medicine, Czarnowiejska 36, 30-054 Kraków, Poland

kacper.jurek@cyfronet.pl, bwojtaro@student.agh.edu.pl,
kzajac@agh.edu.pl, j.roget@sanoscience.org

Keywords: community detection, quantum computing, graphs

1. Introduction

Community detection in complex networks is a fundamental problem in network science, with applications in neuroscience, social analysis, and optimization. As networks grow in size and complexity, the number of possible partitions increases exponentially, making exhaustive search impractical. Classical methods, such as modularity optimization and spectral clustering, become inefficient for large-scale networks due to their computational complexity. Quantum computing, with its ability to explore multiple solutions, offers a promising alternative for addressing combinatorial optimization problems like community detection.

2. Description of the problem

There is no library that integrates various community detection methods into a single framework with a unified interface, forcing researchers to rely on multiple separate tools, which complicates experimentation and result comparison. Additionally, quantum methods for community detection are currently limited to binary partitioning, making them impractical for networks with more complex structures. Since many real-world networks contain more than two communities, existing quantum approaches cannot fully capture their structure. Without a method for multi-community detection, quantum solvers remain constrained in their ability to analyze large-scale networks, limiting their practical applicability.

3. Related work

Our work builds on existing quantum and hybrid optimization tools, particularly QHyper, developed by Cyfronet [1]. QHyper provides a foundation for defining optimization problems, including community detection, and supports various solvers. Additionally, our Qommunity library, which includes the hierarchical partitioning method, was used in recent research to compare its performance against other community detection methods, demonstrating its practical applicability [2].

4. Solution of the problem and conclusions

We introduce Qommunity, a library that integrates classical, quantum, and hybrid approaches for community detection, offering a unified interface for various algorithms. It extends QHyper to support quantum optimization and incorporates hierarchical partitioning to enable multi-community detection. The framework uses quantum annealing with D-Wave's Advantage system, enabling quantum methods for network analysis.

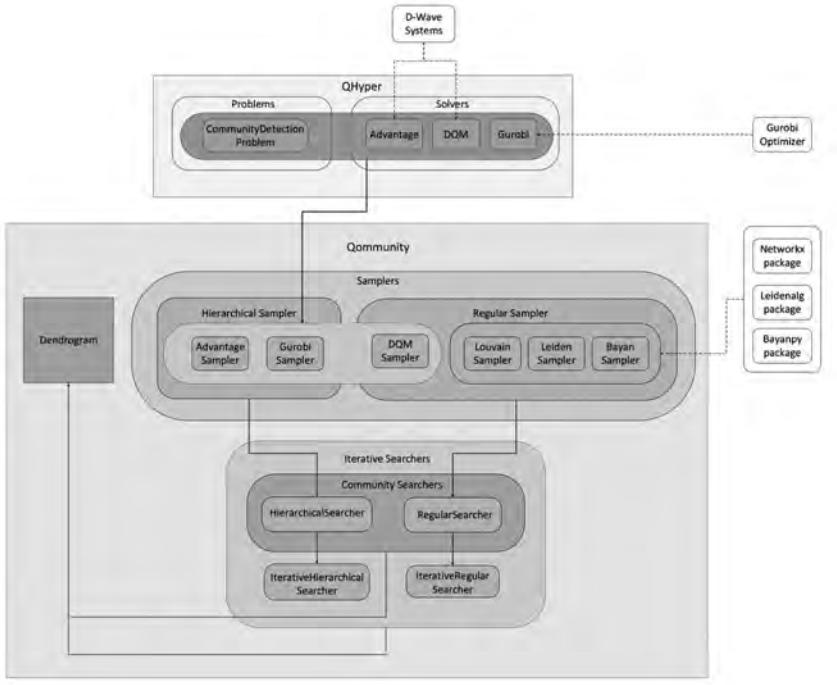

Fig. 1. Qommunity architecture.

A key feature of Qommunity is its ability to provide multiple community detection methods − classical, hybrid, and quantum − within a single framework. It ensures a consistent interface for seamless integration and experimentation while also introducing hierarchical partitioning for algorithms that inherently support only binary division. This expands their usability, enabling the detection of more than two communities in complex networks. By integrating multiple solvers, Qommunity allows users to select the most suitable method − classical, hybrid, or quantum − depending on the specific requirements of their problem.

Acknowledgements. We gratefully acknowledge Polish high-performance computing infrastructure PLGrid (HPC Center: ACK Cyfronet AGH) for providing computer facilities and support within computational grant no. PLG/2024/017717 (B.W.) and grant no. PLG/2024/017911 (K. J.).

References

1. Tomasz Lamża, Justyna Zawalska, Kacper Jurek, Mariusz Sterzel, Katarzyna Rycerz: „QHyper: an integration library for hybrid quantum-classical optimization”, `https://arxiv.org/abs/2409.15926`
2. Joan Falcó-Roget, Kacper Jurek, Barbara Wojtarowicz, Karol Capała, Katarzyna Rycerz: “Modularity maximization and community detection in complex networks through recursive and hierarchical annealing in the D-Wave Advantage quantum processing units”, `https://arxiv.org/abs/2410.07744`
3. Qommunity library repository: `https://github.com/kacper3615/Qommunity`

Designing Graph-Kolmogorov-Arnold Networks for Node Classification with Cartesian Genetic Programming

Maciej Krzywda[1], Chenqing Hua[2,3], Szymon Łukasik[1,4], Amir H. Gandomi[5]

[1] Faculty of Physics and Applied Computer Science, AGH University of Krakow
[2] School of Computer Science, McGill University
[3] Mila-Quebec AI Institute
[4] Systems Research Institute, Polish Academy of Sciences
[5] Faculty of Engineering and IT, University of Technology Sydney

krzywda@agh.edu.pl

Keywords: Graph Neural Network, Graph Kolmogorov Arnold Network ,Kolmogorov Arnold Networks, Neural Architecture Search, Cartesian Genetic Programming, Node Classification

1. Introduction

Neural Architecture Search (NAS) automates the design of neural networks for tasks like classification, segmentation, and regression, eliminating tedious manual configuration. As architectures become more complex, evolutionary optimization–using selection, mutation, and recombination–has proven effective. In particular, Cartesian Genetic Programming (CGP) encodes networks as fixed-size matrices where each cell defines an operator and connections map the data flow. This approach simplifies complex designs and allows dynamic node activation through masking. In our work, we fuse multiple graph convolution layers (GCN, GAT, GIN, GraphSAGE) with a Fourier-transform block, called the Graph Kolmogorov-Arnold Layer, to address node classification. The resulting fixed-size genotype specifies layer types, activation functions, and connections and is optimized via a (1+λ) evolutionary strategy with mutation, automating both architecture and hyperparameter selection.

2. Description of the problem

Optimizing neural network architectures for graph-structured data is challenging due to the vast search space of layer configurations and hyperparameter settings. Manual tuning is labor-intensive and often suboptimal. Our method employs an evolutionary (1 + λ) strategy to automatically evolve architectures that integrate graph convolution layers with a Fourier-based GraphKAN module [5], simultaneously optimizing the network design and training hyperparameters to improve feature extraction and classification performance.

3. Related work

Recent developments in Neural Architecture Search leverage evolutionary algorithms, reinforcement learning, and gradient-based optimization. Several methods [3] have focused on optimizing variants of Graph Convolutional Networks (GCNs) for graph-related tasks. Meanwhile, CGP-based NAS efficiently encodes Convolutional Neural Network architectures using grid representations [4]. Our work sets itself apart by uniquely integrating evolutionary CGP with GraphKAN modules, thereby advancing the automated design of Graph Neural Networks for Node Classification.

4. Solution of the problem

The proposed method implements an evolutionary optimization framework for neural network architectures by integrating graph convolution layers and a Fourier-based GraphKAN

module. The architecture is encoded in a fixed-dimension genotype, where each row specifies the layer type, activation function, and inter-layer connectivity, with an additional mask vector determining active layers. Two primary modules are defined: a graph block that extracts structural information from graph-structured data and a GraphKAN block that employs Fourier transformations. The network is incrementally constructed with fallback mechanisms to ensure functionality even if no layers in a given block are active. Mutation functions introduce stochastic modifications to both the network structure and hyperparameters, including the optimizer, learning rate, and weight decay. The evolutionary process follows a $(1 + \lambda)$ strategy, where a parent network generates multiple offspring through mutations, each of which is individually trained and evaluated. If an offspring outperforms the parent, it replaces the parent for subsequent generations; otherwise, neutral mutations are applied. Performance is assessed using accuracy and the F1 score to guide the iterative optimization.

We use PyTorch and PyTorch Geometric for building and training graph neural networks, and NetworkX for visualizing the architecture. Training is conducted on the Athena cluster at ACC Cyfronet AGH, which offers computing power of over 7.7 PFlops. All the computations were carried out with the mentioned library using 4 CPUs per task. The runtime for a complete simulation on one dataset (covering all generations) ranged from 8645 to 10000 seconds.

5. Conclusions

Our work demonstrates that integrating Cartesian Genetic Programming with evolutionary optimization can effectively automate the design of graph neural network architectures for Node Classification Tasks. Our approach simultaneously evolves network structures and training hyperparameters by fusing diverse graph convolution layers with a Fourier-based GraphKAN module. This method not only alleviates the challenges of manual tuning but also shows promising improvements in node classification performance, paving the way for further advancements in automated architecture search for graph-structured data.

Acknowledgements. The work was supported by statutory tasks of the AGH UST Faculty of Physics and Applied Computer Science within the MEiN grant. The numerical experiment was possible through computing allocation on the Athena system at the Polish high-performance computing infrastructure PLGrid (HPC Center: ACK Cyfronet AGH) under grant no. PLG/2025/018082.

References

1. Miller, J. F. Cartesian genetic programming: its status and future. https://doi.org/10.1007/s10710-019-09360-6
2. Y. Liu, Y. Sun, B. Xue, M. Zhang, G. G. Yen and K. C. Tan, "A Survey on Evolutionary Neural Architecture Search," doi: 10.1109/TNNLS.2021.3100554
3. B. M. Oloulade, J. Gao, J. Chen, T. Lyu and R. Al-Sabri, "Graph neural architecture search: A survey," doi: 10.26599/TST.2021.9010057
4. Krzywda M, Łukasik Sz, Gandomi A. H, "Cartesian Genetic Programming Approach for Designing Convolutional Neural Networks." arXiv preprint arXiv:2410.00129 (2024).
5. GraphKAN-Graph-Kolmogorov-Arnold-Networks implementation: https://github.com/WillHua127/GraphKAN-Graph-Kolmogorov-Arnold-Networks

High-Performance Computing for Event Cameras: DIF Filtering and Graph Convolutional Networks for Object Classification

Marcin Kowalczyk, Kamil Jeziorek, Tomasz Kryjak, Marek Gorgoń

Embedded Vision Systems Group, Department of Automatic Control and Robotics, Faculty of Electrical Engineering, Automatics, Computer Science and Biomedical Engineering AGH, University of Krakow

{kowalczyk, kjeziorek, kryjak, mago}@agh.edu.pl

Keywords: event camera, DVS, CNN, denoising, GCN, SNN, FPGA

1. Introduction

Event cameras are a relatively new vision sensor that capture the change in intensity of light incident on a pixel with microsecond precision, as opposed to an absolute brightness value captured by a frame camera. Their main advantages are their very high temporal resolution, high dynamic range and low latency. This new type of visual information requires the development of techniques to process data as a sparse spatio-temporal point cloud.

Fig. 1. Comparison of a frame from a classic camera and an event frame aggregated over 20 ms.

2. Description of the problem

Our research involved event data filtering and object classification using neural networks. Each of these problems required the processing of large datasets in order to train neural network based solutions or to evaluate proposed algorithms. The requirements of the developed solutions were high throughput and the ability to accelerate them in heterogeneous systems using FPGA resources.

3. Related work

The topic of processing visual event data has been addressed many times in the scientific literature due to its great practical importance. Neural networks for filtering this type of data are presented in [1], while a classical algorithm is presented in [2].

Many approaches to object classification and detection have also been presented in the literature. The vast majority of them are based on neural networks: Convolutional Neural Networks (CNNs) [3], Graph Convolutional Neural Networks (GCNNs) [4] and Spiking Neural Networks (SNNs) [5] are used.

4. Solution of the problem

A modified Distance-based Interpolation with Frequency weights (DIF) algorithm was proposed for event data filtering. The aim was to achieve high filtering efficiency at the highest possible throughput. The solution was based on interpolation of timestamps and event intervals from neighbouring areas of the sensor array. The MATLAB environment was used to design the solution. For the evaluation, however, the C++ language with the Metavision library was used. The programmes were run on the Ares supercomputer to calculate filtering efficiency metrics on large datasets. The necessary test sequences were also generated using the V2E [6] framework on the Athena supercomputer. The intermediate results and data sets were stored on HPC storage at ACK Cyfronet AGH centre.

GCNNs were employed to investigate object classification in event data. The models were developed in Python using the PyTorch and PyTorch Geometric frameworks. The proposed solution utilised lightweight models based on PointNetConv layers. To optimise hyperparameters and adapt the models for implementation on FPGAs, the networks were trained in batches per node, and transfer learning from larger models was applied to enhance their performance. The training process was conducted on the Athena supercomputer, with data stored on the HPC Storage resources at ACK Cyfronet AGH.

5. Conclusions

The research carried out has made it possible to design algorithms with very high efficiency (greater than or comparable to SOTA). In addition, their speed can be significantly increased by using reconfigurable FPGA resources. The design of these algorithms and their evaluation would not have been possible without the use of the computing resources of the ACK Cyfronet AGH centre.

Acknowledgements. This research has been supported by the National Science Centre project no. 2021/41/N/ST6/03915 (first author). The numerical experiment was possible through computing allocation on the Prometheus system at ACC Cyfronet AGH under the grants PLG/2023/016388 and PLG/2023/016897.

References

1. Baldwin, R., et al. “Event probability mask (epm) and event denoising convolutional neural network (edncnn) for neuromorphic cameras.” Proceedings of the IEEE/CVF Conference on Computer Vision and Pattern Recognition. 2020.
2. Xu, Ninghui, et al. “Denoising for dynamic vision sensor based on augmented spatiotemporal correlation.” IEEE Transactions on Circuits and Systems for Video Technology 33.9 (2023): 4812-4824.
3. Perot, Etienne, et al. “Learning to detect objects with a 1 megapixel event camera.” Advances in Neural Information Processing Systems 33 (2020): 16639-16652.
4. Schaefer, Simon, Daniel Gehrig, and Davide Scaramuzza. “Aegnn: Asynchronous event-based graph neural networks.” Proceedings of the IEEE/CVF conference on computer vision and pattern recognition. 2022.
5. Dampfhoffer, Manon, and Thomas Mesquida. “Neuromorphic lip-reading with signed spiking gated recurrent units.” Proceedings of the IEEE/CVF Conference on Computer Vision and Pattern Recognition. 2024.
6. Hu, Yuhuang, Shih-Chii Liu, and Tobi Delbruck. “v2e: From video frames to realistic DVS events.” Proceedings of the IEEE/CVF conference on computer vision and pattern recognition. 2021.

Evaluating Synthetic vs. Real Dynamic Vision Sensor Data for SNN-Based Object Classification

Mustafa Sakhai[1], Kaung Sithu[1], Min Khant Soe Oke[1], Szymon Mazurek[1,2], Maciej Wielgosz[1,2]

[1]AGH University of Krakow, al. Mickiewicza 30, 30-059 Kraków, Poland
[2] ACC Cyfronet AGH, Nawojki 11, 30-950 Kraków, Poland

{msakhai,szmazurek,wielgosz}@agh.edu.pl,
{sithu,oke}@student.agh.edu.pl, s.mazurek@cyfronet.pl

Keywords: Dynamic Vision Sensors, classification, Low-Latency Perception, Spiking Neural Networks

1. Introduction

Real-time perception in autonomous vehicles requires fast, accurate object detection for safe navigation. While RGB cameras offer high spatial resolution, they suffer from latency and high power use. Dynamic Vision Sensors (DVS) capture light changes asynchronously, enabling low--latency detection. Synthetic DVS data provides a cost-effective alternative to physical cameras. This paper compares synthetic and real DVS data with RGB imagery, focusing on detection performance and latency.

2. Description of the problem

Frame-based cameras can cause latency in dynamic environments, limiting real-time detection for robotics and autonomous vehicles. To evaluate synthetic DVS data, JAAD RGB videos were converted into event-based formats using the v2e tool, and an SNN model's performance was tested. The DMT22 dataset, containing real DVS and RGB recordings, enabled direct comparisons between synthetic DVS, real DVS, and RGB, validating synthetic event-based vision as a practical alternative to physical DVS sensors.

3. Related work

Recent developments in event-based vision have underscored the potential of Dynamic Vision Sensors (DVS) for low-latency applications. Sakhai et al. [1] showcased the effectiveness of Spiking Neural Networks (SNNs) in real-time pedestrian classification using DVS even under adverse weather conditions. Gallego et al. [2] provided a comprehensive survey highlighting the latency reduction and computational benefits of DVS. Mueggler et al. [3] established a standardized benchmark for event-based visual odometry and SLAM. In addition, influential data sets such as JAAD [4] and DMT22 [5] have played a crucial role in the advancement of event-based models. Despite these advances, creating high-quality synthetic DVS data that faithfully mimic real-world events remains a challenge, particularly for autonomous driving and robotics.

4. Solution of the problem

Dataset Evaluation: To evaluate the feasibility of synthetic DVS data, we converted RGB videos from the JAAD dataset into event-based formats using the v2e tool. The DMT22 dataset, which includes both RGB and real DVS recordings, was employed as a benchmark for assessing synthetic DVS quality. Synthetic DVS videos generated from DMT22 RGB data were configured to match real DVS specifications (240 × 180 pixels, 30 fps, DAVIS APS format), enabling a direct **quantitative comparison** between synthetic and real DVS data.

Algorithm: We implemented a Spiking Neural Network (SNN) model for **low-latency object detection**, utilizing event-driven computations to enhance efficiency.

Software Tools: The conversion of RGB videos to synthetic AEDAT event files was performed using v2e and jAER, while PyTorch was used to train and evaluate the SNN model.

Compute and Storage Resources: Experiments were carried out on NVIDIA A100 GPUs within the PLGrid infrastructure, optimizing event-driven processing. Additionally, metric evaluations were conducted using **Cyfronet's Athena**, ensuring robust computational support.

5. Results

We compared the performance of synthetic and real DVS data against traditional RGB imagery by evaluating key metrics and the performance of our SNN models. DVS provides 25μs temporal precision, while RGB is 33ms, a lower temporal precision value means more accurate alignment of events over time. The summarized results for DVS are presented in the following table.

Tab.1. Overview of key results.

	Polarity Accuracy	Event Density	MSE	SSIM
DVS	74%	2,797	0.0012	0.4625
SNN Object Detection Performance in Bad Weather (JAAD Dataset)				
Model	Modality	AUROC	F1-Score	
PT ResNet18	DVS	0.5336	85.43	
SPS R18T	DVS	0.5720	86.37	

6. Conclusions

This study demonstrates the comparative analysis between real and synthetic DVS data and validates the feasibility of generating high-quality synthetic event-based datasets for training SNN models.

Acknowledgements. This research was supported by the PLGrid Infrastructure under grant ID: PLG/2024/017775 and plgdyplomanci6. We would also like to thank Cyfronet for providing essential support, especially through the use of Cyfronet's Athena for compute and storage resource management.

References

1. Sakhai, M. and Mazurek, S. and Caputa, J. and Argasiński, J. K. and Wielgosz, M.: "Spiking Neural Networks for Real-Time Pedestrian Street-Crossing Detection Using Dynamic Vision Sensors in Simulated Adverse Weather Conditions", Electronics, vol. 13, p. 4280, 2024.
2. Gallego, G. and Delbruck, T. and Orchard, G. and Bartolozzi, C. and Taba, B. and Censi, A. and Leutenegger, S. and Davison, A. J. and Conradt, J. K. and Daniilidis, K. and Scaramuzza, D.: „ Event-Based Vision: A Survey", IEEE Transactions on Pattern Analysis and Machine Intelligence, vol. 44, no. 1, pp. 154–180, 2020.
3. E. Mueggler, H. Rebecq, G. Gallego, T. Delbruck, and D. Scaramuzza: "The Event-Camera Dataset and Simulator: Event-Based Data for Pose Estimation, Visual Odometry, and SLAM", International Journal of Robotics Research, vol. 36, no. 2, pp. 142–149, 2017.
4. Rasouli, A. and Kotseruba, I. and Tsotsos, J. K.: "JAAD: A Benchmark for Studying Pedestrian Behavior in Traffic Scenes", in Proceedings of IEEE International Conference on Computer Vision Workshops, 2017, pp. 301–309.
5. L. Duarte and P. Neto: "Dmt22 dataset: A benchmark for dynamic vision sensor applications,", Zenodo, 2023.

Calculation of Graph Isomorphisms in the Context of Processing of Big Structured Data

Igor Wojnicki[1], Aleksander Suchorab[2], Andrzej Bielecki[1], Marzena Bielecka[3]

[1] AGH University of Krakow, Faculty of Electrical Engineering, Automatics, Computer Science and Biomedical Engineering, Mickiewicza 30, 30-059 Kraków, Poland.
[2] AGH University of Krakow, Student Scientific Association AI LAB, , Faculty of Electrical Engineering, Automatics, Computer Science and Biomedical Engineering, Mickiewicza 30, 30-059 Kraków, Poland.
[3] AGH University of Krakow, Faculty of Geology, Geophysics and Environmental Protection, Mickiewicza 30, 30-059 Kraków, Poland.

{wojnicki,bielecki,bielecka}@agh.edu.pl, aleksander.suchorab@gmail.com

Keywords: structural information, graph isomorphism, structural data, graph embedding, machine learning

1. Introduction

Machine learning is associated with processing large data sets. If such data is structured, it often takes the form of a graph with a significant number of vertices, not rarely exceeding several hundred thousand of edges. In the context of machine learning, there is a challenge of calculating the amount of information (entropy) of such structured graph structures [1,2,3] to evaluate their suitability for the learning process. It is especially significant if there is a need to transform a data set into yet another form to achieve dimensionality reduction. In such a case it is important to provide an estimation if such a transformation could be successful or how much of the information would be lost during this process. A classic example of this type of task is the embedding problem, related to algorithms for transforming a graph structure into a vector form [4].

2. Description of the problem

The research of structural information in graphs using node-balls requires an effective way of checking if any two node-balls are isomorphic. While graph isomorphism is well researched, checking node-ball isomorphism requires computation of multiple graph isomorphisms, which was found to be difficult on large datasets due to computation complexity. The goal of this research is to design a node-ball isomorphism algorithm aware of the multilayered structure of node-balls, which would let reduce the computation time.

3. Related work

The problem of entropy in graphs is studied since Sixties of the twentieth century [3]. One of the authors introduced the concept of structural information that refers directly to the problem of information in graphs [1,2]. There are many approaches to represent structural information as a vector with use of graph embeddings [5]. They result both in fixed dimensionality and dimensionality reduction compared with the original graph structure. An alternative approach is to use Artificial Neural Networks in a form of Graph Neural Networks [6], which subsequently can be thought how to embed multi-dimensional data. There are several graph benchmarks available in the form of ready-to-use datasets [7], which were subsequently used by the authors.

4. Solution of the problem

The node-ball isomorphism algorithm developed during this research first expands the neighborhoods of both starting nodes and groups them by the iteration they occurred in and by the

in-degrees and out-degrees of each node. Then, it uses an individualisation-refinement approach on the already grouped nodes, similar to many graph isomorphism algorithms, to check for existence of an isomorphism. The algorithm was implemented in C++, using MPI for parallelization and *tbbmalloc* for efficient memory allocation. In order to test the algorithm, large datasets (40k+ vertices) from the *PyKeen* repository [7] were used.

The experiments were conducted with use of ACK Cyfronet Ares, PLGrid grant number PLG/2024/017406. 46 879 hours of CPU time have been consumed, which exhausted the grant quota.

5. Conclusions

Suitability of the proposed algorithm, as well as its computational correctness have been confirmed. Several versions of the algorithm have been proposed, implemented and tested. They offer reduced computational complexity for real-world examples, which would not be feasible without the PLGrid infrastructure.

Acknowledgements. We gratefully acknowledge Polish high-performance computing infrastructure PLGrid (HPC Center: ACK Cyfronet AGH) for providing computer facilities and support within computational grant no. PLG/2024/017406.

References

1. Bielecki A., Schmittel M., The information encoded in structures: Theory and Applications to molecular cybernetics, Foundations of Science, vol.27, 1327-1345, 2022.
2. Bielecki A., Stocki R., The concept of structural information and possible applications, Philosophical Problems in Science, vol.75, 157-183.
3. Dehmer M., Mowshowitz A., A history of graph entropy measures, Information Sciences, vol.181, 57-78, 2011.
4. Wang, Q., Mao, Z., Wang, B., Guo, L.: Knowledge Graph Embedding: A Survey of Approaches and Applications. IEEE Transactions on Knowledge and Data Engineering 29(12), 2724–2743 (Dec 2017).
5. Goyal, P., Huang, D., Goswami, A., Chhetri, S. R., Canedo, A., Ferrara, E.: Benchmarks for Graph Embedding Evaluation (Aug 2019). https://doi.org/10.48550/arXiv.1908.06543
6. Zhou J., Cui G., Hu S., Zhang Z., Yang C., Liu Z. (2020). Graph Neural Networks: A Review of Methods and Applications, AI Open, Elsevier.
7. Ali, M., Berrendorf, M., Hoyt, C. T., Vermue, L., Sharifzadeh, S., Tresp, V., Lehmann, J., PyKEEN 1.0: A Python Library for Training and Evaluating Knowledge Graph Embeddings, Journal of Machine Learning Research, Vol. 22, 2021.

Modeling Texture Evolution in Metals with CA Model

Bartosz Sułkowski

Department of Materials Science and Non-Ferrous Metals Engineering, Faculty of Non-Ferrous Metals, AGH University of Krakow, 30 Mickiewicza Av., Kraków 30-059, Poland

bartosz.sulkowski@agh.edu.pl

Keywords: modeling, cellular automaton, visco-plastic

1. Introduction

Evolution of structure and texture during processing of metals have a great effect on the mechanical properties of final products. Determining these properties requires a lot of experimental work and predicting the final properties is within the area of interest of scientists, producers and customers. To reduce time consuming and expensive experiments of every combination of chemical composition, temperature, strain rate and deformation; modeling and simulations are very helpful. However, there are many models describing evolution of structure and texture in deformed metals. The models are based on different assumptions and are very sensitive on the starting conditions leading to results far from the experiments. Among many, one of the best models and widely used with huge success is visco-plastic self consistent model (vpsc). However, the model is adequate to cold deformation only, where dynamic recrystallization mechanisms can be omitted. For better convergence with experiments the vpsc model can be combined together with the cellular automaton model (CA). The vpsc model is able to predict the deformation texture components while the CA model can trace the texture softening due to the activation of recrystallization processes. The model vpsc+CA was implemented in C++ with the use of the Message Passing Interface (MPI) library to increase the scalability of the calculations.

2. Description of the problem

Evolution of the texture in deformed metals predicted with the vpsc model is based on many different deformation modes such like slip systems and twinning [1-4]. However, at elevated temperatures, in hot deformed metals may appear new components which are the results of recrystallization [5-7]. Thus, the recrystallization mechanisms must be taken into account in the new model. This is necessary to be correct with the experimental results. To enhance the ability of predicting proper texture components in deformed metals at elevated temperatures by the vpsc model the cellular automation model may be woven in. The CA model allows to calculate the energy state of the modeled structure to predict grain nucleation and grain growth.

3. Related work

In the Zecevic model a combination of the vpsc formulation and intragranular orientation gradients and strain energy fields are introduced [8]. The vpsc formulation describes the evolution of the main texture components which come from the slip or twinning. In the prediction of the recrystallization components a driving force for grain boundary migration is based on the total dislocation density stored in the grains. When there is a gradient in dislocation density the driving force moves grain boundary toward grains with more dislocations. This mechanism depicts grain growth. However, when dislocation density reaches certain high level, a new grain nuclei is formed, and this represents recrystallization. The Zacevic model is based on the probability of dislocation density, but for the better simulation results, comparable with the experiments, the distinction between the statistically stored (SSD) and geometrically necessary dislocations (GND) is necessary.

4. Solution of the problem

The combination of the vpsc and CA model is presented in the current study. The vpsc model is responsible for prediction the deformation texture components while with the use of the CA model the recrystallization components are obtained. To achieve good, comparable with the experiments results, the structure was divided into grains represented by orientation, position and the total dislocation density. The orientation and dislocation density evolution are calculated based on the vpsc model formulations. For the CA procedure, each grain is divided into a certain number of subgrains whose orientation and dislocation density differ a little from the parent grain. In the subgrains, the distinction between SSD and GND is achieved based on the local misorientation. The differences of dislocations density in the subgrains allow to determine the driving force for the grain nucleation or grain boundary migration. The calculations formulas in the CA procedure contains the parameters describing the recrystallization mechanisms.

5. Conclusions

The introduction the CA procedure into vpsc model allows for better texture prediction. However, the combined model needs much more computational power. Using parallel computing methods such like openMP and MPI significantly reduces simulations time.

Acknowledgements. We gratefully acknowledge Polish high-performance computing infrastructure PLGrid (HPC Centers: ACK Cyfronet AGH, WCSS, CI TASK) for providing computer facilities and support within computational grant no. PLG/2023/016844.

References

1. R. A. Lebensohn, C. N. Tomé, A self-consistent anisotropic approach for the simulation of plastic deformation and texture development of polycrystals: application to zirconium alloys, Acta Metall. Mater. 41 (1993) 2611–2624.
2. P. Van Houtte, A comprehensive mathematical formulation of an extended Taylor-Bishop-Hill model featuring relaxed constraints, the Renouard-Wintenberger theory and a strain rate sensitivity model, Textures Microstruct. 8 & 9 (1988) 313–350.
3. H. R. Piehler, Crystal-Plasticity Fundamentals, ASM Handbook Volume 22A: Fundamentals of Modeling for Metals Processing (#05215G), 2009.
4. A. Chapuis, Q. Liu, Modeling strain rate sensitivity and high temperature deformation of mg-3Al-1Zn alloy, J. Magnes. Alloys 7 (2019) 433–443, https://doi.org/10.1016/j.jma.2019.04.004
5. S. R. Agnew, M. H. Yoo, C. N. Tome, Application of texture simulation to understanding mechanical behavior of mg and solid solution alloys containing Li or Y, Acta Mater. 49 (2001) 4277–4289.
6. A. Chapuis, Z. Wang, Q. Liu, Influence of material parameters on modeling plastic deformation of mg alloys, Mater. Sci. Eng. A 655 (2016) 244–250.
7. B. Sułkowski, R. Chulist, Materials Characterization 201 (2023) 112968.
8. M. Zecevic, R. A. Lebensohn, R. J. McCabe, M. Knezevic, Acta Mater. 164 (2019) 530–546.

Fast Simulation of the FoCal-H Detector with Machine Learning

Łukasz Dubiel, Piotr Ludynia, Emilia Majerz

AGH University of Krakow

{lukdubiel, piotrztych}@student.agh.edu.pl, majerz@agh.edu.pl

Keywords: high energy physics, fast simulation, generative neural networks, calorimeter simulation, focal

1. Introduction

The currently utilised approach to calorimeter simulation at CERN is based on Monte Carlo computations. Such a method provides accurate results, yet requires substantial computational resources and involves many steps of the algorithm, thus making it time-consuming. With the recent developments in the Machine Learning (ML) field, researchers seek ML-based methods to speed up the simulation. It is crucial for effective preparations for Large Hadron Collider (LHC) runs.

2. Description of the problem

Here, we address the simulation of the ALICE experiment's forward hadronic calorimeter (FoCal-H). We verify the effectiveness of cutting-edge generative neural networks for producing 2-dimensional showers. The dataset was created using the GEANT4 software and comprises vectors containing particle features, treated in this study as input data, and matrices representing the energy detected by the FoCal-H in response to the incoming particles, which we simulate with neural networks.

3. Related work

Numerous studies addressed the topic of calorimeter simulation. They mainly concentrate on the use of GANs [1-3], VAEs [1,2,4], NFs [2,5], and diffusion models [1,2,6]. Each framework features a tradeoff between the simulation fidelity and speed [1,2]; NFs and diffusion excel in the former, while GANs and VAEs - in the latter.

4. Solution of the problem

We started with exploring GAN, VAE and diffusion architectures. In the case of diffusions, we investigated the DDIM model with a cross-attention block with just 50 inference steps, which showed promising effectiveness in terms of simulation fidelity in single- and multi-shower simulations. An alternative approach with VAEs generated blurred results, yet we were able to approximate the locations of particle shower centres well. GANs allowed for obtaining encouraging results regarding shower positions and radii, and are especially worth investigating as one of the fastest frameworks. We show example results simulated with a GAN in Fig. 1. Throughout the experiments, we used mainly TensorFlow, PyTorch, JAX, NumPy, scikit-learn and Uproot libraries, and the Weights & Biases platform. All computations were performed on a single NVIDIA A100 GPU available on the Athena cluster.

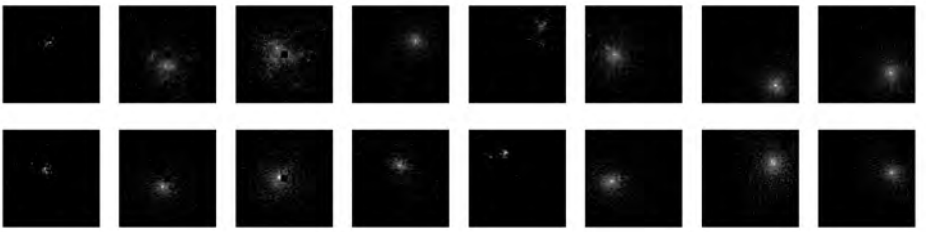

Fig. 1. Example simulations of the FoCal-H detector generated with a GAN. Top: reference, bottom: generated.

5. Conclusions

We investigated the use of several deep-learning generation methods for the task of fast simulation of the FoCal-H detector. We observed promising results with GAN and diffusion models, and want to focus on them in further experiments.

Acknowledgements. This work is co-financed and in part supported by the Ministry of Science and Higher Education (Agreement Nr 2023/WK/07) by the program entitled "PMW" and by the Ministry funds assigned to AGH University in Krakow. The numerical experiment was possible through computing allocation on the Athena system at ACC Cyfronet AGH under the grant PLG/2024/017264.

References

1. M. Wojnar, E. Majerz, and W. Dzwinel, "Fast Simulation of the Zero Degree Calorimeter Responses with Generative Neural Networks," Computing and Software for Big Science, vol. 9, no. 1, pp. 1–18, Jan. 2025, doi: 10.1007/s41781-025-00130-x
2. C. Krause et al., "CaloChallenge 2022: A Community Challenge for Fast Calorimeter Simulation," arXiv.org. [Online]. Available: https://arxiv.org/abs/2410.21611
3. M. F. Giannelli and R. Zhang, "CaloShowerGAN, a generative adversarial network model for fast calorimeter shower simulation," The European Physical Journal Plus, vol. 139, no. 7, p. 597, 0 2024, doi: 10.1140/epjp/s13360-024-05397-4
4. K. Deja, J. Dubinski, P. Nowak, S. Wenzel, P. Spurek, and T. Trzcinski, "End-to-End Sinkhorn Autoencoder With Noise Generator," IEEE Access, vol. 9, pp. 7211–7219, 2021, doi: 10.1109/access.2020.3048622
5. T. Buss, F. Gaede, G. Kasieczka, C. Krause, and D. Shih, "Convolutional L2LFlows: generating accurate showers in highly granular calorimeters using convolutional normalizing flows," Journal of Instrumentation, vol. 19, no. 09, p. P09003, 0 2024, doi: 10.1088/1748-0221/19/09/P09003
6. O. Amram and K. Pedro, "Denoising diffusion models with geometry adaptation for high fidelity calorimeter simulation," Physical Review D, vol. 108, Oct. 2023, doi: 10.1103/PhysRevD.108.072014

Self-Gravity, Perturbations, and Magnetic Fields in Gamma-Ray Burst Progenitors

Piotr Płonka[1], Agnieszka Janiuk[2]

[1] Warsaw University Observatory, Al. Ujazdowskie 4, 00-478 Warsaw, Poland
[2] Center for Theoretical Physics, Al. Lotników 32/46, 02-668 Warsaw, Poland

p.plonka@student.uw.edu.pl, agnes@cft.edu.pl

Keywords: gamma-ray bursts, computational astrophysics, numerical relativity, relativistic magnetohydrodynamics, black holes

1. Introduction

Gamma-ray bursts are among the most energetic phenomena in the Universe, releasing more energy in just a few seconds than the Sun does over its entire lifetime. Long gamma-ray bursts occur when massive stars collapse into black holes, with their outer layers accreting onto the central object. This study examines how the self-gravity of the stellar envelope affects the structure of the accretion disk, the accretion rate, and the evolution of a black hole during extreme astrophysical events.

2. Description of the problem

Within the collapsar model, we examine the influence of self-gravity using detailed magnetohydrodynamics simulations to study the interaction between plasma and magnetic fields within a general relativistic framework.

3. Related work

Previous 2D simulations [1] demonstrated that the self-gravitating stellar envelope influences black hole spin evolution and mass accretion. In this study, we extend these findings by performing 3D simulations and analyzing the impact of self-gravity in the collapsar model with three different magnetic field configurations.

4. Solution of the problem

We conducted twelve 3D simulations on a 256 × 128 × 64 grid, equally divided between self-gravitating and non-self-gravitating cases (six simulations each). The simulations used a modified version of the GR MHD code HARM [2], which implements a conservative shock--capturing scheme with the HLLE method—a Riemann solver—for flux computations. At its core, HARM reconstructs the primitive variables (density, velocity, internal energy, and magnetic field) from the conservative values using the Newton-Raphson method. Furthermore, the simulations incorporate the dynamical Kerr metric to model spacetime and track the evolution of the black hole's mass and angular momentum [3].

5. Conclusions

Self-gravity plays a crucial role in collapsar dynamics by stabilizing the stellar envelope and influencing black hole evolution. Our results from 3D simulations are consistent with previous 2D studies and reveal additional details about the effects of self-gravity in extreme astrophysical conditions.

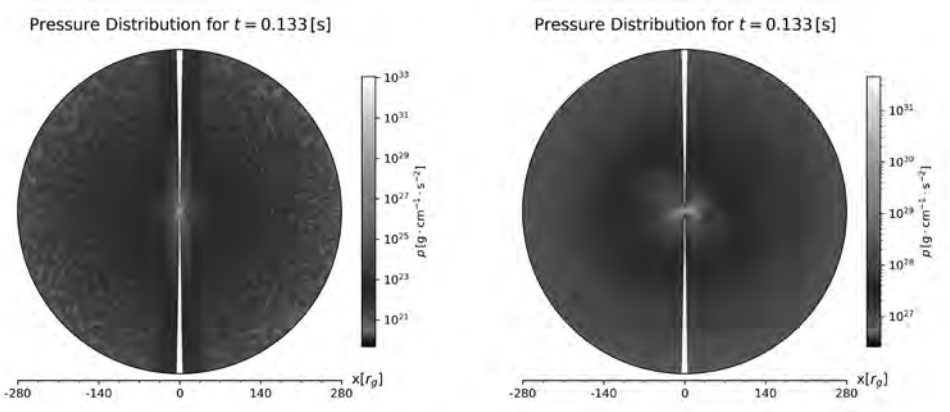

Fig. 1. Pressure distribution in collapsars: slices along the black hole's axis comparing non-self-gravitating (right) and self-gravitating (left) cases, with identical initial conditions.

Acknowledgements. We gratefully acknowledge the Polish high-performance computing infrastructure PLGrid (HPC Center: ACK Cyfronet AGH) for providing the computational facilities and support under computational grant no. PLG/2024/017013.

References

1. A. Janiuk, N. Shahamat Dehsorkh, and D. L. Król. Self-gravitating collapsing star and black hole spin-up in long gamma ray bursts. Astronomy & Astrophysics, 677:A19, Sept. 2023.
2. C. F. Gammie, J. C. McKinney, and G. Tóth. HARM: A Numerical Scheme for General Relativistic Magnetohydrodynamics. The Astrophysical Journal, 589(1):444–457, May 2003.
3. A. Janiuk, P. Sukova, and I. Palit. Accretion in a Dynamical Spacetime and the Spinning Up of the Black Hole in the Gamma-Ray Burst Central Engine. The Astrophysical Journal, 868(1):68, Nov. 2018.

Mildly Relativistic Shocks at High Magnetization Using PIC Simulations

Gabriel Torralba Paz[1], Masahiro Hoshino[2], Takanobu Amano[2], Shuichi Matsukiyo[3], Jacek Niemiec[1]

[1] Institute of Nuclear Physics Polish Academy of Sciences, Krakow, 31-342 Poland
[2] University of Tokyo, Tokyo, 113-8654 Japan
[3] Kyushu University, Fukuoka, 819-0395 Japan

gtorralba@ifj.edu.pl

Keywords: cosmic plasma, astrophysical jets, shocks, PIC simulations, particle acceleration

1. Introduction

Collisionless plasma shocks are believed to be the primary sources of particle acceleration responsible for the X-ray and γ-ray emissions of astrophysical objects, as well as the cosmic rays detected on Earth. Understanding particle acceleration at these shocks requires computational simulations to explore the underlying mechanisms. In particular, Particle-In-Cell (PIC) simulations provide valuable insights into the small-scale processes governing collisionless shocks. This abstract presents recent PIC simulation results of mildly relativistic shocks in a highly magnetized medium, with applications to Active Galactic Nuclei and microquasar jets.

2. Description of the problem

Ultra-relativistic shocks inherently exhibit quasi-perpendicular superluminal conditions. Mildly relativistic shocks, however, present a broad range of obliquities, allowing for subluminal configurations that enable particle reflection off the shock. This, in turn, opens the door to previously unexplored yet potentially efficient acceleration mechanisms.

3. Related work

Ultra-relativistic shocks generate electromagnetic precursor waves through the synchrotron maser instability (SMI) and efficiently accelerate electrons via wakefield acceleration (WFA) [1]. In the mildly relativistic regime, however, WFA is not efficient [2]. Recently, mildly relativistic shocks were studied in the low magnetization regime [3] showing efficient electron acceleration. Nevertheless, the regime of high magnetisation provides new and efficient mechanisms for both ion and electron acceleration as it is shown in this abstract.

4. Solution of the problem

We perform a 2D Particle-In-Cell (PIC) simulation to model an oblique, mildly relativistic shock in a highly magnetized medium. The shock has a Lorentz factor of , with upstream magnetization, defined as the squared ratio of the cyclotron frequency to the plasma frequency and an obliquity of , defined as the angle between the upstream magnetic field and shock velocity. Using the fully relativistic parallelized PIC code THATMPI, the simulation runs on the Ares cluster at ACC Cyfronet AGH with 1440 processes across 30 nodes, each consisting of 2 Intel Xeon Platinum 8268 CPUs. The simulation took 121 hours and generated 6 TB of data.

The simulation reveals an unusual shock transition characterized by strong soliton waves, each associated to significant electrostatic potential jumps. Figure 1 (top) shows the electrosta-

tic potential and normalized ion density across the shock, while the electron phase-space plot (bottom) demonstrates electron trapping within the potential peaks of the top panel, leading to extremely high energies. As described in [4], sufficiently strong magnetosonic waves can reflect and trap electrons, causing a continuous acceleration while the electrons oscillate within the electrostatic peak. In our highly magnetized, mildly relativistic shock, this mechanism proves significantly more effective than the non-relativistic case shown in [4], enabling the production of very high energy electrons and ions.

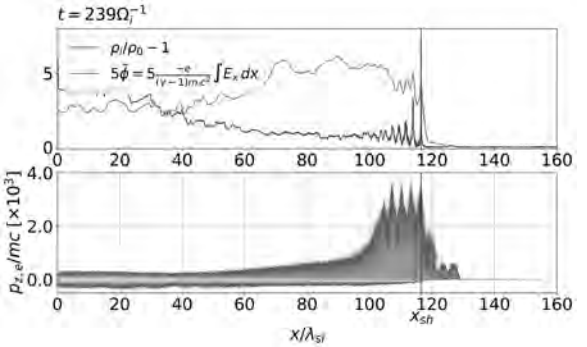

Fig. 1. Top: Normalized ion density and electrostatic potential profiles along the shock propagation direction at time. Bottom: z-component of the electron normalised momentum.

5. Conclusions

By using PIC simulations to model a highly magnetised, mildly relativistic shock in an oblique configuration of the magnetic field, we observe significant electron and ion acceleration. Electrons become trapped by the electrostatic potential generated by the soliton waves at the shock transition and are further accelerated by the transverse electrostatic field. Over multiple acceleration cycles, electrons gain ultra-relativistic energies. This intense acceleration could potentially explain the production of energetic particles responsible for high-energy emissions observed in AGN hotspots or the jets of microquasars.

Acknowledgements. This work has been supported by Narodowe Centrum Nauki through the project 2019/33/B/ST9/02569. This research was supported by PLGrid Infrastructure. We gratefully acknowledge Polish high-performance computing infrastructure PLGrid (HPC Center: ACK Cyfronet AGH, Kraków, Poland) for providing computer facilities and support within computational grant no. PLG/2023/016861 and for awarding this project access to the LUMI supercomputer, owned by the EuroHPC Joint Undertaking, hosted by CSC (Finland) and the LUMI consortium through PLL/2024/06/017077. This research also used computational resources from HPCI (Tokyo, Japan) System Research Project (Project ID: hp240019).

References

1. M. Hoshino: “Wakefield Acceleration by Radiation Pressure in Relativistic Shock Waves” in ApJ, 2008, 672(2), pp. 940-56.
2. A. Ligorini, et al.: “Mildly relativistic magnetized shocks in electron-ion plasmas - II. Particle acceleration and heating” in MNRAS, 2021, 502, pp. 5065-74.
3. P. Crumley, et al.: “Kinetic simulations of mildly relativistic shocks - I. Particle acceleration in high Mach number shocks” in MNRAS, 2019, 485, pp. 5105-19.
4. N. Bessho and Y. Ohsawa: “Electron acceleration and trapping by an oblique shock wave” in Phys. Plasmas, 2002, 9(3), pp. 979-86.

Modelling High Energy Fermi Gamma-Ray Bursts Using GRMHD Simulations

Joseph Saji[1], Shubham Bhardwaj[2], Maria Giovanna Dainotti[2], Agnieszka Janiuk[1]

[1] Center for Theoretical Physics, Polish Academy of Sciences, Al. Lotnikow 32/46, 02-668 Warsaw
[2] Division of Science, National Astronomical Observatory of Japan, Mitaka, Tokyo 181-8588, Japan

jsaji@cft.edu.pl, shubham.bhardwaj@grad.nao.ac.jp,
maria.dainotti@nao.ac.jp, agnieszka.janiuk@cft.edu.pl

Keywords: computational astrophysics, numerical relativity, magnetohydrodynamics (MHD)

1. Introduction

Gamma-ray bursts (GRBs) are the most energetic explosions in the universe, originating from collapsing massive stars or neutron star (NS) mergers. Despite decades of observations, the physics of GRB jets remains poorly understood. Multi-wavelength observations reveal key emission processes, while General relativistic magnetohydrodynamic (GRMHD) simulations model jet dynamics. Combining both approaches helps uncover the underlying physics.

2. Description of the problem

A major challenge in GRB studies is reproducing observed properties, such as jet energy, structure, opening angles, Lorentz factor, & variability, through numerical modelling. GRB090510 [1], one of the brightest short GRB observed by the Fermi gamma-ray telescope exhibits an isotropic energy of 9.97×10^{52} ergs, a 10.04° opening angle, and a 4.9 ms minimum variability timescale (MTS). We use 2D & 3D GRMHD simulations to precisely simulate observed properties of GRB090510.

3. Related work

The formation and dynamics of GRB jets have been extensively studied. References [2] & [3] have conducted 3D simulations to explore jet evolution. [3] also investigated how different initial conditions in the NS merger environment influence the resulting observational signatures.

4. Solution of the problem

We have performed GRMHD simulations of accretion flow around a Kerr black hole (BH) using the code HARM [4,5], a finite volume, shock-capturing scheme to solve the hyperbolic system of partial differential equations in their conservative form. We modelled accretion disk mass ranging from $\sim10^{-3}$ - 10^{-1} solar mass. We tried a range of magnetic field strengths, BH spins, and other initial parameters. For a few models, we have also implemented an expanding dynamic ejecta to study the effect of pre-merger mass ejecta on jet dynamics. We found three models that produce energy, luminosity, jet opening angle, and MTS comparable to GRB090510 within 1-sigma confidence. Different models also create a wide range of jet structures, different orders of energy ranges and opening angles.

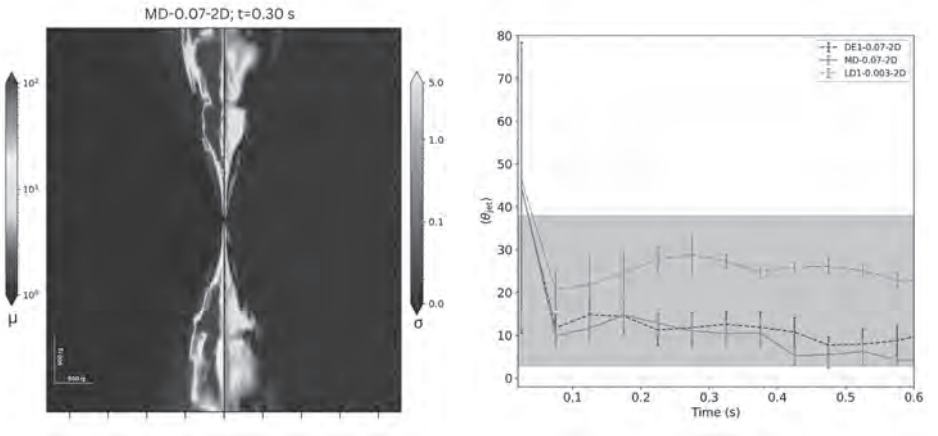

Fig. 1. Left Panel: Jet structure characterised by jet energetics parameter (μ) and jet magnetisation parameter (σ). Right Panel: Opening angle evolution over time. Models DE1 & MD are chosen to represent GRB090510 properties.

5. Conclusions

1. Through GRMHD simulations, we developed numerical models that explain key jet properties of GRB090510, such as energy, opening angle, and variability.
2. By exploring a broader range of models, we provide insights into the dynamics and structure of short GRB jets in general.

Acknowledgements. This work was supported by the grant 2019/35/B/ST9/04000 from the Polish National Science Center. The numerical experiment was possible through computing allocation on the Prometheus system at ACC Cyfronet AGH under the grant PLG/2024/017347.

References

1. M. Ackermann et al, “Fermi Observations Of GRB 090510: A Short–Hard Gamma-Ray Burst with An Additional, Hard Power-Law Component From 10 Kev To Gev Energies” 2010 ApJ 716 1178.
2. Bestin James et al, “Modeling the Gamma-Ray Burst Jet Properties with 3D General Relativistic Simulations of Magnetically Arrested Accretion Flows”, 2022 ApJ 935 176.
3. Ore Gottlieb et al, “On the Jet–Ejecta Interaction in 3D GRMHD Simulations of a Binary Neutron Star Merger Aftermath” 2022 ApJL 933 L2.
4. C. Gammie, McKinney, J. C., & Tóth, G. “HARM: A Numerical Scheme for General Relativistic Magnetohydrodynamics”, 2003 ApJ 589 444 .
5. K. Sapountzis, K. and A. Janiuk, “The MRI Imprint on the Short-GRB Jets”, 2019 ApJ 873 12.

PIC Simulations of Particle Acceleration at Astrophysical Shocks: Study of the Parameter Reduction Effects

Oleh Kobzar, Gabriel Krężel

Astronomical Observatory, Jagiellonian University, ul. Orla 171, 30-244 Kraków, Poland

metho638.krezel@student.uj.edu.pl, oleh.kobzar@uj.edu.pl

Keywords: shock waves, particle acceleration, magnetic waves, PIC simulations

1. Introduction

Acceleration of particles is one of the cornerstone problems in astrophysics. Shock waves in cosmic plasmas are generally considered as most appropriate candidates for the role of particle accelerators. They can be found at wide variety of astrophysical objects, up to Mpc-scale shocks in galaxy clusters. Because of strong nonlinearity, possibilities to study such objects with analytical methods are limited. Therefore numerical methods, such as kinetic Particle-In-Cell (PIC) simulations are widely applied for this purpose.

2. Particle-In-Cell simulations of astrophysical shocks

PIC-simulations is a first-principle method for collisionless plasma, which solves Maxwell's equations for EM-fields on a spatial grid and follows the motion of individual particles with finite time steps. It requires high-performance computing with thousands of CPUs and up to tens of TB of RAM. To fit into the available resources, simulations are often carried out with reduced physical parameters, such as ion-to-electron mass ratio. The obtained results thus require an extrapolation and proper interpretation, which is not always obvious.

3. Related work

In our resent research we modeled the electron acceleration processes at rippled low-Mach--number shocks in galaxy clusters [1]. The ion-to-electron mass ratio was reduced to 100, while realistic one is 1836. This could change the interaction level between electronic and ionic processes, finally affecting the electron acceleration efficiency.

4. Simulation setup and results

Like in the previous study [1], in the current numerical experiment we use the advanced MPI-based parallel relativistic code TRISTAN [2], rewritten in FORTRAN90 and modified to use the HDF5 file format libraries and improved algorithm of the particle sorting [3]. All simulations were performed in so called 2D-3V setup, where particles are positioned only with 2 spatial coordinates, but all 3 components are treated for their velocities and fields.

We performed series of the large-scale simulations with the same set of physical parameters as in [1], appropriate for shock waves in the galaxy clusters, but with set of different mass ratios: 50, 100, 200, 400. Other parameters of these simulations are listed in Table 1. In each case we followed the time evolution of the electron energies under their energization through shock drift acceleration (SDA) and stochastic SDA (SSDA) processes. The obtained electron energy distributions are presented in Figure 1. The supra-thermal tails of these spectra are formed by the populations of the accelerated and reflected electrons.

Tab. 1. List of the main simulation parameters.

Setup	m-50	m-100	m-200	m-400
Mass ratio, m_i/m_e	50	100	200	400
CPU-hours used	~ 150 k	~ 300 k	~ 500 k	~ 1000 k
Disk space used	~ 5 TB	~ 10 TB	~ 20 TB	~ 40 TB
CPUs/nodes (max.)	1680/35	3840/80	4800/100	7200/150

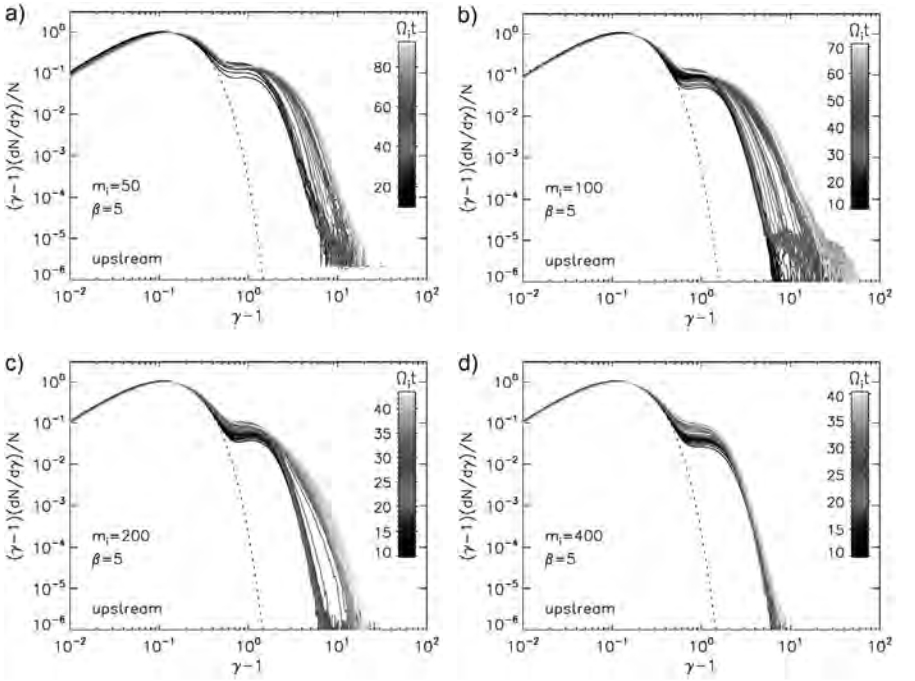

Fig. 1. Evolution of the electron energy spectra in runs m-50 (a), m-100 (b), m-200 (c) and m-400 (d).

5. Conclusions

SSDA process is much more efficient for electron acceleration than SDA. In simulations we observe the transition from SDA to SSDA mediated by the electron interaction with ion-scale waves, which is simpler at smaller ion-to-electron mass ratio. For higher mass ratio the difference between electron and ion scales increases, being unfavorable for SDA-to-SSDA transition (Fig. 1 d). This needs to be studied in a wider range of the physical conditions.

Acknowledgements. The numerical experiment was possible through computing allocation on the Ares system at ACC Cyfronet AGH under the grant “heapic” (PLG/2024/017211).

References

1. O. Kobzar, J. Niemiec, T. Amano et.al. 2021, Astrophys. J., 919, 97.
2. J. Niemiec, M. Pohl, T. Stroman, K.-I. Nishikawa, 2008, Astrophys. J., 684, 1174.
3. A. Dorobisz, M. Kotwica, J. Niemiec, O. Kobzar, A. Bohdan, K. Wiatr, 2018, LNSC, 10777, 156.

High-Resolution Atmospheric Simulations in Areas with Complicated Topography, Based on the Example of the Tatra Mountains

Adrian Góra[1], Mirosław Zimnoch[1], Michał Gałkowski[1,2]

[1] AGH University of Krakow, Faculty of Physics and Applied Computer Science, Kraków, Poland
[2] Max Planck Institute for Biogeochemistry, Department of Biogeochemical Signals, Jena, Germany

adriangora@student.agh.edu.pl, zimnoch@agh.edu.pl,
michal.galkowski@fis.agh.edu.pl

Keywords: atmospheric simulations, mountain terrain, meteorology, WRF model, numerical model error

1. Introduction

Accurate measurements of trace gases' background levels are crucial for estimation of greenhouse gas emissions. AGH operates the KASLAB station on Kasprowy Wierch to monitor CO_2 and CH_4 molar fractions. Cities like nearby Zakopane may influence the measurements. Gas transport is governed by advection and diffusion, and its investigation requires precise meteorological models. This project evaluates WRF model errors in complex terrain, its capability to simulate mountain weather at different resolutions, and key factors affecting the discrepancies.

2. Description of the problem

Simulating mountain weather is challenging, as terrain height can vary by hundreds of meters within a single grid cell. Phenomena like foehn winds and mountain breezes require precise mapping of the topography, and valley geometry, while gravity waves require high resolution due to their wavelength [1]. Higher resolution improves topography, but do not unambiguously improve the wind predictions [2], and can lead to computational instability. Determining optimal resolution requires case-specific testing. The problem is still within current research interest of many groups (e.g. [3] [4]).

3. Solution of the problem

The WRF-ARW (Advanced Weather Research and Forecasting) model [5] has been configured in a spatial resolution of 5 km and 1 km over central Europe with an embedded domain over the Tatra Mountains (Fig. 1.). The simulations have been performed in parallel WRF configuration on 6 nodes of Ares cluster in ACC Cyfronet AGH using approximately 4k computational hours and 130 GB of storage. Three-day simulation periods were selected for extreme wind events (Great Tatra Windstorm of 2013 and an extremely windy summer period in 2021).

The simulation results (pressure, temperature, humidity, and wind) were compared with meteorological measurements available for IMGW synoptic stations located within domains. The 1 km model successfully simulated effects of foehn wind, gravitational wave, and mountain breezes, while the 5 km model was insubstantial in simulating those effects. On the other hand, the comparison of RMSE (root mean square error) showed better performance of 5 km compared to the 1 km simulation.

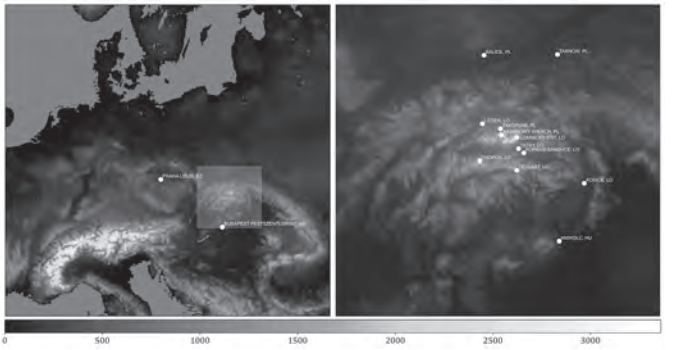

Fig. 1. Topography maps (scale in meters a.s.l.) of 5 km domain (left) and 1 km domain (right) with marked locations of synoptic stations used for data analysis, and boundary of the nested 1 km domain (on left map).

4. Conclusions

Results suggests that one of the crucial elements in comparison between model results and observations is a proper selection of grid cell which is not necessary representing location of the observation point in computational grid (especially its altitude).e). The spatial resolution of 5 km is insufficient for Tatra region simulations and a resolution of 1 km is required for an accurate simulation of mountain climate phenomena. At the same time, the 1 km model performed worse than 5 km in the RMSE analysis, because of the limitations mentioned above. Further investigation with higher spatial resolution (eq. 200m) may improve the agreement between model and observations.

Acknowledgements. This project has been partially supported by the European Union's Horizon Europe Green research and innovation programme, grant agreement No. 101183460, and the Polish high-performance computing infrastructure PLGrid (HPC Center ACC Cyfronet AGH), which is greatly acknowledged for providing computer facilities and support within computational grant PLG/2024/017757.

References

1. Skamarock, William C., Chris Snyder, Joseph B. Klemp, and Sang-Hun Park: "Vertical Resolution Requirements in Atmospheric Simulation", in Monthly Weather Review 147.7., 2019, pp. 2641-2656.
2. Mass, Clifford F., David Ovens, Ken Westrick, and Brian A Colle: "DOES INCREASING HORIZONTAL RESOLUTION PRODUCE MORE SKILLFUL FORECASTS?: The Results of Two Years of Real-Time Numerical Weather Prediction over the Pacific Northwest", in Bulletin of the American Meteorological Society 83.3 2002, pp. 407-430.
3. Park, J.-R., Kim, J.-H., Shin, Y., Kim, S.-H., Chun, H.-Y., Jang, W., Tsai, C.-L., & Lee, G: "A numerical simulation of a strong windstorm event in the Taebaek Mountain Region in Korea during the ICE-POP 2018", in Atmospheric Research, 2022, Vol. 272, p. 10615.
4. Zhang, M., Luo, G., Hamdi, R., Qiu, Y., Wang, X., Maeyer, P. D., & Kurban, A: "Numerical Simulations of the Impacts of Mountain on Oasis Effects, in Arid Central Asia", in Atmosphere, 2017, Vol. 8, Issue 11, p. 212.
5. Skamarock, W. C., J. B. Klemp, J. Dudhia, D. O. Gill, Z. Liu, J. Berner, W. Wang, J. G. Powers, M. G. Duda, D. M. Barker, and X.-Y. Huang, 2019: A Description of the Advanced Research WRF Version 4. NCAR Tech. Note NCAR/TN-556+STR.

Deep Learning for Cancer Cell Detection in Veterinary Cytology

Jan Krupiński[3], Ernest Jamro[1,2], Maciej Wielgosz[2], Paweł Russek[1,2], Agnieszka Dąbrowska-Boruch[1,2], Kazimierz Wiatr[1]

[1] ACC Cyfronet AGH, Nawojki 11, 30-950 Kraków, Poland
[2] AGH University of Krakow, al. Mickiewicza 30, 30-059 Kraków, Poland
[3] Cracow University of Technology, Warszawska 24, 31-155 Kraków, Poland

jan.krupinski@pk.edu.pl, {jamro, wielgosz, russek, adabrow, wiatr}@agh.edu.pl

Keywords: cytology, deep learning, cell detection, skin cancer

1. Introduction

Detection of neoplastic cells in veterinary cytology enables quick and minimally invasive skin cancer diagnostics. Although the fine needle aspiration procedure is technically simple, abnormal cells may require further visual verification by a specialist. This paper describes improvements to the system presented in [1] that aims to support the detection of malignant cells using deep learning (DL). Moreover, the cytological data used has been significantly expanded with the addition of third-party sources.

2. Description of the problem

In the literature, datasets often contain many images taken from the same source or slide. This is due to limited data availability. To ensure that the system performs reliably in a clinical setting, it should be trained and tested on diverse data. Furthermore, training data must be separated temporally and geographically from the data used for model testing. In the case of cytological images, the method of their acquisition may vary, and they may contain many artifacts. While a human specialist did not have difficulty interpreting such samples, the performance of the deep learning models dropped significantly under such conditions. This revealed that the used dataset introduced an undeniable bias.

3. Related Work

The use of DL models has been largely explored in gynecological cancer cytology [2], however research for its use in other forms of cytopathology is limited [3]. Studies have been performed on relatively small datasets and would require further validation before clinical use.

Fig. 1. Lack of similarity between used data, shown using ViT-L [4] output features and t-SNE.

4. Solution of the problem

Our new experiments shifted the focus in the development of the system to emphasize model generalizability. While Cascade R-CNN [4] performed well on the former, more homogeneous data, smaller models such as YOLOv8 [5] were now employed to prevent overfitting. However, these changes were not sufficient to yield significant improvement due to substantial differences in the third-party data, as shown in Figure 1.

Figure 1 visualizes the activations of a deep learning model's backbone (i.e., the model output before the final classification layers) for all the images in the used datasets. The distance between points is an indication of their similarity. While some of the third-party data resembles the previous dataset, the vast majority of it does not. The previous dataset forms clusters corresponding to different skin cancer types, while there is no such clear differentiation in the third-party data. In its case, the variability between image sources outweighs the variability between different neoplasia. This suggested that the training dataset should be expanded.

Annotating new images is a labor-intensive task, as thousands of cells need to be labeled. This process was significantly accelerated using already developed models, which were employed to locate the cells on the images. Preliminary classes were assigned to the cells, leveraging the fact that the type of cancer on the image was known. Using this process, over 1,200 third-party images were annotated, containing a total of 75,000 cells.

After collecting new data, the model was trained again, giving a substantial improvement in performance. On the old data the mAP@IoU0.5 metric increased from 0.78 to 0.88, while testing on the more varied images the metric increased from 0.26 to 0.54. The improvements in detection of specific cancer types in third-party images are presented in Table 1.

Tab. 1. Detection metric AP@IoU0.5 per cancer cell class, YOLOv8 trained on old and new datasets.

Training dataset	Melanoma	Plasmacytoma	MCT	Lymphoma	Histiocytoma	Histiocytic Sarcoma	STS
old	0.21	0.33	0.72	0.32	0.01	0.02	0.19
new	0.50	0.80	0.71	0.20	0.69	0.31	0.55

5. Conclusions

The performance of a deep learning model needs to be evaluated on an entirely separate dataset to test generalizability. This can reveal biases in the training data, which can only be solved by expanding the dataset. This process can be automated to an extent, and training a new model on the resultant data can bring significant improvement.

Acknowledgements. The numerical experiment was possible through computing allocation on the Athena system at ACC Cyfronet AGH under the grants plglaoisi24, plgdyplomanci6.

References

1. R. Frączek, M. Karwatowski, J. Grzeszczyk, J. Caputa, D. Łukasik, M. Wielgosz, P. Russek et al., „The System for Automatic Skin Cancer Detection – Achievements and Challenges", KUKDM 2024: Sixteenth ACC Cyfronet AGH HPC Users' Conference, 13-15 March 2024: proceedings.
2. H. Jianga, et al., „Deep Learning for Computational Cytology: A Survey", Med. Image Analysis, 2022.
3. N. Thakur et al., „Recent Application of Artificial Intelligence in Non-Gynecological Cancer Cytopathology: A Systematic Review", Cancers (Basel) 2022, 14, 5382.
4. Z. Cai and N. Vasconcelos: „Cascade R-CNN: Delving into High Quality Object Detection", in Proc. IEEE/CVF Conference on Computer Vision and Pattern Recognition, 2018, pp. 6154-6162.
5. G. Jocher, J. Qiu and A. Chaurasia: „Ultralytics YOLO (Version 8.0.0)": `http://github.com/ultralytics/ultralytics`
6. A. Dosovitskiy, L. Beyer, et. al., "An image is worth 16x16 words: Transformers for image recognition at scale" ICLR, 2021.

Treatment Prediction of Head and Neck Cancer with Vision-Language Modeling

Filip Ręka, Bartosz Minch

AGH University of Krakow, Kraków, Poland

{filipreka, minch}@agh.edu.pl

Keywords: large language models, clip, computer vision, medicine

1. Introduction

This work presents a novel approach to simulating medical treatment outcomes by embedding medical images and their corresponding descriptions into a shared vector space. By leveraging diffusion models for image synthesis, the method aims to generate clinically coherent medical images (such as CT scans or X-rays) reflecting post-treatment conditions. This research addresses key challenges in medical imaging and offers potential tools for predicting disease progression and supporting clinical decision-making.

2. Description of the problem

Accurately predicting disease progression through medical imaging remains challenging, especially when visualizing treatment outcomes over time. A tool that simulates various treatment options and identifies the most promising one could support doctors in selecting the best approach for a patient. Showing patients potential outcomes without treatment may also help them make informed decisions about their care.

3. Related work

Similar research has been done showing that diffusion models can produce meaningful images of chest X-Rays [1] based on textual input. Both text and image are being encoded into the same vector space defined by fine-tuned MedCLIP model [2]. Fine-tuned large language models can be leveraged for medical image analysis, enabling the generation of accurate clinical descriptions [3].

4. Solution of the problem

To establish a meaningful connection between text and images, we fine-tuned the MedCLIP model using a curated dataset. CLIP models typically consist of text and image embedding components, often based on transformer architectures. Fine-tuning the existing MedCLIP model for improved understanding of head and neck cancer images, along with training a diffusion model from scratch, requires substantial computational resources. All computations were conducted on the Athena supercomputer, equipped with NVIDIA A100 GPUs. By leveraging textual embeddings, a generative model can be trained to produce images that accurately reflect their corresponding descriptions. Through prompt engineering, it becomes possible to describe potential patient states and treatments, thereby generating relevant medical images. Large language models (LLMs) can subsequently analyze the generated images and provide descriptive feedback to assist clinicians in the decision-making process.

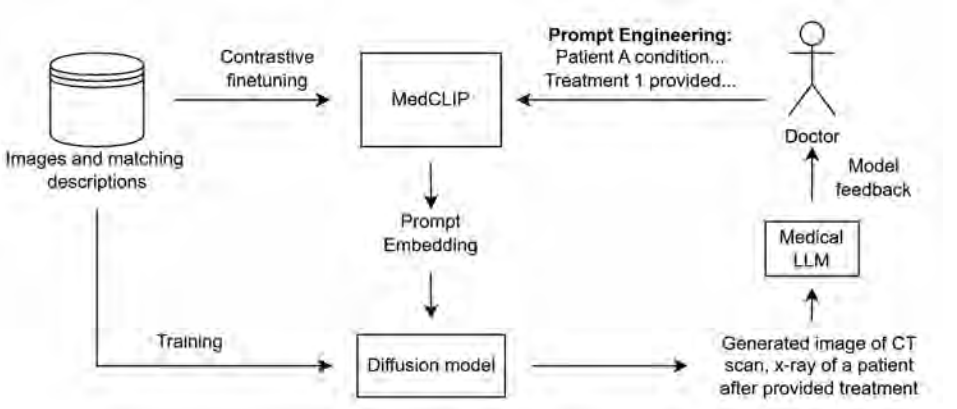

Fig. 1. Schema of proposed solution.

Acknowledgements. We gratefully acknowledge Polish high-performance computing infrastructure PLGrid (HPC Center: ACK Cyfronet AGH) for providing computer facilities and support within computational grant no. PLG/2024/017794.

We gratefully acknowledge Witold Dzwinel for his invaluable supervision of our research and the Maria Sklodowska-Curie National Research Institute of Oncology in Gliwice for providing the data and offering essential scientific and medical support.

References

1. Peng Huang, Xue Gao, Lihong Huang, Jing Jiao, Xiaokang Li, Yuanyuan Wang, & Yi Guo. (2024). Chest-Diffusion: A Light-Weight Text-to-Image Model for Report-to-CXR Generation.
2. Zifeng Wang, Zhenbang Wu, Dinesh Agarwal, & Jimeng Sun. (2022). MedCLIP: Contrastive Learning from Unpaired Medical Images and Text.
3. Omkar Thawkar, J., & Fahad Shahbaz Khan (2023). XrayGPT: Chest Radiographs Summarization using Large Medical Vision-Language Models. arXiv: 2306.07971.

GaNDLF-Synth: a Framework for Generative AI in Biomedical Imaging

Sarthak Pati[1,2], Szymon Mazurek[3,4], Akis Lindaros[1], Spyridon Bakas[1,2]

[1] Indiana University, Indianapolis, 46202 USA
[2] Medical AI Working Group, MLCommons, San Francisco, CA, USA
[3] AGH University of Krakow, Krakow, 30-059 Poland
[4] ACC Cyfronet AGH, Krakow, 30-950 Poland

{patis,aklina,spbakas}@iu.edu, s.mazurek@agh.edu.pl

Keywords: deep learning, framework, medical imaging, generative AI, image synthesis

1. Introduction

Recent AI advances have expanded its applications, notably in computational medicine, which relies on large, complex datasets. However, medical data is scarce and legally restricted. Generative AI (GenAI) addresses this by enabling deep learning (DL) models to generate synthetic data, aiding dataset augmentation [4], improving AI validation, and tackling privacy and class imbalance issues. We introduce the **G**enerally **N**uanced **D**eep **L**earning **F**ramework for **Synth**esis - **GaNDLF-Synth**. It is a low/no-code Python framework for biomedical image synthesis. Integrated with **GaNDLF-core** [1], it offers a simple interface, multi-modal data support, and scalability, lowering the entry barrier for GenAI in biomedical imaging research.

2. Description of the problem

The development and usage of DL methods requires extensive technical knowledge. Applying it in the domain of biomedical imaging increases the complexity even further, creating an entry barrier for researchers, which limits the progress of the field.

3. Related work

Open-source GenAI frameworks for biomedical imaging are limited, lacking flexibility and reusable workflows for diverse data and models. Python library MONAI Generative [2], built on MONAI [3], is the most comprehensive option but still demands significant technical expertise.

4. Solution of the problem

We design and implement GaNDLF-Synth as a general-purpose Python library for both the computational and clinical researchers interested in exploring and evaluating various GenAI approaches for a given biomedical imaging task. It offers a simple CLI interface for running and processing data, configured via simple YAML files. We have implemented numerous popular neural network architectures like autoencoders, generative adversarial networks (GANs), and diffusion models. Furthermore, model training and inference is highly scalable to multiple GPUs and nodes through integration with the DeepSpeed library [5]. Due to modular design based on Pytorch Lightning, it allows for simple extension and customization, allowing adaptability for the complex landscape of GenAI. The overview of the GaNDLF-Synth logic can be seen in Figure 1. The development, testing, and scalability benchmarking were conducted using the Athena supercomputer, using up to 8 compute nodes, each containing 8 Nvidia A100 GPUs and 2 AMD EPYC 7742 CPUs. Cyfronet storage system was used for storing and versioning datasets, requiring up to 1 TB of space.

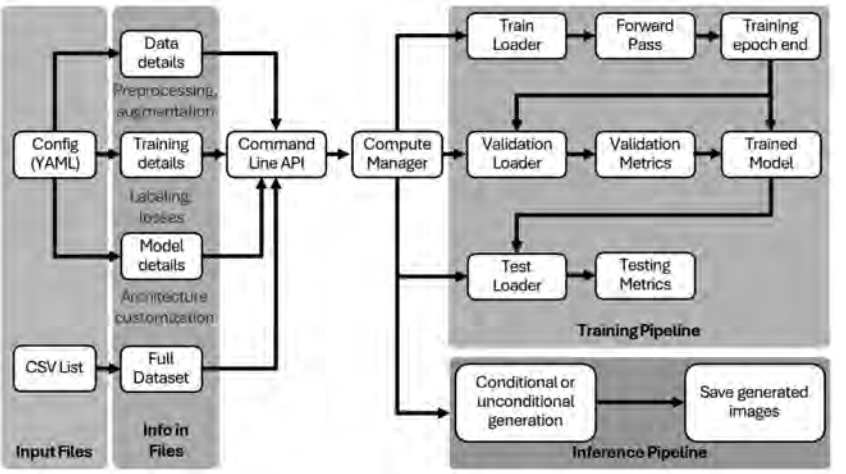

Fig. 1. GaNDLF-Synth workflow.

5. Conclusions

We introduce GaNDLF-Synth, a novel low/no-code framework for creating GenAI models for biomedical imaging. With its simple interface and modularity, it comes in handy for researchers not proficient in programming, as well as experienced ones aiming to customize used methods. Thus, it paves a way for democratizing usage of AI in medicine. The library is openly available under `github.com/mlcommons/GaNDLF-Synth`. Website of the project can be found under `gandlf-synth.org`.

Acknowledgements. We gratefully acknowledge Polish high-performance computing infrastructure PLGrid (HPC Center: ACK Cyfronet AGH) for providing computer facilities and support within computational grant no. PLG/2024/017091. Research reported in this publication was partly supported by the National Institutes of Health (NIH) under award numbers U01CA242871 and U24CA279629. The content of this publication is solely the responsibility of the authors and does not represent the official views of the NIH.

References

1. Koohi-Moghadam, M. et al. Generative AI in Medical Imaging: Applications, Challenges, and Ethics. J Med Syst 47, 94 (2023).
2. Pati, S., Thakur, S. P., Hamamcı, İ. E. et al. GaNDLF: the generally nuanced deep learning framework for scalable end-to-end clinical workflows. Commun Eng 2, 23 (2023).
3. Pinaya, W. H. L. et al. Generative AI for Medical Imaging: extending the MONAI Framework. arXiv 2307.15208 (2023).
4. Cardoso, M. J. et al. MONAI: An open-source framework for deep learning in healthcare. arXiv 2211.02701 (2022).
5. Aminabadi, R. Y. et al. DeepSpeed Inference: Enabling Efficient Inference of Transformer Models at Unprecedented Scale. arXiv 2207.00032 (2022).

Comparative Computational Study of Isomeric TFSI and FPFSI Anions in Li-Ion Electrolytes

Andrzej Eilmes[1], Piotr Kubisiak[1], Domantas Narkevičius[1,2], Chiara Nicotri[1,3]

[1] Jagiellonian University, Faculty of Chemistry, Gronostajowa 2, 30-387 Kraków, Poland
[2] Faculty of Physics, Vilnius University, LT-01513 Vilnius, Lithuania
[3] Department of Applied Science and Technology, Politecnico di Torino, 10129 Torino, Italy

{eilmes,kubisiak}@chemia.uj.edu.pl,
domantas.narkevicius@alumni.vu.lt, chiara.nicotri@student.uj.edu.pl

Keywords: Li-ion electrolytes, molecular dynamics, ion complexation, vibrational spectra

1. Introduction

Although Li-ion batteries have been commercially available since the 1990s of the 20th century, a large effort is being invested in the development of new, more effective, safe and environment-friendly devices. One of key components of a metal-ion battery is the ion-conducting electrolyte, typically a Li salt solution in a molecular liquid. The optimized electrolyte contributes to the overall performance of the battery.

2. Description of the problem

In the search for better Li-conducting electrolytes several promising salts with weakly coordinating anions are experimentally investigated, e.g. lithium bis(trifluoromethanesulfonyl) imide (LiTFSI). Recently, some asymmetric perfluorinated sulfonimide anions were studied, including the TFSI isomer, (fluorosulfonyl)(pentafluoroethanesulfonyl)imide (FPFSI) [1].

Fig. 1. Structure of TFSI and FPFSI anions.

3. Related work

The more commonly used TFSI anion has been thoroughly theoretically investigated. On the other hand, not much computational modeling was done on the FPFSI isomer. Density functional (DFT) calculations were reported for perfluorinated anions and their complexes with Li^+ using an implicit solvent model [2]. In another work, DFT screening was performed for a set of salts in vacuum [3]. Neither of these works discussed the effects of Li-anion interactions on vibrational spectra, used to monitor ion coordination in experiments.

4. Solution of the problem

Quantum chemical calculations for isolated anions and their complexes with Li cations were performed using the MP2 method and three DFT functionals: PBE, B3LYP and M062X. Ab initio molecular dynamics (AIMD) simulations employing the density DFT methodology with the PBE functional, the empirical dispersion correction D3, Goedecker's pseudopotentials and a molecularly optimized DZVP basis set were performed in the CP2K program [4] for LiTFSI and LiFPFSI solutions in tetraglyme. Two salt concentrations for each system were simulated for 50 ps with a time step of 1 fs in the NVT ensemble at T = 298 K using the Nosé--Hoover thermostat.

The infrared (IR) spectra were obtained from the recorded AIMD trajectories as the Fourier transforms (FTs) of the autocorrelation function of the dipole moment. In order to analyze the effect of ion aggregation on the vibrational frequencies, FTs of selected bond lengths were calculated, yielding the power spectra of local vibrations.

5. Conclusions

The FPFSI anion has more low-energy conformations and its asymmetry increases the number of possible Li-FPFSI complexes. For both anions, the preferred geometry of an ion pair in the solvent is the bidentate coordination of Li^+ by two oxygen atoms. The binding effect is only slightly weaker for FPFSI. The PBE results are the most close to the MP2 structural data, which rationalizes the choice of this relatively cheap functional in the AIMD simulations.

Analysis of the AIMD trajectories revealed that the amount of Li^+ coordination to the tetraglyme solvent increases in the LiFPFSI electrolytes. Vibrational spectra of anions and ion pairs and the analysis of the IR spectra obtained from AIMD have indicated that the S-F stretching mode (IR and Raman active) at ~ 600 cm^{-1} can be potentially used in experiments to monitor the FPFSI interactions with cations in the electrolytes [5].

Acknowledgements. The numerical experiment was possible through computing allocation on the Ares system at ACC Cyfronet AGH under the grant plgaenael8. The AIMD simulations were running on 1-2 nodes (48-96 CPU cores) and consumed about 420 k CPU hours.

References

1. P. Deng, H. Zhang, W. Feng, Z. Zhou, M. Armand, J. Nie: Lithium (Fluorosulfonyl) (pentafluoroethanesufonyl)imide/poly(ethylene oxide) Polymer Electrolyte: Physical and Electrochemical Properties, in Solid State Ionics 2019, 338, 161-167.
2. H. Zhang, O. Arcelus, J. Carrasco: Role of Asymmetry in the Physicochemical and Electrochemical Behaviors of Perfluorinated Sulfonimide Anions for Lithium Batteries: A DFT Study, in Electrochim. Acta 2018, 280, 290-299.
3. D. A. Osborne, M. Breedon, T. Rüther, M. J. S. Spencer: Towards Higher Electrochemical Stability of Electrolytes: Lithium Salt Design Through in Silico Screening, in J. Mater. Chem. A 2022, 10, 13254-13265.
4. J. Hutter, M. Iannuzzi, F. Schiffmann, J. VandeVondele: CP2K: Atomistic Simulations of Condensed Matter Systems, in Wiley Interdiscip. Rev.: Comput. Mol. Sci 2014, 4, 15-25.
5. P. Kubisiak, A. Eilmes, D. Narkevičius, C. Nicotri: Comparative Study of Isomeric TFSI and FPFSI Anions in Li-Ion Electrolytes Using Quantum Chemistry and Ab Initio Molecular Dynamics, in J. Phys. Chem. B 2025, DOI: 10.1021/acs.jpcb.4c08414

Enhancing Ni_xAu_{1-x} Thermoelectric Performance through Resonant Scattering

Kacper Pryga, Bartłomiej Wiendlocha

AGH University of Krakow, Faculty of Physics and Applied Computer Science,
Aleja Mickiewicza 30, 30-059 Krakow, Poland

pryga@agh.edu.pl

Keywords: thermoelectric materials, DFT, intermetallic compounds, NiAu, resonant level

1. Introduction

Growing energy concerns in the current world are leading to intensive search for efficient and green alternatives to available energy sources. Thermoelectric materials (TEs) bring aid to this issue due to their capability to convert temperature gradient to electricity with no emissions whatsoever. So far, TEs have been utilized for example in space exploration to power satellites and rovers due to their robustness and low maintenance requirements. Such characteristics cause TEs to be now sought in waste-heat recovery applications.

2. Description of the problem

Unfortunately, current thermoelectric generators have relatively low efficiency, which in TEs is usually described by a figure of merit $zT = \sigma S^2 \kappa^{-1} T$. Obtaining high zT is a challenging task as Seebeck coefficient (S), electrical conductivity (σ) and thermal conductivity (κ) are intertwined through electronic structure, requiring careful optimization. This endeavor can be aided by joint experimental and theoretical analysis to understand its mechanism and to be able to further improve TE performance through e.g. band engineering or introducing resonant levels.

3. Related work

In 2023, a study on Ni-Au alloy [1] reported that it has a record high power factor ($PF = \sigma S^2$) of > 30 $mWm^{-1}K^{-2}$ surpassing any known bulk material and a zT of ~0.5. However the electronic structure and transport properties have not been studied in detail from theoretical standpoint, leaving room for improvement.

4. Solution of the problem

Here we present the results of *ab-initio* study of electronic structure and transport properties of Ni_xAu_{1-x} metallic binary alloy. Calculations were performed on the Ares system at ACK Cyfronet AGH using the KKR-CPA (Korringa-Kohn-Rostoker with coherent potential approximation) method based on Density Functional Theory as implemented in the Munich SPRKKR package. Energy dependent transport function was calculated within the Kubo-Greenwood formalism, and the Seebeck coefficient was estimated using the full Fermi integrals.

5. Conclusions

We have found out that the primary cause determining high thermoelectric performance of Ni_xAu_{1-x} is the difference in resonant scattering around the Fermi level. This is analyzed with a side-by-side study of constantan alloy.

Acknowledgements. This work has been supported by the ’Excellence Initiative – Research University’ program at AGH University of Krakow. We gratefully acknowledge Polish high-performance computing infrastructure PLGrid (HPC Center: ACK Cyfronet AGH) for providing computer facilities and support within computational grant no. PLG/2024/017306.

References

1. F. Garmroudi, M. Parzer, A. Riss, C. Bourgès, S. Khmelevskyi, T. Mori, E. Bauer, A. Pustogow: „High thermoelectric performance in metallic NiAu alloys via interband scattering”, in Science Advances, 2023, 9 (37), eadj1611.

Highly Accurate *ab initio* Calculations of the Excited Electronic States of the Helium Molecule

Dawid Dąbrowski[1], Marcin Gronowski[1], Michał Przybytek[2], Michał Tomza[1]

[1] Faculty of Physics, University of Warsaw, Pasteura 5, 02-093 Warsaw, Poland
[2] Faculty of Chemistry, University of Warsaw, Pasteura 1, 02-093 Warsaw, Poland

d.dabrowsk12@student.uw.edu.pl, michal.tomza@fuw.edu.pl

Keywords: *ab initio* electronic structure calculations, ultracold molecules, Rydberg molecules, helium dimer, excited states, Coupled Cluster theory, Configuration Interaction theory

1. Introduction

The helium dimer serves as an exemplary system for advancing our understanding of few-body physics, high-resolution laser spectroscopy, and the properties of ultracold molecules. The electronic structure of four-electron systems, like He2, can be calculated with unparalleled accuracy. Highly accurate ab initio results not only allow for a direct comparison with experimental data but also guide upcoming experiments and pave the way towards the verification of the Standard Model.

2. Description of the problem

This study aims to achieve benchmark-quality potential energy curves (PECs) with the highest possible accuracy for the few lowest excited states of He_2. We systematically explore these states using various methods and basis sets to provide reliable estimate of accuracy of our computations. After incorporating relativistic and adiabatic corrections, we achieve an exceptional level of accuracy, which is essential for guiding ongoing experiments.

3. Related work

While previous *in silico* studies have attained a reasonable level of accuracy, they remain insufficient for reliably guiding and interpreting state-of-the-art experiments. Last high-accuracy calculation [1] deviates from the experimental results by approximately 1.5%, which is still inadequate for making direct comparisons and providing meaningful insights for cutting-edge spectroscopic research.

4. Solution of the problem

We utilize an extensive range of molecular electronic structure theory methods, including coupled cluster (CCSD(T), CCSDT, EOM-CCSD, EOM-CC3), and configuration interaction (FCI) methods. We develop basis sets for the $He(^1S) + He(^3S)$ states with cardinal numbers up to 10Z and energies are extrapolated to the complete basis set limit. Potential energy curves are calculated for distances up to 50 a_0. The states from the first four asymptotes are computed using the FCI method with basis sets up to 7Z and the various CC methods with basis sets up to 8Z. We also provide a single point calculation for the and states in the 8Z basis set using the FCI and in the 10Z basis set using EOM-CC3 to demonstrate convergence at the global minimum. Our theoretical accuracy reaches 1.0 cm^{-1} (0.006%-0.02%) over the minimum.

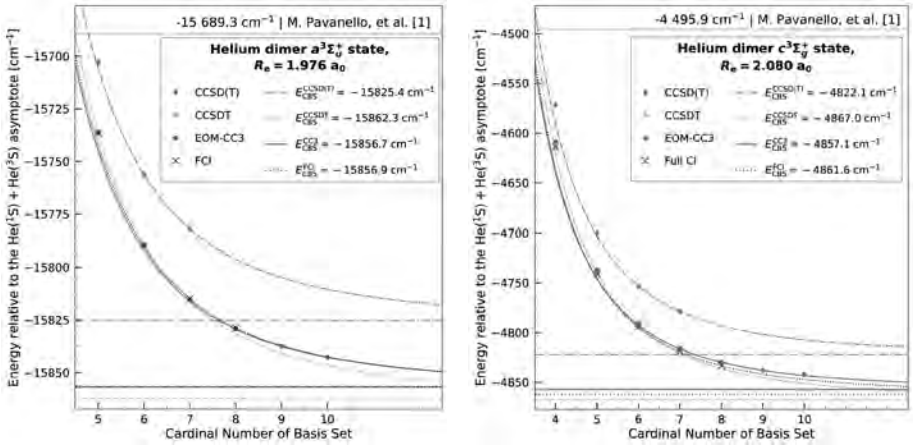

Fig. 1. Energy convergence for $He_2(a^3\Sigma_u^+)$ and $He_2(c^3\Sigma_g^+)$.

The computational workflow involves multiple quantum chemistry programs and algorithms, each selected for its specific strengths. Initially, we employed MOLPRO [3] due to its highly efficient and parallelized implementation of the CCSD(T) method. Next, we utilized MRCC [4], which provides a robust implementation of CCSDT. Subsequently, DALTON [5] was chosen for efficient handling of high angular momentum basis functions, and well-implemented EOM-CC3 method for excited-state computations. In parallel, we carried out FCI calculations using HECTOR [6]. In this project, we utilized three high-performance computing clusters, accumulating a total of approximately 8 million CPU hours.

5. Conclusions

The results of our calculations provide highly accurate data, enabling the calculation of Franck-Condon factors for higher Rydberg states of the helium dimer or the helium molecular ion [2]. We report that our study has achieved the highest accuracy worldwide for the He_2 in excited electronic states.

Acknowledgements. The numerical experiment was possible through computing allocation on the ARES and HELIOS system at ACC Cyfronet AGH under the grants no. PLG/2023/016878 and PLG/2024/017527. National Science Centre, Poland, grant no. 2020/38/E/ST2/00564.

References

1. M. Pavanello, et al. Int. J. Quantum Chem. 108, 2291 (2008).
2. J. Gębala, et al. Phys. Rev. A 108, 052821(2023).
3. MOLPRO, 2023, a package of ab initio programs, H. J. Werner, P. J. Knowles, and others.
4. MRCC quantum package, v2018.
5. Dalton, a molecular electronic structure program, Release v2020.1.
6. M. Przybytek, General FCI program Hector (2014).

Application of Differential Molecular Electrostatic Potential (ΔMEP) in a Description of Chemical Bonding and Reactivity

Olga Żurowska[1,2], Artur Michalak[1]

[1] Jagiellonian University, Faculty of Chemistry, Gronostajowa St 2, PL30387, Cracow, Poland
[2] Jagiellonian University, Doctoral School of Exact and Natural Sciences, Prof. St. Łojasiewicza St 11, PL30348, Cracow, Poland

olga.zurowska@doctoral.uj.edu.pl

Keywords: differential molecular electrostatic potential, chemical bonding, ETS-NOCV, non-covalent interactions, reaction pathways

1. Introduction

Differential Molecular Electrostatic Potential (ΔMEP) [1-3] is a novel tool for chemical bonding analysis. In previous studies [1], we demonstrated that a description based on MEP deformation (ΔMEP) is consistent with ETS-NOCV [4] analysis: key features of chemical bonding revealed in ETS-NOCV are reflected in ΔMEP. However, the methods are not entirely equivalent, as ΔMEP more explicitly illustrates the polarization of molecular fragments.

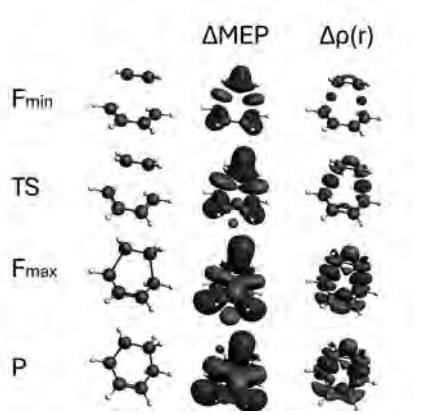

Fig. 1. The examination of ΔMEP and Δρ(r) along the reaction path for the Diels-Alder reaction of 1,3-butadiene and ethylene. The analysis is presented for characteristic points along the path: Fmin (minimum reaction force), TS (transition state), Fmax (maximum reaction force), and P (products). The contour value for ΔMEP is 0.01 a.u., and for Δρ(r), it is 0.005 a.u.

2. Description of the problem

We demonstrate several applications of ΔMEP, including the analysis of covalent bonds, weak non-covalent interactions, tuning halogen bond strength, and tracking changes in chemical bonding along reaction pathways. These applications cover both model reactions and the decomposition of the carbazolium cation by OH^- [5], a process relevant to fuel cells and anion-exchange membranes. The combination of ΔMEP with ETS-NOCV offers a more comprehensive and intuitive representation of chemical interactions.

3. Related work

Previous studies [1-3] have confirmed that ΔMEP effectively characterizes both covalent and non-covalent interactions. ETS-NOCV has been applied in such analyses, but ΔMEP complements it by emphasizing molecular polarization effects and charge redistribution.

4. Solution of the problem

ΔMEP is computed as the difference between the molecular electrostatic potential V(r) of the full system and the sum of $V_0(r)$ for isolated fragments in their geometries from the full system:

$$\Delta MEP = V(r) - \Sigma V_0(r)$$

This approach isolates the effects of bond formation and polarization. To implement this methodology, we use the Amsterdam Density Functional (ADF) software within the AMS package (AMS 2023.104). Calculations are performed using the GGA and hybrid functionals with appropriate basis sets to ensure accurate electrostatic potential evaluation.

The computational workflow includes:

- Optimization of the molecule using DFT calculations.
- Electrostatic potential calculations (Single Point) for both the molecule and its isolated fragments.
- Subtraction of fragment potentials from the total molecular potential.

All computations are carried out using high-performance computing (HPC) resources provided by PLGrid infrastructure.

5. Conclusions

ΔMEP serves as a powerful and intuitive tool for analyzing chemical bonding dynamics. By offering a detailed view of charge redistribution, it provides a valuable complement to ETS-NOCV, facilitating a deeper understanding of chemical interactions and chemical reactions in complex systems.

Acknowledgements. The research was funded by the National Science Centre, Poland, Grant UMO-2022/04/Y/ST4/00154 (M-ERA.NET 3 Call 2022). We gratefully acknowledge Polish high-performance computing infrastructure PLGrid (HPC Center: ACK Cyfronet AGH) for providing computer facilities and support within computational grant no. PLG/2024/017261.

References

1. Żurowska, O., Mitoraj, M. P., Michalak, A.: ETS-NOCV and Molecular Electrostatic Potential-Based Picture of Chemical Bonding. In Advances in Quantum Chemistry; Musiał, M. Grabowski, I., Eds.; Academic Press, 2023; Vol. 87, pp 375–396.
2. Kukułka, M., Żurowska, O., Mitoraj, M. et al.: ETS-NOCV description of chemical bonding: from covalent bonds to non-covalent interactions. J Mol Model 2025, 31, 6.
3. Żurowska, O., Michalak, A.: Description of changes in chemical bonding along the pathways of chemical reactions by deformation of the molecular electrostatic potential. J Mol Model 2025, 31, 33.
4. Mitoraj, M., Michalak, A.: Natural orbitals for chemical valence as descriptors of chemical bonding in transition metal complexes. J Mol Model 2007, 13 (2), 347–355.
5. Nansi Gjineci, Sinai Aharonovich, Sapir Willdorf-Cohen, Dario R. Dekel, and Charles E. Diesendruck. ACS Appl. Mater. Interfaces 2020, 12, 49617−49625.

Theoretical Study on Photophysical Properties of a Coumarin Derivative

Dominika Tabor[1,2], Monika Srebro-Hooper[1]

[1] Department of Theoretical Chemistry, Faculty of Chemistry,
Jagiellonian University, Gronostajowa 2, 30-387 Kraków, Poland
[2] Jagiellonian University, Doctoral School of Exact and Natural Sciences
Prof. St. Łojasiewicza 11, 30-348 Kraków, Poland

dominika.tabor@doctoral.uj.edu.pl, monika.srebro@uj.edu.pl

Keywords: coumarin, fluorescence, phosphorescence, TD-DFT, spin-orbit coupling

1. Introduction

Dual fluorescence (*DF*) produced by a single excitation and room-temperature phosphorescence (*RTP*) phenomena have been gaining increasing attention due to broad applications in optoelectronics and bioimaging [1,2]. In this context, systems based on purely organic molecules emerge as particularly attractive because of such favorable properties as good processability, low cost, and high biocompatibility, with coumarin derivatives as especially promising due to their photostability, high quantum yield, and ability to tune their properties through structural modifications.

2. Description of the problem

Recently, a coumarin derivative with an electron-withdrawing ester and electron-donating hydroxyl groups at positions 3 and 7, respectively (Fig. 1), have been synthesized and its photophysical properties have been experimentally studied, showing occurrence of dual fluorescence in methanol (with maxima at ca. 405 (3.06) and 445 (2.79) nm (eV)) [3]. The goal of the presented work is to develop a reliable theoretical model to explain observed emission properties and comment on *RTP* capabilities of the system.

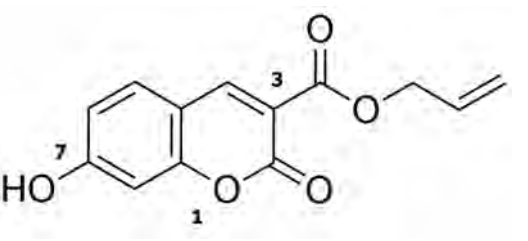

Fig. 1. Examined coumarin derivative.

3. Related work

DF occurrence is usually explained based on the co-existence of multiple emissive states in different electronic and/or molecular structures, breaching the Kasha's rule as well as aggregation effects, while for appearance of *RTP* promotion of intersystem crossing (ISC) and reduction of non-radiative relaxation processes are crucial [4,5]. In understanding of both phenomena theoretical studies via quantum-chemical calculations appear indispensable.

4. Solution of the problem

The calculations included geometry optimizations of the examined coumarin in the ground S_0 and excited S_1 and T_1 states employing density functional theory (DFT) and its time-dependent variant (TD-DFT) with solvent (methanol) effects modelled via a polarizable continuum

model. Additionally, a wavefunction-based correlation method at the coupled cluster (CC) level was used to assess emission energies. To comment on a possibility of ISC and occurrence of *RTP*, spin-orbit coupling (SOC) interactions between S_1 and low-energy triplet excited states were calculated. Conformational analysis in S_0 was performed with the conformer-rotamer sampling tool CREST; (TD-)DFT and CCSD calculations were carried out using the Gaussian 16 and Orca 6 programs. The example results are presented in Fig. 2.

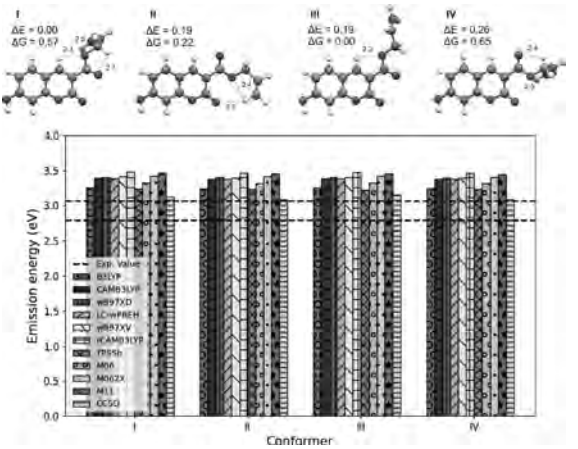

Fig. 2. Top: Optimized (DFT-B3LYP/6-311++G(d,p)) low-energy structures of the examined coumarin in S_0. Bottom: The corresponding fluorescence energy values obtained at the TD-DFT-X/6-311++G(d,p) level with X representing different density functionals and via STEOM-DLPNO-CCSD/def2-TZVP calculations at TD-DFT-B3LYP-optimized S_1 structures. Dashed lines indicate experimental values representing the two maxima in dual fluorescence spectrum in methanol obtained for the examined coumarin.

5. Conclusions

The fluorescence emission energies computed for different conformers change rather negligibly with changes in ester substituent arrangement and seem to correspond well to higher-energy signal in the experimental fluorescence spectrum, especially for CCSD which provides quantitative agreement with the measured value (as can be seen in Fig. 2, TD-DFT tends to overestimate it). *DF* effect cannot be thus explained based on co-existence of various rotameric structures; on-going studies consider aggregation and explicit solvent effects to explain this phenomenon. Interestingly, while ester substituent arrangement, particularly a position of the carbonyl group relative to the coumarin ring, does not affect much fluorescence energy, the obtained SOC values indicate its strong impact on ISC efficiency.

Acknowledgements. We gratefully acknowledge Polish high-performance computing infrastructure PLGrid (HPC Center: ACK Cyfronet AGH) for providing computer facilities and support within computational grant no. PLG/2024/017662.

References

1. Belmonte-Vázquez, J. L. et al., Chem. Mater. 2021, 33 (18), 7160–7184.
2. Wu, H. et al., Adv. Funct. Mater. 2021, 31 (32), 2101656.
3. Matwijczuk, A., private communication, 2024.
4. Behera, S. K. et al.; Angew. Chem. Int. Ed. 2021, 60 (42), 22624–22638.
5. Dong, M. et al., J. Mater. Chem. C 2024, 12 (2), 443–448.

Quantum-Chemical Modelling of Photophysical and Chiroptical Properties of a Helical Molecular System with a Potential Application in CP-OLEDs

Dominika Jelonek[1,2], Monika Srebro-Hooper[2]

[1] Doctoral School of Exact and Natural Sciences, Jagiellonian University, Prof. St. Łojasiewicza 11, Cracow, Poland
[2] Faculty of Chemistry, Jagiellonian University, Gronostajowa 2, Cracow, Poland

dominika.jelonek@doctoral.uj.edu.pl, monika.srebro@uj.edu.pl

Keywords: CPL, MR-TADF, helicenes, (TDA-)TDDFT, spin-orbit coupling

1. Introduction

Combining circularly polarized luminescence (CPL) and multiple resonance thermally activated delayed fluorescence (MR-TADF) has been attracting an increasing interest in the development of molecular systems for organic light-emitting diode (OLED) applications. Currently, integration of helical chirality with MR-TADF core is seen as a promising design approach [1]. In this context, supplementing experimental data with quantum-chemical (QM) calculations may pave the way for better understanding of the experimentally observed photophysical and chiroptical features of such systems.

2. Description of the problem

The main goal of the presented study is to provide a theoretical description and rationalization of the experimentally observed photophysical and chiroptical features of CP-MR-TADF double hetero[5]helicene (Fig. 1), reported by Yang et al. [2], who used its enantiomers in the construction of the OLED devices with beneficial electroluminescence (EL) and CPEL characteristics. Additionally, to comment on helical chirality effects in the examined system, the obtained results are compared with those for its corresponding non-helicenic MR-TADF analogue.

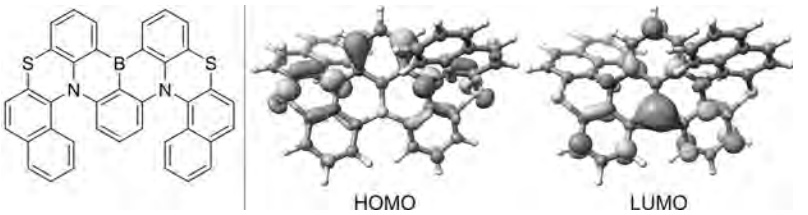

Fig. 1. Left: Chemical structure of the studied system. Right: Isosurfaces of its frontier molecular orbitals computed with PBE0/def2-SVP/CPCM(toluene).

3. Related work

Accurate theoretical modelling of the excited states of the MR-TADF/helically chiral CP--MR-TADF systems rises some notable challenges, concerned with, e.g., determination of reliable values of energy gap(s) between singlet and triplet excited states, ΔE_{ST}. As literature data indicate, for the correct theoretical description it may be necessary to utilize wavefunction-based methods such as SCS–CC2, SCS–ADC(2) and STEOM-DLPNO-CCSD [3,4,5], which induce

high computational cost. Recently, Shizu et al. proposed a cost-effective computational protocol and successfully used it to study the photophysics of the non-chiral MR-TADF molecule based on the analogous core as in the examined here helicene [6].

4. Solution of the problem

In this contribution, the computational protocol adapted from Shizu et al. [6] and based on (time-dependent) density functional theory ((TD)DFT) calculations was used, employing the ORCA 6, Gaussian 16, and Amsterdam Density Functional (ADF) programs.

Computations were performed for the double hetero[5]helicene in the P stereochemistry and its non-helicenic analogue, and involved geometry optimizations in the ground state and S1 and T1 excited states, simulations of the UV-Vis and ECD spectra, and evaluation of the spin-orbit coupling matrix elements (SOCMEs), vertical emission energies, and luminescence dissymmetry factors.

5. Conclusions

To understand experimentally observed photophysical and chiroptical features of the CP-MR-TADF double hetero[5]helicene, QM calculations have been carried out using the protocol adapted from the studies on the photophysical properties of the non-chiral analogue. The computational results obtained and their comparative analysis with those derived for the non-helicenic system allowed to establish the structure-properties relationships in the studied compounds.

Acknowledgements. The numerical experiment was possible through computing allocation on the Ares system at ACC Cyfronet AGH under the grant PLG/2024/017882.

References

1. Y. Xu et al. Chem. Eur. J. 2023, 29(12), e202203414.
2. Yang, W. et al. CCS Chem. 2022, 4(11), 3463-3471.
3. Pershin, A. et al. Nat. Commun. 2019, 10, 597.
4. Wang J., et al. Chem. Sci., 2024, 15(41), 16917-16927.
5. Pratik M. S. et al. Chem. Mater. 2022, 34(17), 8022-8030
6. Shizu, K. et al. Nat. Commun. 2024, 15, 4723.

Study of Lattice Dynamics and Electron-Phonon Interaction in SnTe:In and PbTe:Tl

Gabriel Kuderowicz, Bartlomiej Wiendlocha

Faculty of Physics and Applied Computer Science, AGH University of Krakow, Krakow, Poland

gabriel.kuderowicz@fis.agh.edu.pl

Keywords: superconductivity, density functional theory, electron-phonon interaction, semiconductors, resonant dopants, disorder

1. Introduction

Resonantly doped SnTe and PbTe are well known for their exceptional thermoelectric performance, thus they have been extensively researched for decades. However, some of their properties are still not well understood. Upon doping $Sn_{1-x}In_xTe$ and $Pb_{1-x}Tl_xTe$, these compounds become superconductors with critical temperatures of few Kelvins, despite having very low carrier concentration. With so few carriers to form Cooper pairs, unconventional superconductivity of non electron-phonon origin is often proposed.

2. Description of the problem

One way of studying superconductivity with ab initio calculations in disordered systems is rigid muffin tin approximation which decouples electron-phonon interaction into two separate terms. The electronic one can be calculated using KKR-CPA method but lattice dynamics is much harder to obtain as it requires large supercells. Those problems can be overcome thanks to high-performance computing infrastructure. Moreover, electron-phonon interaction can be calculated more precisely from density functional perturbation theory.

3. Related work

Highest critical temperature of $Pb_{1-x}Tl_xTe$ occurs at solubility limit of 1.4% Tl [1] and valence skipping behaviour is a proposed pairing mechanism [2]. $Sn_{1-x}In_xTe$ can be doped up to 40% and undergoes multiple phase transitions depending on concentration and temperatures. However, electron-phonon coupling constant estimated from experimental data is sufficiently large to explain superconductivity [3] which asks for more theoretical calculations to follow.

4. Solution of the problem

Electronic structure, phonons and electron-phonon interaction was calculated using Quantum Espresso package [4]. Parallelization on Prometheus and Ares supercomputers were done by submitting jobs for few irreducible representations of each dynamical matrix per run. Every job was run on a single node with 12 or 24 cores. The most demanding calculations required 270 GB memory that could not be split between nodes thus bigmem partition was essential. Overall, calculations consumed over million hours of CPU time and output files filled over 2 TB disk space. Other calculations in VASP [5], Phonopy [6] and KKR-CPA code [7] were performed outside of the PLGrid infrastructure.

5. Conclusions

Structure relaxation lowers average phonon frequencies and enhances electron-phonon interaction around dopant atoms and neighbouring Te. Obtained electron-phonon coupling constant

$\lambda \approx 0.22$ in $Sn_{31}In_1Te_{32}$ does not rule out phonon mediated pairing. Accounting for rombohedral distortion resulted in slightly higher value of λ.

Acknowledgements. This work has been supported by the 'Excellence Initiative – Research University' program at AGH University of Krakow. We gratefully acknowledge Polish high-performance computing infrastructure PLGrid (HPC Center: ACK Cyfronet AGH) for providing computer facilities and support within computational grant no. PLG/2024/017305 and PLG/2024/017661.

References

1. Y. Matsushita, P. A. Wianecki, A. T. Sommer, T. H. Geballe, and I. R. Fisher: Type II superconducting parameters of Tl-doped PbTe determined from heat capacity and electronic transport measurements, Physical Review B 74, 134512 (2006).
2. A. Erickson: Pairing mechanism in superconductors with valence-skipping dopants, PhD thesis, Stanford university USA (2009).
3. Shantanu Misra, Bartlomiej Wiendlocha, Janusz Tobola, Petr Levinsky, Jiri Hejtmanek, Sylvie Migot, Jaafar Ghaanbaja, Anne Dausher, Bertrand Lenoir, and Christophe Candolfi: Influence of In-induced resonant level on the normal-state and superconducting properties of $Sn_{1.03}Te$, Physical Review B 106, 075205 (2022).
4. Giannozzi, P., et al. Quantum ESPRESSO toward the exascale. J. Chem. Phys. 152, 154105 (2020).
5. G. Kresse and J. Furthmüller. Efficient iterative schemes for *ab initio* total-energy calculations using a plane-wave basis set. Phys. Rev. B 54, 11169 (1996).
6. Togo, A. and Chaput, L. First-principles Phonon Calculations with Phonopy and Phono3py. J. Phys. Soc. Jpn., 92, 012001-1-21 (2023).
7. A. Bansil, S. Kaprzyk, P. E. Mijnarends, and J. Tobola. Electronic structure and magnetism of $Fe_{3-x}V_xX$ (X = Si, Ga, and Al) alloys by the KKR-CPA method. Phys. Rev. B 60, 13396 (1999).

Experimental and Theoretical Studies of the Structure of Selected Styrene-Divinylbenzene Ion Exchange Resins

Katarzyna Chruszcz-Lipska

AGH University of Krakow, al. Mickiewicza 30, 30-059 Kraków, Poland

lipska@agh.edu.pl

Keywords: anion exchange resin, quaternary ammonium functional group, infrared spectroscopy, DFT calculations

1. Introduction

Ion exchange resins have multifunctional applications. They are used in various industrial processes in the pharmaceutical, food, mining and hydrometallurgical industries. The use of ion exchange resins in water/wastewater treatment has also gained considerable attention over the past few decades [1]. The majority of commercially available ion-exchange resins are based on cross-linked polystyrene-divinylbenzene copolymers with ion-exchanging functional groups (Fig. 1).

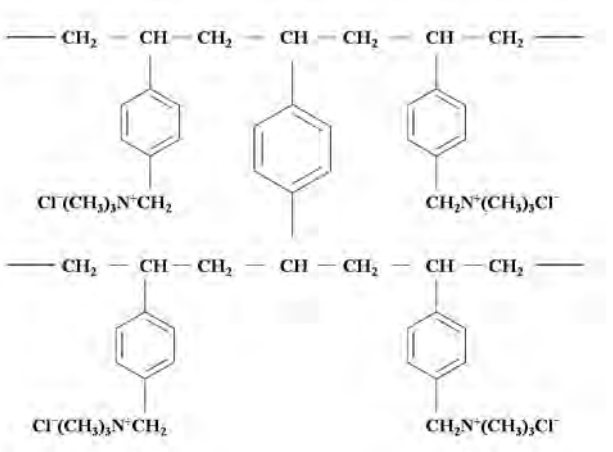

Fig. 1. The chemical structure of the styrene–divinylbenzene anion exchange resin with an ammonium functional group (Cl^- form).

2. Description of the problem

Spectroscopic techniques such as IR spectroscopy are very well suited to study the structure of the resin and then understand what changes occur in its structure during interaction with various chemicals. However, the interpretation of the infrared spectra of styrene-divinylbenzene resins is difficult because they are very band-rich. Quantum chemical calculations leading to theoretical infrared spectra are extremely helpful in the detailed description of experimental data.

3. Related work

Literature data show that IR spectroscopy is used to characterize styrene-divinylbenzene resins. However, a detailed description of the infrared spectra (supported by DFT calculations) for this type of resins is still a knowledge gap.

4. Solution of the problem

All calculations were performed using the Gaussian 16 software packages and were performed at the DFT level, with the B3LYP functional and the 6-31g** basis set.

The solution of the research problem were proceeded in the following order:

- experimental IR spectra of the styrene–divinylbenzene anion exchange resins with an ammonium functional group (Amberlite®IRA402 and Amberlite®IRA900) were measured,
- an appropriate model reflecting the structure of the tested resins (Fig. 1) were selected,
- the structure geometries were fully optimized without any restriction,
- the infrared frequencies were calculated,
- theoretical IR spectra of the model structures of exchange resin were obtained by representing each IR band as a Lorentzian curve,
- the assignment of individual IR experimental bands to the corresponding modes was based on a direct comparison of the experimental and calculated spectra (taking into account the frequency sequence and intensity pattern).

5. Conclusions

For the first time, quantum chemical calculations (DFT/B3LYP/6-31g**) allowed for a detailed assignment of IR bands in the spectra of styrene-divinylbenzene resins with a trimethylammonium functional group Amberlite®IRA402 (Cl^- form) and Amberlite®IRA900 (Cl^- form) [2].

Acknowledgements. This research was supported in part by PL-Grid Infrastructure. The DFT calculation was possible through computing time on the Ares system at ACC Cyfronet AGH under the grants (no. PLG/2022/015763 and PLG/2023/016729). This research was partly supported by "Excellence Initiative-Research University" program for AGH University of Krakow and was partly funded by AGH University of Krakow, The Faculty of Drilling, Oil and Gas (No. 16.16.190.779).

References

1. S. D. Alexandratos: Ion-Exchange Resins: A Retrospective from Industrial and Engineering Chemistry Research. Ind. Eng. Chem. Res. 2009, 48, 388–398.
2. K. Chruszcz-Lipska, E. Szostak: A Study of the Structure of an Anion Exchange Resin with a Quaternary Ammonium Functional Group by Using Infrared Spectroscopy and DFT Calculations, Materials, 2024, 17(24), 6132.

Cellular Automaton Approach to Estimation of Neurotransmitter Flow Parameters in a Presynaptic Bouton of a Neuron

Andrzej Bielecki , Maciej Gierdziewicz

AGH University of Krakow, Al. Adama Mickiewicza 30, 30-059 Kraków, Poland

{bielecki, gierdzma}@agh.edu.pl

Keywords: simulation, neurotransmitter, synapse, diffusion coefficient, cellular automaton

1. Introduction

The reaction-diffusion parameters of neurotransmitter (NT) flow inside the presynaptic bouton of the synapse have been estimated by using partial differential equation (PDE) and cellular automaton (CA). PDE models are more accurate but also more computationally complex. In the present version of the computer program, the performance was improved as well as data quality although the detected spatio-temporal distributions obtained with PDE and CA are still slightly different.

2. Description of the problem

Simulation experiments help estimate parameters of transmission of nerve impulses in the presynaptic bouton. Neurotransmitter molecules diffuse freely or as a content of synaptic vesicles. The process may be modeled by using partial differential equations (PDE) [1] or cellular automata (CA) [2]. The use of CA seems to give less accurate results, but still acceptable precision, with a less complex algorithm. The results presented below show how unknown biological quantities may be estimated by using both PDE and CA.

3. Related work

Mixed continuous and discrete calculations used a 3D bouton model [3], then supply zone, a release site [4], asymmetric design and NT vesicle pools. Next, the quality of the three-dimensional bouton mesh was improved because it may be critical for the speed and accuracy of calculations [5,6].

4. Solution of the problem

The bouton was implemented as a tetrahedral mesh like before [7] but the quality of the mesh was improved; the new one was better and smaller and this speeded up the calculations. Each of the elements (tetrahedrons) was connected maximum 4 other elements. The equation used to model the reaction-diffusion (Equation 1) was a partial differential equation:

$$\partial_t q = D\nabla^2 q + R(q) = f(q, a, a, b, \rho^0) \quad (1)$$

where q was the vector of unknowns, D was the diagonal matrix of diffusion coefficients, and R contains all local reactions. The parameters of the simulation were: a – the diffusion coefficient, a – the permeability coefficient of the secretion zone, b – the synthesis coefficient, and ρ^0 was the threshold density value triggering NT supply. The values of a, a, b, ρ^0 for which the obtained results were similar to the real ones were 6μm^2/s, 80μm^3/s, 50/s, and 370/μm^3, respectively. The CA approach required including additional parameters: distances between neighboring mesh elements and areas of connecting faces. The simulated time was 0.1s and the frequency of stimulation was 200Hz. The computer used for calculations was Ares supercomputer installed in

Academic Computer Center Cyfronet AGH. The amount of time was about 1.5h (for PDE) and 0.75h (for CA and memory use around 4GB compared with 6h and 6GB in [7].

Two example output graphs are presented below (Figure 1). The process of synaptic depression is captured. Unlike the previous results [7], here the restoration of NT amount between impulses is clearly visible for both methods (PDE and CA).

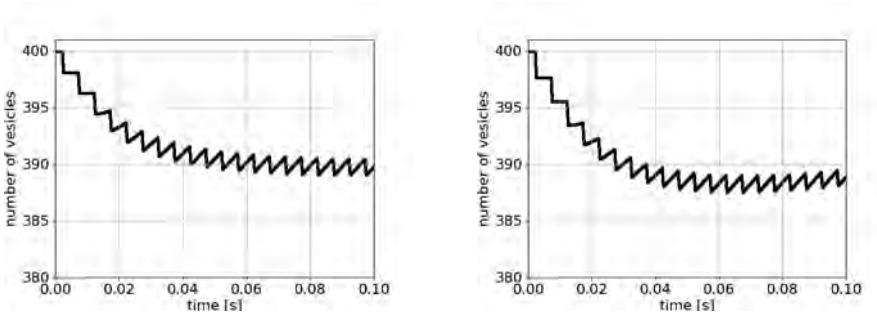

Fig. 1. The change in the amount of NT vesicles in the presynaptic bouton in time. Left, PDE, Right, CA.

5. Conclusions

The research showed that the cellular automaton methodology is capable of estimating parameters of neurotransmitter vesicles transport, synthesis and release in the presynaptic bouton of the neuron. Applying both partial differential equations and cellular automaton reached similar results, including the clear visibility of the neurotransmitter supply.

Acknowledgements. The numerical experiment was possible through computing allocation on the Ares system at ACC Cyfronet AGH under the grant *plgneuron2024*.

References

1. A. Bielecki and M. Gierdziewicz: „Simulation of neurotransmitter flow in three dimensional model of presynaptic bouton", Lecture Notes in Computer Science, 12139, 2020, pp. 132-143.
2. A. Strader, K. E. Schubert, M. Quintana, E. Gomez, J. Curnutt and P. Boston: „Estimation, Modeling, and Simulation of Patterned Growth in Extreme Environments", in Arabnia, H. and Tran, Q. N.(eds.): „Software Tools and Algorithms for Biological Systems. Advances in Experimental Medicine and Biology", Springer, New York, USA, 696, 2011.
3. M. M. Knoedel et al.: "Synaptic bouton properties are tuned to best fit the prevailing firing pattern", Frontiers in Computational Neuroscience, 8:101, pp. 1-16, 2014.
4. A. Bielecki, M. Gierdziewicz and P. Kalita: „Three-dimensional model of signal processing in the presynaptic bouton of the neuron", Lecture Notes in Artificial Intelligence 10841:3-14, 2018.
5. M. Gierdziewicz: Relations between geometric parameters and numerical simulation accuracy in modeling signal transmission in the presynaptic bouton. Applied Sciences 11:2811, 2021.
6. M. Gierdziewicz: Simulation of processes and structures in the synapse in the context of tetrahedral mesh quality. Computers and Mathematics with Applications 145:58-64, 2023.
7. A. Bielecki, M. Gierdziewicz: Simulation of Neurotransmitter Flow in a Presynaptic Bouton of a Neuron with Cellular Automaton. KUKDM 2024: Proc. Of the XVIth ACC Cyfronet AGH HPC Users' Conference, 13-15 March 2024, 33-34, 2024.

Design of Alkylxanthine Derivatives of 3,4-dihydroquinazoline-2-amine as Potential Serotonin Receptor Ligands Using Molecular Modelling Methods

Natalia Kozień[1], Przemysław Zaręba[2]

[1] Cracow University of Technology, Faculty of Chemical Engineering and Technology, 24 Warszawska Street, 31-155 Cracow, Poland

[2] Cracow University of Technology, Faculty of Chemical Engineering and Technology, Department of Chemical Technology and Environmental Analytics, 24 Warszawska Street, 31-155 Cracow, Poland

natalia.kozien@student.pk.edu.pl, przemyslaw.zareba@pk.edu.pl

Keywords: serotonin, 5-HT_{5A}, anticancer, 3,4-dihydroquinazoline-2-amine, molecular modeling

1. Introduction

Oncological diseases are the leading cause of deaths. According to the World Health Organization (WHO), the most common organs attacked by cancer are the lungs, large intestine with rectum, liver, stomach and breasts. [1] Numerous scientific studies have shown that ligands of serotonin receptors can be widely used in their treatment. The 5-HT_{5A}R is the least known of the serotonin receptors. However, there are reports that selective antagonists of this receptor may be anticancer drugs in the future [2].

2. Description of the problem

There are reports of antitumor activity of 5-HT_{5A}R antagonist, but there are no compounds with the desired pharmacological properties. Therefore it is important to design new group of this receptor ligands that could be a candidate for usage as a monotherapy or in combination therapy in the treatment of cancer, for example in combination with compounds targeting adenosine receptors. Molecular modeling can be used in their design.

3. Related work

Selective 5-HT_{5A} receptor antagonists could be future anti-cancer agents [3]. It has been proven that they reduce the frequency of tumorsphere initiating cells residing in breast tumor cell lines [4]. The studies also identified 5-HT_{5A} receptor as a promising therapeutic target for prostate cancer via its interaction with AR signaling [5].

4. Solution of the problem

In light of the presented reports, it was decided to design compounds with potential activity directed at 5-HT_{5A} and adenosine receptors using molecular modeling. Two groups of 3,4-dihydroquinazoline-2-amine derivatives were selected and obtained. The results of computer simulations have been confirmed in biological studies. The crystal structure of the receptor (PDB ID:7UM4, from PDB RSCB) was used. Molecular docking was performed in Schödinger's Maestro program in the Induced Fit Docking protocol. The grid box was centered on the $D^{3.32}$ using "Glide". The structures were prepared using "LigPrep". The membrane (POPC) and dynamics simulation system were created using QwikMD in VMD 1.9.3. The simulation was performed in NAMD using CHARMM. The results of trajectory analysis obtained using Chimera MD.

5. Conclusions

The molecular modeling researches showed that compounds arranged themselves coherently in the protein and molecular dynamics simulation showed that designed ligand-protein complex is stable with permanent interactions with $D^{3.32}$. The obtained compounds appeared to be a moderate ligands of 5-HT_{5A}R, biological results showed medium affinity for the receptor (K_i within 555-203 nM), which initiated a new, unique chemotype of long-chain 5-HT_{5A}R ligands.

Acknowledgements. The research has been supported by the project „Nowe ligandy receptora 5-HT_{5A} zdolne do hamowania sygnalizacji szlaku PI3K/Akt/mTOR jako dualne podeście w leczeniu opornego na kastracje raka gruczołu krokowego" LIDER14/0035/2023, financed by NCBR. The numerical experiment was possible through computing allocation on the Ares system at ACC Cyfronet AGH under the grants plgzzb5.

References

1. WHO web site: `https://www.who.int/news-room/fact-sheets/detail/cancer`
2. D. Ye, H. Xu, Q. Tang, H. Xia, C. Zhang, F. Bi, "The role of 5-HT metabolism in cancer", BBA, 2021, pp. 188618.
3. W. D. Gwynne et al., "Antagonists of the serotonin receptor 5A target human breast tumor initiating cells", BMC Cancer, 2020, pp.724.
4. W. D. Gwynne, M. S. Shakeel, A. Girgis-Gabardo et al., "Antagonists of the serotonin receptor 5A target human breast tumor initiating cells" BMC Cancer, 2020, pp.724.
5. Itsumi M., Shiota M., Sekino Y. et al., "High-throughput screen identifies 5-HT receptor as a modulator of AR and a therapeutic target for prostate cancer", The Prostate, 2020, pp. 885–894.

Author Index

Published by

ACC Cyfronet AGH
ul. Nawojki 11
30-950 Kraków
www.cyfronet.pl

Sponsors

ISBN 978-83-61433-48-4